E L E C T R I C R O C K B R E A K I N G F O R

S O U T H A F R I C A N O R E B O D I E S

Hartmut Johannes Ilgner

A dissertation submitted to the Faculty of Engineering and the Built Environment, University of the Witwatersrand, Johannesburg, in fulfilment of the requirements for the degree of Master of Science in Engineering.

Johannesburg, 2006

DECLARATION

I declare that this dissertation is my own work, unaided work, except where otherwise acknowledged. It is being submitted for the Degree of Master of Science in Engineering in the University of the Witwatersrand, Johannesburg. It has not been submitted before for any degree or examination in any other University.

_____

_____ day of _____ _____

ABSTRACT

Although pulsed power has been used in many parts of the world over the last few decades to initiate high-voltage discharges through rock, no systematic test work on South African ore bodies and related rock types has been done so far.

As part of CSIR Miningtek's integrated approach of combining underground comminution with a novel Tore© hydrotransport system, which has been shown to operate well with coarse particles up to 10 mm, various rock types were fragmented in single discharge mode under laboratory conditions.

The work was conducted at the University of the Witwatersrand's high-voltage laboratory with a custom-designed test rig. The rig configuration was based on a critical review and analysis of the literature and on assessments of existing test facilities elsewhere. Core samples with diameters ranging from 16 to 48 mm were cut from test specimens with thicknesses ranging from 8 to 48 mm. Rock types included Ventersdorp Contact Reef, Carbon Leader, Elsburg Formation, UG2 and Merensky, as well as pure quartz, shales, lava and dykes.

A six-stage Marx generator provided a voltage rise time of 2 000 kV/µs to create a discharge through the rock, in preference to a discharge through the surrounding water, which acts as an insulator at ramp-up times faster than 0,5 µs. High-speed photography, and an analysis of the voltage and current signals for various rock types and for water alone, were used to quantify the potential benefits of rock breaking by electric discharge.

It was found that some Kimberlite specimens and mineralised gold-bearing reefs were much easier to fragment than hanging wall or footwall material. Merensky reef appeared to be more susceptible than the less brittle UG2 material. A correlation was derived between the dynamic resistivity of various rock types, measured at 16 MHz excitation frequency, and the electrical breakdown strength at which discharge took place.

The fragments created had a more cubical shape than would be created by conventional impact crushing. However, the high voltage requirements of about 30 to 35 kV per millimetre of rock thickness would necessitate not only efficient mechanical and electrical contact between the electrodes and the rock, but also considerable safety features for underground installations.

The clearly identified, preferential fracturing of reef rock types, compared with the hanging or footwall materials, suggests that the greater benefit of electric rock breaking may lie in primary

rock breaking as a mining method, rather than in secondary comminution of broken rock to enable hydraulic transportation by pipeline to surface.

ACKNOWLEDGEMENTS

I wish to thank the CSIR for providing the funds to conduct this research, and for the many discussions with Horst Haase and Peter Kramers during the initial phases of this research project. Many thanks also to my supervisors Prof's B W Skews and E A Moss for their guidance and patience.

Also, I would like to thank the team at the Forschungszentrum Karlsruhe (FZK) in Germany, particularly Hans Joachim Bluhm and Wolfgang Frey, for accommodating my visit to their facilities in 1998. The existing facilities are an inspiration and I was able to witness the first electric rock-breaking test conducted on my samples with one of their older test rigs.

I would like specifically to thank Thomas Wallmach for the many hours of microscopic observations and discussions, and Philamon Moseme for conducting some geological characterisation of the many test specimens prior to fragmentation. A big thank you goes to Jonathan Manganye, who, as always, did a superb job in preparing and polishing the disc samples, providing thin sections for microscopic interpretations, and conducting the 16 MHz tests to determine the dynamic electric properties of the many 8 by 32 mm samples.

The technical know-how and support of Shawn Nielson and Andreas Beutel from the High-Voltage Laboratory at Wits in building the electric circuit, based on the information obtained during the literature search and site visits, were also invaluable. Thanks also goes to Murray Bredin from the University of the Witwatersrand's Photographic Section who provided the two high-speed black and white cameras, with advice on how to operate them, to complement the colour camera equipment provided by the author. Thanks also to Dirk Albrecht for converting the many analogue, colour video images into individual frames for detailed analysis.

Finally, a huge, special thank you goes to my family, Liz, Nicola and Laura, for providing the space and support to burn the midnight oil so often.

CONTENTS

Page

DECLARATION.....I

ABSTRACT.....II

ACKNOWLEDGEMENTS.....IV

LIST OF FIGURES.....VIII

LIST OF TABLES.....XIV

NOMENCLATURE AND DEFINITION OF TERMS.....XV

1 INTRODUCTION.....1

2 BACKGROUND AND MOTIVATION.....1

3 AIMS OF THE STUDY.....3

4 METHODOLOGY.....4

4.1 Literature Review.....4
4.2 Assessment of Equipment Available Worldwide 4
4.3 Test Work on Electric Rock Breaking 5
4.4 Analyses and Discussion.....5

5 LITERATURE REVIEW OF ELECTRIC ROCK BREAKING.....7

5.1 Classic Lightning Theory.....8
5.2 Budenstein's Theory.....11
5.3 Dielectric Measurements of Homogeneous Material.....16
5.4 High-Frequency, Dry Applications.....16
5.5 First Discharges with Submerged Specimens.....19
5.6 Power Consumptions.....23
5.7 Rock Types Used in Previous Studies.....23
5.8 Black Granite Test Series.....24
5.9 Electric Discharge Paths.....26
5.10 Summary.....30

6 ASSESSMENT OF POTENTIAL RIGS AND INITIAL TESTS.....32

6.1 Functional Test Rigs Outside South Africa.....32
6.1.1 TZN, Germany.....32
6.1.2 IEEE (Switzerland).....33
6.1.3 Aerie Partners (USA).....33
6.1.4 Euro-Pulse (UK).....39
6.2 Forschungszentrum Karlsruhe (FZK), Germany.....41
6.2.1 Batch rig.....42
6.2.2 Continuous rig.....44
6.2.3 Challenges for continuous rock-breaking plant.....46

6.3 Evaluation of Rock Specimens Fractured at FZK....46
6.3.1 Macroscopic and microscopic analyses before fragmentation....46
6.3.2 Initial tests at FZK, Germany....50
6.3.3 Particle size distributions (PSDs)....57
6.3.4 Particle shape definitions....57
6.3.5 Comparisons of settling velocities....59
6.4 Success Criteria for Electric Rock-Breaking Tests....62
6.4.1 Importance of voltage rise time....62
6.4.2 Submergence in water....62
6.4.3 Single shots for investigations into the breakage of various rock types....62
6.4.4 Electrical instrumentation....63
6.4.5 Clamping of rock samples....63
6.4.6 Sampling facility....63
6.5 Summary....64

7 RIG CONFIGURATION USED FOR LOCAL TEST WORK....66

7.1 Requirements for Local Test Equipment....66
7.2 Identification of State-of-the-Art, Local Equipment....66
7.2.1 Apollo....66
7.2.2 Potchefstroom University....67
7.2.3 Atomic Energy Corporation....68
7.2.4 High-Voltage Laboratory at the University of the Witwatersrand....68
7.2.5 Comparisons of equipment....69
7.3 Test Rig for Electric Rock Breaking....69
7.3.1 High-voltage circuit....69
7.3.2 Rock-breaking chamber....74
7.3.3 Signal conversions....76
7.3.4 Cameras and lighting settings....76
7.3.5 Photographic settings for discharges through water....81
7.3.6 Photographic settings for rock-breaking sequences....84
7.4 Quantification of the effect of the water gap on breakdown delays....86
7.4.1 Voltage rise times and strength level....86
7.4.2 Discharge delay with applied high voltage....87
7.4.3 Current wave-form during discharge....88
7.4.4 Breakdown delays through water....90
7.5 Summary....92

8 ELECTRIC ROCK BREAKING TEST WORK....93

8.1 Geometries of Various Rock Types....93
8.2 Evaluation of Electric Rock Breaking Signals....93
8.2.1 Breakdown through reef....96
8.2.2 Unsuitable rock types – unwanted discharge through water....98
8.3 Associated Currents to Above-Voltage Signals....98
8.4 Energy Consumption....100
8.5 Electrical Rock Properties....101
8.6 Correlation of Electrical Rock Properties and Breakdown Voltage....102
8.7 Correlation between dynamic resistivity and breakdown field strength....103
8.8 Assessment of Reef Type, Fragments and Specimen Thickness....104
8.9 Effect of specimen thickness on breakdown voltage....106
8.10 Electron Microscope Images....111
8.11 Summary....113

9 DISCUSSION OF RESULTS AND OBSERVATIONS 114

9.1 Potential Effect on Flotation Recovery.....114
9.2 Selective Fracturing along Grain Boundaries.....114
9.3 Effect of Ore Body Type.....115
9.3.1 Gold reef material.....115
9.3.2 Foot wall and hanging wall rock types.....115
9.3.3 Platinum reef specimens.....115
9.3.4 Kimberlite specimens.....117
9.3.5 Foscor specimens.....118
9.4 Utilisation of High-Speed Photographic Evidence.....119
9.4.1 Unwanted flashovers.....119
9.4.2 Carbon Leader Reef footwall, 'blown off' 120
9.4.3 Cavitation due to moving fragments.....120
9.4.4 Raising air bubbles 122
9.4.5 Design of comminution chamber components.....122
9.4.6 Insulation failure for upper electrode.....123
9.4.7 Photographic Evidence and Acoustic Emissions.....124
9.5 Implications for Underground Equipment.....124
9.6 Review of Objectives and Potential Benefits of the Technology.....125
9.7 Summary.....126

10 CONCLUSIONS.....127

11 RECOMMENDATIONS FOR FUTURE RESEARCH.....128

12 REFERENCES.....130

13 BIBLIOGRAPHY.....132

14 APPENDIX A: FZK DRAFT CONTRACT AGREEMENT (NEVER BEEN SIGNED).....135

15 APPENDIX B: CHRONOLOGICAL DEVELOPMENTS AND SEQUENCE OF COMRO AND CSIR INVOLVEMENT WITH 'ELECTRIC SHOCK WAVE COMMINUTION' TECHNOLOGY.....153

16 APPENDIX C: PEOPLE SIGNIFICANTLY INVOLVED IN SOUTH AFRICA WITH ELECTRIC ROCK BREAKING FOR THIS PROJECT.....155

17 APPENDIX D: VOLTAGE AND CURRENT TRACES FROM OTHER TEST RIGS.....157

LIST OF FIGURES

Page

FIGURE -1: ENVISAGED INTEGRATION OF ELECTRIC ROCK-BREAKING AND PUMPING.....3

FIGURE -2: ELECTRIC DISCHARGES IN NATURE (AFTER NATIONAL GEOGRAPHIC, 2002).....9

FIGURE -3: ERUPTING VOLCANIC DEBRIS, ILLUMINATED BY LIGHTNING DURING A THUNDERSTORM (THORARINSON, 1964).....10

FIGURE -4: INITIAL, FORMATIVE PHASE OF POLARISATION.....11

FIGURE -5: FIELD ENHANCEMENTS DURING INITIATION PHASE.....12

FIGURE -6: TREEING AND LUMINANCE PRODUCED.....12

FIGURE -7: CHANNEL ENLARGEMENT AND CURRENT FLOW.....13

FIGURE -8: EXPANDING PLASMA AND DESTRUCTION.....14

FIGURE -9: DIFFERENT CRACK CREATION MECHANISMS FOR VERTICAL LOADING (MEYERS, 1996).....15

FIGURE -10: ACCURATE SET-UP FOR ELECTRICAL BREAKDOWN TESTS (WHITEHEAD, 1951).....16

FIGURE -11: TRUCK-MOUNTED BOULDER BREAKER FOR QUARRIES (AFTER SARAPUU, 1973).....18

FIGURE -12: POTENTIAL UNDERGROUND APPLICATION (AFTER SARAPUU, 1973) 18

FIGURE -13: ADDITIONAL, ELECTRICAL IMPULSE GENERATOR TO BREAK ROCK AFTER THERMAL HEATING (SEGSWORTH AND KUHN, 1975).....19

FIGURE -14: YUTKIN'S UNDERWATER CRUSHING (AFTER MAROUDAS, 1967).....20

FIGURE -15: UNDERWATER CRUSHING (LEFT) AND PARTICLE SIZE DISTRIBUTIONS PRODUCED (RIGHT) (AFTER BERGSTROM, 1961).....21

FIGURE -16: UNDERWATER CONTINUOUS CRUSHER (ANDRES, 1976).....22

FIGURE -17: TEST RESULTS FROM SINGLE SHOTS WITH FINE-GRAINED BLACK SOUTH AFRICAN GRANITE (ANDRES, 1989).....25

FIGURE -18: DIFFERENCES BETWEEN INDIRECT AND DIRECT COMMINUTION.....27

FIGURE -19: SCHEMATIC OF BREAKDOWN STRENGTH VS. DELAY 28

FIGURE -20: BREAKDOWN CURVES FOR WATER AND CONCRETE (HOPPE ET AL., 1998).....29

FIGURE -21: ARTIST'S IMPRESSION OF TZN'S COMMINUTION RIG.....32

FIGURE -22: FRAGMENTATION OF CARBON LEADER REEF (CLR) (AFTER COMRO, 1990).....33

FIGURE -23: AERIE PARTNERS' MOBILE RIG 34

FIGURE -24: AERIE'S ROCK-BREAKING CHAMBER.....35

FIGURE -25: GRAIN BOUNDARY BREAKAGE BY AERIE EPD UNIT (AERIE PARTNERS, PROPRIETARY DATA).....35

FIGURE -26: CONCEPT FOR A LARGE-SCALE COMMINUTION PLANT (AERIE PARTNERS).....36

FIGURE -27: BATCH DISCHARGE ONTO SCREEN (AERIE PARTNERS).....37

FIGURE -28: VARIOUS GOLD ASSOCIATIONS WITH HOST ROCK.....38

FIGURE -29: TYPICAL VOLTAGE AND CURRENT SIGNALS DURING DISCHARGE (EURO-PULSE SET UP, AFTER KRAMERS, 1997).....40

FIGURE -30: EURO-PULSE: ROCK LOADED (LEFT), EXPLOSIVE LIFTING OF LID, FRAGMENTS (RIGHT).....40

FIGURE -31: SCHEMATIC OF BATCH RIG AT FZK, 'FRANKA-0'.....42

FIGURE -32: COLLECTOR BASE WITH SCREEN ON TOP (LEFT) AND CONICAL COMMINUTION CHAMBER (RIGHT).....43

FIGURE -33: FZK'S FRANKA-0 MARX GENERATOR.....43

FIGURE -34: SCHEMATIC OF FZK'S 'FRANKA-STEIN' CONTINUOUS RIG (HOPPE ET AL., 1998).....44

FIGURE -35: MARX GENERATOR FOR CONTINUOUS RIG.....45

FIGURE -36: LAVA: INITIAL, SMALL CHIP FROM CORE SAMPLE.....50

FIGURE -37: LAVA: CHIPPING AND CRACKING NEAR EDGE OF CORE SAMPLE (PENCIL TIP WITH LEAD PROVIDES A RELATIVE SCALE) 51

FIGURE -38: EVIDENCE OF GLASS PARTICLES IN THE DISCHARGE PATH.....51

FIGURE -39: SPOTTED DYKE: CRACKS ALONG THE SURFACE OF THE POLISHED SAMPLE 52

FIGURE -40: SULPHUR STAINING ALONG THE CRACKS OF THE CRUSHED SPOTTED DYKE SAMPLE, AND FRACTURING ALONG THE GRAIN BOUNDARIES.....53

FIGURE -41: MULTI-STRIATED JOINTING IN VEIN QUARTZ.....54

FIGURE -42: INDICATIVE PLATINUM PSDS FROM FZK'S BATCH RIG.....55

FIGURE -43: VCR: PYRITE SEAMED BY CHLORITE.....56

FIGURE -44: VCR: INDICATIONS OF SPALLING AT THE EDGE OF THE SAMPLE.....56

FIGURE -45: GOLD-MINE-RELATED PARTICLE SIZE DISTRIBUTIONS – FZK BATCH RIG 57

FIGURE -46: THREE PRINCIPAL AXES FOR FRAGMENT SIZE DETERMINATION (AFTER PETTIJOHN, 1949).....58

FIGURE -47: PARTICLE SHAPE DEFINITIONS (AFTER PETTIJOHN, 1949).....58

FIGURE -48: CORRECTION FACTORS FOR NON-SPHERICAL PARTICLES (AFTER MCNOWN AND MALAIKA, 1950).....59

FIGURE -49: SPHERICITIES OF ESWC-CRUSHED AND IMPACT-CRUSHED PARTICLES 60

FIGURE -50: SETTLING VELOCITIES FOR FRAGMENTS.....61

FIGURE -51: NETFA'S 18-STAGE MARX GENERATOR, CONTROL ROOM, CONCRETE TOWER AND CAPACITOR BANKS.....66

FIGURE -52: NETFA'S EIGHT-STAGE MARX GENERATOR WITH CONTROL PANEL.....67

FIGURE -53: AEC'S POTENTIAL TEST SET-UP (AFTER TURNER, 1999).....68

FIGURE -54: TEST RIG – ELECTRICAL LAYOUT.....71

FIGURE -55: WITS' MARX GENERATOR AND HIGH-VOLTAGE TRANSFORMER 71

FIGURE -56: SHIELDED CAMERAS, FLASHCAM (LEFT) AND SONY (RIGHT).....72

FIGURE -57: OSCILLOSCOPE TRACES FOR VCR AND QUARTZ SPECIMENS.....95

FIGURE -58: OSCILLOSCOPE TRACES WITH DELAYED BREAKDOWN FOR KUDU DYKE AND LAVA.....96

FIGURE -59: OSCILLOSCOPE TRACE COMPARISON: VCR SPARE PEBBLE MARKER..96

FIGURE -60: PREFERENTIAL DISCHARGE THROUGH REEF TYPES, 20 MM THICK.....97

FIGURE -61: DISCHARGE THROUGH VCR, KUDU DYKE AND LAVA, 8 MM THICK 98

FIGURE -62: CURRENT TRACES THROUGH VCR, 8 MM THICK, MOVING AVERAGE OF 5.....99

FIGURE -63: CURRENT TRACES FOR KUDU DYKE AND LAVA, 8 MM THICK.....100

FIGURE -64: COMPLEX ELECTRICAL PROPERTIES OF ROCK (SARAPUU, 1973).....101

FIGURE -65: ELECTRO-DYNAMIC ROCK PROPERTIES.....102

FIGURE -66: BREAKDOWN FIELD STRENGTHS FOR VARIOUS ROCK TYPES.....103

FIGURE -67: CORRELATION WITH QUARTZ RESULTS.....103

FIGURE -68: CORRELATION WITHOUT QUARTZ RESULTS.....104

FIGURE -69: CARBON LEADER REEF, NO FINES CREATION.....105

FIGURE -70: UG2 SPECIMENS, 8 MM THICK (LEFT) AND 40 MM THICK (RIGHT).....105

FIGURE -71: GOLD REEF, ELSBURG FORMATION, SAMPLE FRAGMENTS.....106

FIGURE -72: EFFECT OF SPECIMEN THICKNESS ON BREAKDOWN VOLTAGES.....107

FIGURE -73: VOLTAGE BREAKDOWN PATTERNS FOR KIMBERLITE 'A' SPECIMENS 108

FIGURE -74: VOLTAGE BREAKDOWN PATTERNS FOR GOLD REEF SPECIMENS.....109

FIGURE -75: VOLTAGE BREAKDOWN PATTERNS FOR TWO UG2 SPECIMENS AND WATER.....110

FIGURE -76: SUMMARY OF BREAKDOWN FIELD STRENGTHS VS. THICKNESSES….111

FIGURE -77: ELECTRON MICROSCOPE IMAGES – TENSILE-FRACTURED LAVA (LEFT) AND EVIDENCE OF SMALL PLASMA TRACES (RIGHT).....112

FIGURE -78: DETAILED AIR-ENTRAPMENT IN SOLIDIFIED PLASMA (PICTURE WIDTH IS APPROXIMATELY 300 MM).....112

FIGURE -79: ELECTRIC DISCHARGE BURN MARKS AT UG2 FRACTURE PLANE.....114

FIGURE -80: FRAGMENTATION DISCHARGE AND REMAINING CRACKS INSIDE THE 40-MM-THICK UG2 SPECIMEN.....116

FIGURE -81: PLASMA TRACE THROUGH A 30-MM-THICK MERENSKY REEF SPECIMEN AND REMAINING TENSILE CRACKS.....117

FIGURE -82: PLASMA TRACES THROUGH 56-MM-THICK KIMBERLITE 'A' SAMPLE…117

FIGURE -83: FRACTURE SEQUENCE OF 10 MM FOSCOR SPECIMEN.....118

FIGURE -84: HOUR-GLASS-SHAPED PLASMA TRACE THROUGH 30 MM FOSCOR SPECIMEN.....119

FIGURE -85: UNDESIRED FLASHOVER NEXT TO ROCK.....119

FIGURE -86: BLOWN-OFF, SMALL CARBON LEADER REEF FOOTWALL SAMPLE.….120

FIGURE -87: CAVITATION EVIDENCE FOR 35-MM-THICK COARSELY GRAINED GOLD REEF SAMPLE, ELSBURG FORMATION (SONY CAMERA).....121

FIGURE -88: RADIAL SEPARATION OF FRACTURED PARTICLES (SONY CAMERA)….121

FIGURE -89: RISING AIR BUBBLES (SONY CAMERA).....122

FIGURE -90: FLASHOVER TO AN EXTERNAL, METAL BOLT 123

FIGURE -91: 'MINING MOLE', BASED ON ELECTRIC ROCK BREAKING.....129

LIST OF TABLES

Page

TABLE -1: COMPARISON OF OPERATING CONDITIONS AND ENERGY LEVELS.....30

TABLE -2: IMPROVED RECOVERY WITH ELECTRIC ROCK BREAKING (AFTER HINDE AND JOOSUB, 1998).....39

TABLE -3: XRD ANALYSES 47

TABLE -4: XRF ANALYSES.....48

TABLE -5: SUMMARY OF GEOLOGICAL ASSESSMENT.....49

TABLE -6: FEATURES AND LIMITATIONS OF THE FZK ESWC EQUIPMENT.....64

TABLE -7: COMPARISON BETWEEN THE ENERGY PER PULSE OF POTENTIAL TEST RIGS.....69

TABLE -8: CALIBRATION FACTORS FOR OSCILLOSCOPE.....76

TABLE -9: POTENTIAL RISKS AND BENEFITS OF ESWC TECHNOLOGY.....125

NOMENCLATURE AND DEFINITION OF TERMS

(McGraw-Hill Dictionary, 1984)

AEC	Atomic Energy Corporation (South Africa)
CLR	Carbon Leader Reef specimen
Comminution	Breaking up into small fragments
CoMRO	Chamber of Mines Research Organization (South Africa)
D	Longest measured lengths of a fragmented rock specimen
d	Nominal particle diameter, based on its mass, and assuming a spherical particle shape
Dielectric breakdown	Breakdown that occurs in an alkali halide crystal at field strengths in the order of 10^6 volts per centimetre
Dielectric	A material which is an electrical insulator or in which an electric field can be sustained with a minimum dissipation of power
Euro-Pulse	UK-based company with pulsed-power test equipment
EPD	Electric Pulse Disaggregation [Aerie Partners' (1996) terminology]
Eskom	Electricity Supply Commission (South Africa)
ESWC	Electric Shock Wave Comminution
FZK	Forschungszentrum (Research Centre) Karlsruhe, Germany
K	Dimensionless correction factor for settling velocities
kc/s	Kilo cycles per second, unit used in pulsed-power equipment
Marx Circuit	An electric circuit used in an impulse generator in which capacitors are charged in parallel through charging resistors, and are then connected in series and discharged through the test piece by the simultaneous spark over of spark gaps (also known as a Marx Generator)

MR	Main Reef specimen
NETFA	National Electricity Testing Facility
Paroxysms	A volcanic eruption characterised by periodic explosive events
PGM	Platinum Group Metals
ppm	Parts per million
PSD	Particle size distribution
Pt	Platinum materials
Pyroclastic rock	A rock that is composed of fragmented volcanic products ejected from volcanoes in explosive events
R	Used by McNown and Malaika (1950) for Reynolds number
ROM	Run-of-mine rock, particle sizes from 0 to about 0,5 m
S	Sphericity, a measure to quantify how closely an uneven particle resembles the ideal sphere at S=1
SABS	South African Bureau of Standards
Tephra	Denotes all pyroclastic rocks of a volcano
Tore®	Registered trademark of Merpro Process Technologies for a water-driven slurry pump
TTL	Transistor Transistor Logic, circuit configuration for triggering other components
VCR	Ventersdorp Contact Reef specimen
WDL	Western Deep Levels gold mine
Wits	University of the Witwatersrand
XRD	X-Ray Diffraction (method of analysis)

XRF	X-Ray Fluorescence (method of analysis)

1 INTRODUCTION

As part of the ongoing research into novel, more effective ways of achieving primary rock breaking at the face, previous work by the Chamber of Mines Research Organization identified the potential of electric rock breaking (CoMRO, 1990). The application of high voltages across solid matter, which results in dielectric breakdown, is not limited to primary rock breaking at the face, but can also be applied to rock that is already broken. If high-voltage technology could provide high energy densities from compact equipment, it could result in an important innovation for narrow gold mining operations. Furthermore, the rock could be comminuted sufficiently, i.e. reduced in size by either crushing, milling or other means, to enable its removal from the stope by means of pipelines.

This dissertation evaluates the possibility of applying electric rock breaking as a secondary comminution process for various typical South African rock and ore body types.

2 BACKGROUND AND MOTIVATION

It is widely accepted that the single most important change that will increase the productivity of future ultra-deep South African mines will be the introduction of continuous, concentrated mining with significantly increased face advance rates (Haase, 1997). Various methods for breaking the rock from the face are constantly being investigated and reviewed worldwide.

Conventional rock handling methods used underground are not only hazardous with regard to injuries, but often lead to delays, which can result in loss of productivity. Therefore, hydraulic transportation for the continuous removal of reef from the face is worth considering as an alternative. However, the maximum particle size of the solids has to be limited to about 5 to 15 mm – suitable for introduction as a coarse slurry into a pipeline, which eventually enables hydro-hoisting.

In the past, many concepts for underground crushing and milling have been investigated with the aim of transporting the reef hydraulically or even hydrohoisting it. If conventional impact comminution equipment were to be used, this would require a major comminution plant to be installed close to the stope,

which is regarded as uneconomical. A lack of economy of scale also made the introduction of conventional satellite crushers non-viable (Kramers, 1986). The dust emission at the crushers would be a hazard to the work force and the over-production of fine particles would result in high pipeline pressure losses. The dewatering of such slurry underground would be expensive and impractical.

Preliminary laboratory comminution conducted overseas, using electric shock wave technology on rock samples submersed in water, indicated that in principle a relatively coarse reef product can be obtained (Edinger *et al.*, 1995). Due to inter-granular crushing, very few fine particles were evident and the particle shape was more blocky and less flaky than that of the particles typically produced by conventional impact crushing. The fast settling properties of the coarse solids would make this product ideal for use with a novel Tore pump system, which is preferably driven by hydropower (Chard *et al*., 1997). Such a pump system was installed at the CSIR in the last years of the 1990s for evaluation.

However, there are problems with the commercial application of these two technologies. Firstly, there is a lack of fundamental data, detailed understanding and knowledge of how, why and to what extent South African ore bodies can be disintegrated by electric shock waves created by direct discharge. No information is available on the power intensities of applied electric pulses and their practical implications.

Secondly, there is limited knowledge about the effect of this innovative comminution process on the hydraulic transportability of the product obtained with regard to critical deposition velocity, pipeline wear, pipeline pressure losses and the ability to dewater the discharged slurry after it has been hydrohoisted. If a way could be found to successfully transport the electrically broken rock hydraulically, this would offer an innovative means for the continuous removal of reef from the stope up to surface (Ilgner, 1997). The integration of electric rock breaking into the transportation process is shown schematically in Figure -1.

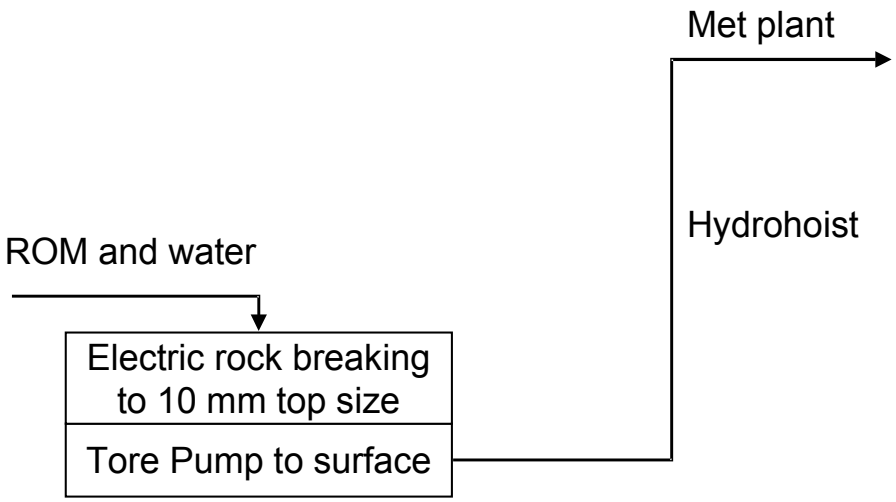


Figure -1: Envisaged integration of electric rock-breaking and pumping

In short, no systematic investigation into the rock disintegration process by dielectric breakdown has been conducted on South African reef, nor has its effect on the hydraulic transportability of the product been assessed.

3 AIMS OF THE STUDY

The aims of this study were as follows:

- Conduct a literature study on the historical development of electric rock breaking.
- Improve the understanding of the process of electric rock breaking.
- Correlate the properties of various types of rock with their suitability for electric rock breaking.
- Quantify the requirements for and assess the effect of electric rock breaking on different rock types by conducting test work, using a single discharge on a variety of rock types.
- Assess the feasibility of using electric rock breaking for underground mining (primary mining and secondary comminution).
- Assess potential applications for electric rock-breaking technology in mining.

4 METHODOLOGY

This section describes the methodology that was applied during the execution of the research. The initial assumption in 1998 was that electric comminution equipment would be purchased by the CSIR from the Forschungszentrum Karlsruhe (FZK) in Germany to conduct tests in South Africa and develop the technology further. The draft agreement, which was never signed due to financial constraints, is provided in Appendix A for reference. In the absence of equipment from FZK, the scope of the study now also includes an assessment of alternative equipment for use during testing, and the design and configuration of a test facility in South Africa. The chronological developments leading up to the initiation of this study are tabulated in Appendix B. The team members from South Africa and their role and contribution to "electric shock wave comminution" (ESWC), which was the phrase originally coined by CSIR, are listed in Appendix C. .

4.1 Literature Review

An assessment of the historical developments in electric rock breaking technology was undertaken to identify any fundamental principles and competence leaders in the world. The physical mechanisms of dielectric breakdown for rock breaking were described in earlier work on insulation failures.

Recent work in Germany by FZK quantified the importance of the electrical impulse rise time to ensure discharge through rock, rather than through the surrounding medium (oil or water). This information was used to configure the test rig in South Africa. Other researchers were less open about their equipment and operating parameters.

4.2 Assessment of Equipment Available Worldwide

During the contract negotiation phase, preliminary fragmentation tests at FZK in Germany were possible and thereafter the first rock fragments could be analysed in South Africa. The analysis included particle shapes and their effect on the particle settling rate as this was important for hydraulic transportation behaviour, and microscopic investigations.

FZK has developed the ability to conduct theoretical modelling of the circuits and the dynamic response of the circuit during discharge. This was seen as a major strength for optimum component specification and operational safety.

Wits University was identified as the most suitable collaborator for conducting the research and providing the necessary skills to design and operate a high-voltage circuit with fast ramp-up times. All the information gathered from the literature review, a visit by the author to FZK, and some photos provided by Peter Kramers (former CSIR employee) from his visit to Euro-Pulse in the UK were analysed to design a suitable test rig at Wits.

4.3 Test Work on Electric Rock Breaking

Various South African reef and rock specimens were prepared to specific geometries (8 by 32 mm) to enable the electric resistivity determination, using a specialised set-up at the CSIR for geophysical characterisation. This rock-specific property was then correlated with the breakdown voltage measured during the fragmentation tests.

Various types of high-speed photographic equipment were tested and utilised to gain insight into the explosive nature of discharge and fragmentation. This approach proved to provide valuable insight which assisted with the analysis.

In order to provide some repeatable reference performance data for the test rig, various water tests were performed, whenever possible. Some electrical components, such as the mechanical trigger box for the Marx generator, and the fine adjustment of the charge-up voltage, were improved as the test programme progressed.

Systematic testing of various rock types with different geometries was conducted with gold reefs, hanging wall and footwall specimens, platinum reefs, Kimberlite and Foscor samples, up to a maximum thickness of 56 mm for Kimberlite.

4.4 Analyses and Discussion

The ability of specimens to attract discharge through the rock and the field strength at which dielectric breakdown took place was used as a measure to determine the suitability of the specimens for electric shock wave comminution.

The resistivities measured prior to the fragmentation by electric discharge were correlated with the voltages at which electric field breakdown occurred, leading to dielectric failure and fragmentation. Broken fragments and the amount of fines generated were assessed to estimate the effectiveness of the discharge.

An analysis of the problems encountered during the test programme was done as a means of critically reviewing the applicability of this technology for the intended purpose of underground crushing of mined rock to enable hydraulic transportation. However, from the excellent fragmentation results of the highly mineralised gold reef specimens, a rough concept was developed of how, potentially, to use electric rock breaking as a primary mining method if various design challenges could be overcome.

5 LITERATURE REVIEW OF ELECTRIC ROCK BREAKING

Mechanical stresses can cause rock to break either by tensile cleavage fracture or by compressive shear fracture. Fracturing occurs when the actual stress system within a rock, which can be either compressive or tensile by nature, satisfies the appropriate criterion of failure. The stress field can either be statically or impulsively generated, an impulsive stress being defined by its extreme rapidity of application and brevity of duration. Many of the commercial methods of rock fracture depend on the initiation of compressive stresses.

When a rock is impulsively loaded, the mode of failure is directly influenced by the mechanics of shock wave propagation. In the case of explosive-based shock generation, a high-pressure compressive wave is released and travels through the rock mass. However, as rocks and other brittle materials are much stronger in compression than in tension, this compressive shock wave has a limited effect – only the material in direct proximity to the explosion will be crushed immediately. Nevertheless, the compressive wave is reflected at a free surface and returns as a tensile wave back towards the centre of the rock, thus weakening grain boundaries.

If the rock mass to be fragmented is submersed under water, the specific gravity (density) of the surrounding water is lower than that of the rock transmitting the shock wave. Thus, spallation or 'scabbing' can occur when the tensile stress is higher than the failure strength of the rock. When fracturing proceeds, energy is absorbed in creating new surface areas.

Parekh *et al.* (1984) claim that comminution efficiencies could be greatly increased if, instead of indiscriminately applying the breakage force to the entire rock mass as in a typical ball mill, new technology could be developed to focus comminution energy at intergranular boundaries. If this could be done, the mono-mineral grains would remain uncrushed as the comminution action would be more selective and would, in overall terms, be substantially more efficient. Kanellopoulus and Ball (1975), who experimented with thermal fracturing of quartzite to induce tensile fracturing, also advocated this approach in principle.

In the past, dielectric breakdown occurred only as a result of gradual ageing of large isolator components in the power distribution industry. During service, a

process known as ‘treeing’ developed slowly along preferential paths between the electrical contacts. Only when the treeing process was completed between the electrodes did an unwanted discharge take place, resulting in an unwanted sudden explosion of the dielectric material.

In recent years, experiments have been conducted with applying pulsed power to rocks with the aim of creating this preferential discharge path through the dielectric rock and thereby crushing the rock into smaller pieces.

Sarapuu (1973) points out that the ability to convert any electrical energy into mechanical fragmentation is the key to the successful application of electro-fracturing.

5.1 Classic Lightning Theory

The following information was obtained from *National Geographic’s* website on 7 January 2002.

“A lightning flash can happen within fractions of a second. During the discharge, the lightning flash superheats the surrounding air to a temperature five times hotter than the surface of the sun. Nearby air expands and vibrates, creating sound waves that can be heard as thunder. The lightning is created by the following physical conditions. The cloud bottom carries a negative charge. Positive charges may collect on the ground, buildings, boat masts, people, mountain tops or trees. A ‘stepped leader’ – that is a negative electrical charge made of zigzagging segments, or steps – comes partway down from the cloud. These steps are invisible; each one about 50 m long. When a stepped leader gets within 50 m of a positive charge, a ‘streamer’ (surge of positive electricity) rises to meet it. Then the leader and the streamer make a channel. An electrical current from an object on the ground surges upward through the channel. It shows a bright display called the ‘return stroke’.

“There are many different forms of strokes and some do not even touch the ground – they are called ‘cloud’ lightning. ‘Spider’ lightning crawls across the sky for up to 60 km.”

Figure -2 below shows some exceptional natural electric discharges. The photos were taken by Warren Faidley, (left), William L. Wantland (middle) and Jonny Autery (right), and were downloaded from *National Geographic's* website.



Figure -2: Electric discharges in nature (after National Geographic, 2002)

"The picture on the left shows a lightning flash which hit the desert of Tucson, Arizona. Film exposure was 5 min. Each flash contains about one billion volts of electricity. The middle picture shows the effect of treeing, which means that one channel can branch away into multiple sub-channels. The picture on the right shows a 20-m Sycamore tree, which is illuminated from top to bottom by a direct lightning strike. Although lightning often destroys trees, this tree in Alabama was reported to be thriving even 12 years after the event."

An indication of the immense power that can be released by an electric discharge in nature is shown in Figure -3.

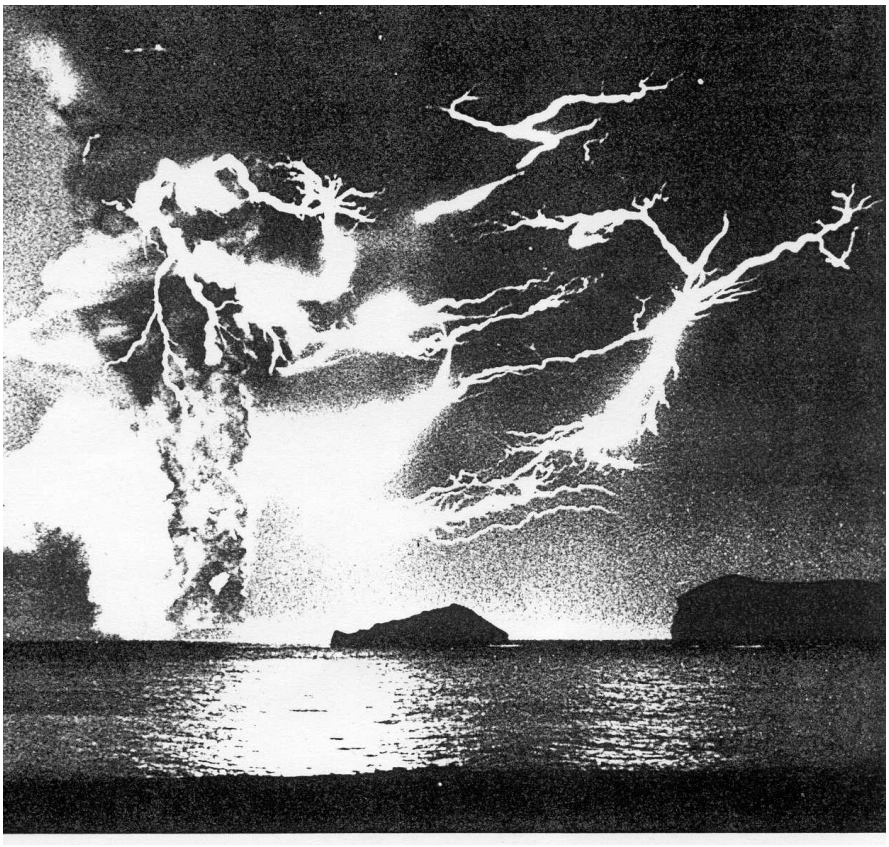


Figure -3: Erupting volcanic debris, illuminated by lightning during a thunderstorm (Thorarinson, 1964)

In the above-photographed event, submarine eruptions had been taking place for a few days before the photo was taken. It is reported that during the most violent tephra-producing paroxysms (i.e. an event in which volcanic products are emitted), the vertical column of molten rock actually made a physical connection between the sea's surface and the thunderstorm clouds. The tephra column, as shown on the left side of Figure -3, was ablaze with lightning flashes. This magnificent event was captured on 1 December 1963 near the Surtsey islands (Thorarinson, 1964). It demonstrates that electric charges use preferential paths for discharge. Here the atmospheric air was less conductive that the debris ejected from the volcano, which was probably semi-saturated with saline sea-water since the volcanic eruption took place under the sea. Photography is the only method that can 'capture' such a large phenomenon. No instrumentation could be applied to measure either the voltage or the current associated with an event of that magnitude.

However, research has recently been conducted in the USA in which special rockets (about 1 m in length) are launched into charged clouds with the intention of triggering lightning through the rocket, which is connected by a wire to the base station. Once the wire on the rocket has linked the electrical charges from the cloud to earth, the discharge power can be measured (source: DSTV programme).

5.2 Budenstein's Theory

The early theories about the dielectric breakdown of solids, which were developed by von Hoppe, were replaced by the theory developed by Budenstein (1980). The following sequence shows five individual stages which take place to enable and complete electric breakdown. Assuming good electrical contact between the electrodes and the rock specimen, free charges within the rock will polarise according to the electrical field applied. The rock (or dielectric) is intact and its insulation properties are undisturbed. The following five figures (Figure -4 to Figure -8) were taken from Le Sueur (1995).

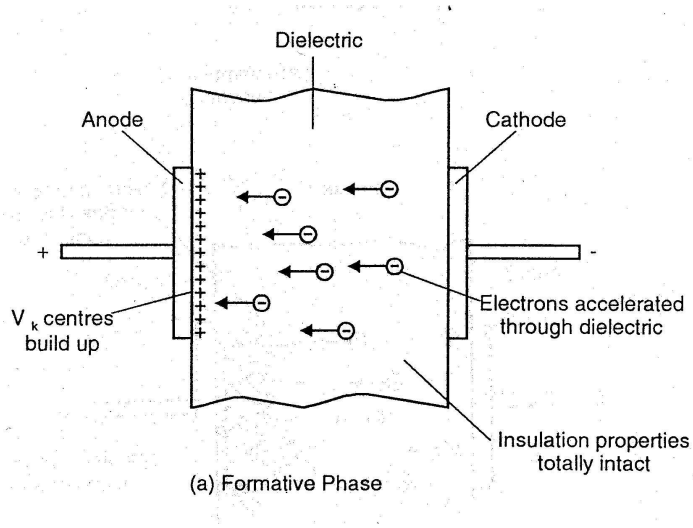


Figure -4: Initial, formative phase of polarisation

After the initial phase, field enhancements are created at bond defects at the anode.

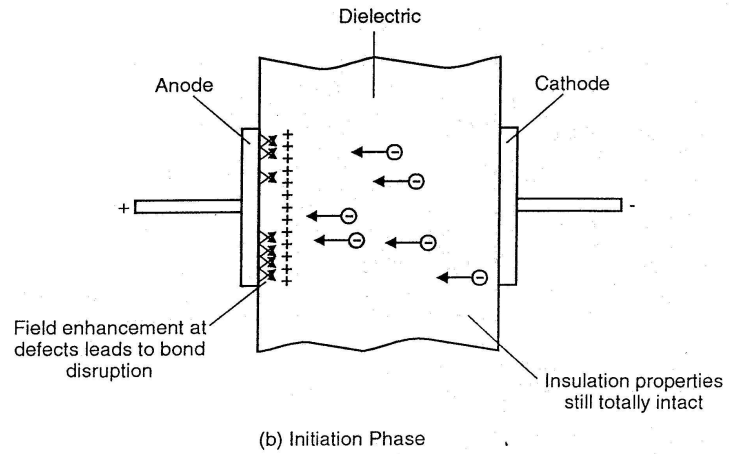


Figure -5: Field enhancements during initiation phase

Material bonds disrupt and the process of treeing starts. The trunks of the tree formation are charged with ionised material which will later grow into the plasma channel.

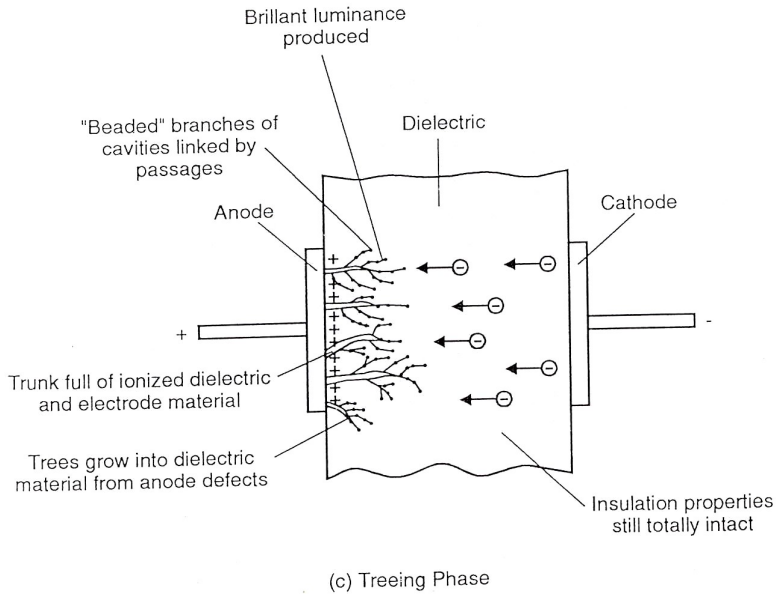


Figure -6: Treeing and luminance produced

Luminescence is starting due to treeing into the dielectric material from anode defects. The insulation properties are still dominant, but the physical properties of the solid matter (i.e. the particles) are changing.

As soon as a conductive channel with ionised material is created between the anode and cathode on opposite sides of the test material, the insulating (dielectric) properties fail. A current starts to flow and creates joule heating in the plasma, which creates pressure inside the 'return streamer'. This is the same physical phenomenon as was described above for when lightning hits the earth. However, due to mechanical confinement, the pressure creates tensile fracturing. The strength of the grain (particle) boundaries, as well as the material's micro-structure with regard to conductive paths and resistivity, will determine where the discharge takes place.

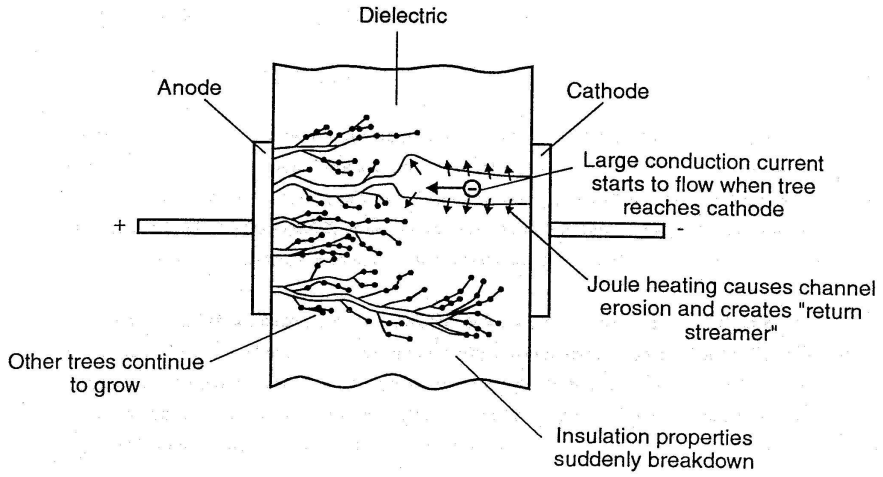


Figure -7: Channel enlargement and current flow

The amount of charge available and its rapid release from the energy store will determine the extent of plasma heating and damage. Also, the larger the contact area, the more channels can be created simultaneously.

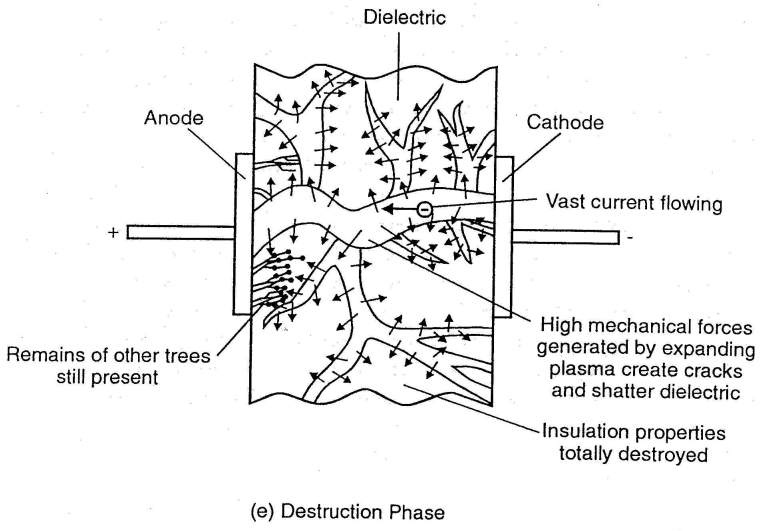


Figure -8: Expanding plasma and destruction

As the dielectric (rock) expands, the contact area between the electrodes and the rock changes and this may limit the time available for the transfer of energy into the plasma channel.

Although tensile stresses are created by the plasma, compressive stresses are also created due to shock waves, which reflect as tensile waves at the particle-to-water interface.

Meyers (1996) postulated three different generic types of mechanism for crack creation in solid matter due to shock loading. This is particularly relevant to the heterogeneous nature of sedimentary rock, even though the different causes of crack creation within the complex physical matrix of reef types are endless.

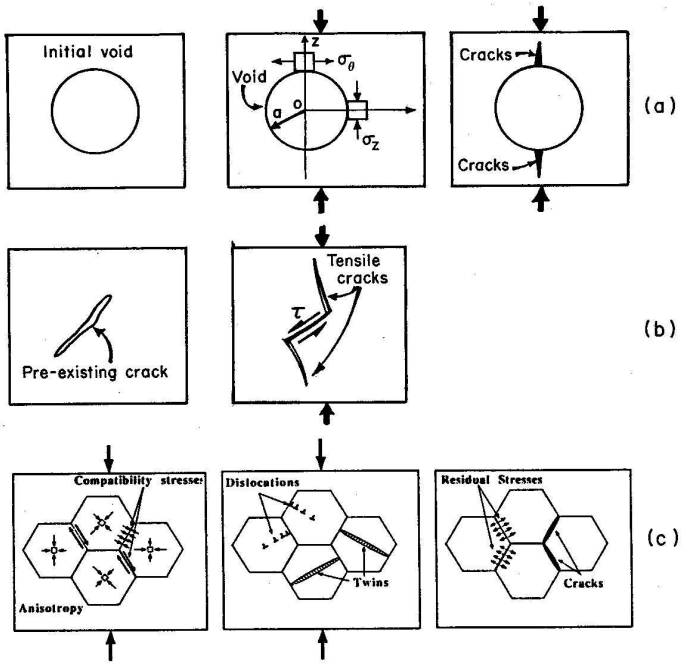


Figure 2.31. Schematic representation of different mechanisms of crack nucleation in ceramics subjected to compressive stress pulses; (a) nucleation at spherical void; (b) nucleation at elliptical flaw; (c) nucleation due to elastic anisotropy of grains.

Figure -9: Different crack creation mechanisms for vertical loading (Meyers, 1996)

Meyers (1996) explains that pores (voids) and grain boundaries are the main nucleation sites for new flaws. Thus, material with smaller grain sizes can exhibit greater damage under the same (mechanical) loading conditions. He describes three different mechanisms of crack nucleation, represented in Figure -9:

a) Existing spherical voids within solid matter, when subjected to compression, generate localised tensile stresses, orientated parallel to the load application.

b) Pre-existing cracks or ellipsoidal flaws under compressive load create shear stresses. These in turn create tensile fractures at the extremities of the elliptical flaw. If the tensile stress exceeds the tensile strength, permanent cracks develop.

c) Elastic anisotropy of polycrystalline materials can lead to incompatibility stresses at the grain boundaries, where softer and stiffer materials interface. After plastic deformation under shock wave (compressive) loading has occurred, localised regions of tension may be created once the stress pulse has passed. Repeated loading could eventually lead to separation along

those grain boundaries. In the rock to be tested, all the crack-creation mechanisms described above may occur in various mutations and to various extents.

5.3 Dielectric Measurements of Homogeneous Material

The measurement of the electric strength of solid matter requires carefully designed test apparatus to ensure good contact between the electrodes, as well as a specimen of defined thickness. Discharges have frequently occurred in weaker parts of the field, which is an undesirable event when determining a material's electrical properties (Whitehead, 1951). A set-up that ensures good electrical contact between the metal electrodes and the specimen is required (see Figure -10). It must also allow the electrical field to be focused within a narrow section across the specimen.

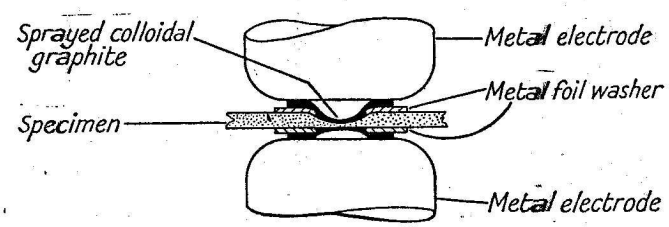


FIG. 2. Recessed specimen with electrodes.
(Austen and Whitehead.)

Figure -10: Accurate set-up for electrical breakdown tests (Whitehead, 1951)

5.4 High-Frequency, Dry Applications

The following sections provide a chronological review of published reports on the use of electric discharges to break rock.

According to Young (1961), secondary breaking tests with rocks were successfully conducted at the following institutes:

1. Montana School of Mines Electrical Laboratory in Butte, Montana, USA

2. General Electric's General Engineering Laboratory, Schenectady, New York, USA

3. Westinghouse Electrical Corporation's Radio Frequency Heating Laboratory, Baltimore, Maryland, USA.

The frequency range for the AC field was varied between 100 kilocycles/s and 27 Megacycles/s. Rock samples were heated by means of an oscillating field, which was induced by voltages between 4,3 and 6,8 kV. Single rock lumps of mainly low-grade dissedimentary copper ore were used. The electrode spacing was varied between 3 cm and 16 cm. It was reported that the resistance of the rocks varied substantially during the heating.

The working voltage was found to be critical as a minimum voltage was normally required to achieve physical fragmentation. The power consumption increased substantially with an increase in the working voltage, but the energy consumption decreased. The decrease in energy consumption was due to the reduction in the overall time needed for fragmentation. The fracture analysis was very difficult as various degrees of cracking were observed, which appeared gradually during heating. In general, it appears that the equipment was not powerful enough to generate energy levels sufficient to enable fracturing within seconds. Breakage was generally achieved within a few minutes, except for a large quartz crystal, which was not fractured. This selective fracturing provides an opportunity for sorting underground as the valuable minerals contained in grain boundaries could be liberated from the larger quartz pebbles.

It is interesting to note that Young (1961) reported the unsuccessful use of capacitor banks. The reason for the lack of success could be that the limited voltage was not able to drive sufficient current through the selected rock sample, i.e. sufficient in terms of its geophysical properties and geometrical size.

Kravchenko (1961) conducted comprehensive test work with high-frequency technology, also based on the phenomenon of thermal breakthrough. Again, electrodes were placed onto the rock (either a semi-conductor or dielectric), and

the heating resulted in a decrease in the resistivity of the rock. He reported that a temperature increase from 20 °C to 200 °C decreased the rock's resistivity from 40 W/cm to 5,2 W/cm.

Sarapuu (1973) designed a dozer-mounted electro-breaker to demolish large boulders in a quarry application, as shown below in Figure -11.

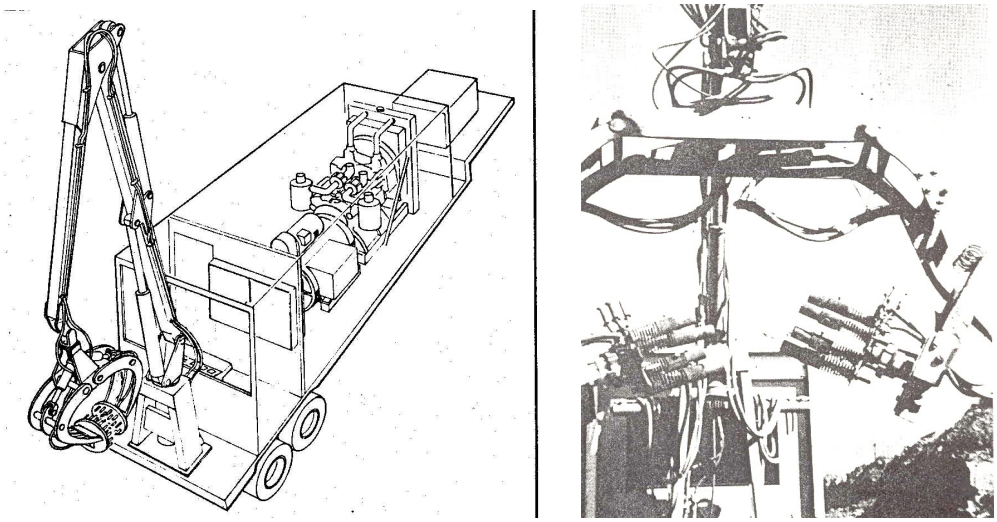


Figure -11: Truck-mounted boulder breaker for quarries (after Sarapuu, 1973)

A possible underground installation was conceived to look like the schematic in Figure -12 below.

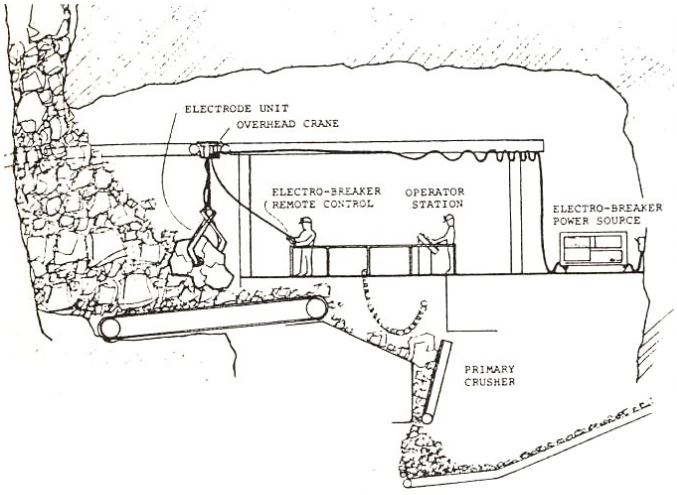


Figure -12: Potential underground application (after Sarapuu, 1973)

However, no such underground installation was ever done.

Segsworth and Kuhn (1975) added a DC pulse to fragment a rock lump finally by dielectric breakdown after the initial high-frequency heat treatment. They found that a critical voltage of about 4,5 kV was required for a 20-mm-thick marble to break down electrically. They concluded that after the rock had been weakened by the high-frequency treatment (which produced a conducting path), the capacitor discharge for the final single DC shot was vital to achieve fracturing.

This thermal heating concept was followed later by the addition of a single-pulse discharge to provide the necessary, spontaneous breaking energy. A simplistic circuit is shown below in Figure -13.

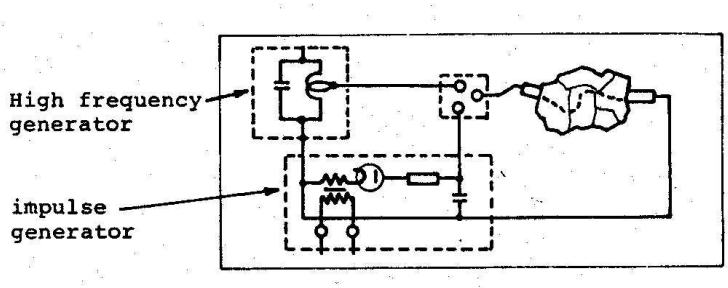


Figure -13: Additional, electrical impulse generator to break rock after thermal heating (Segsworth and Kuhn, 1975)

5.5 First Discharges with Submerged Specimens

Bergstrom (1961) provides a (Cold War, politically motivated) comparison of the developments relating to electro-crushing in the then USSR and the USA. Basically, it is claimed that Allis Chalmers had documented unpublished reports on electric comminution as early as October 1952, whereas Yutkin first published results in 1955.

A basic diagram of Yutkin's rock-crushing device is given by Maroudas (1967), and is shown in Figure -14 below.

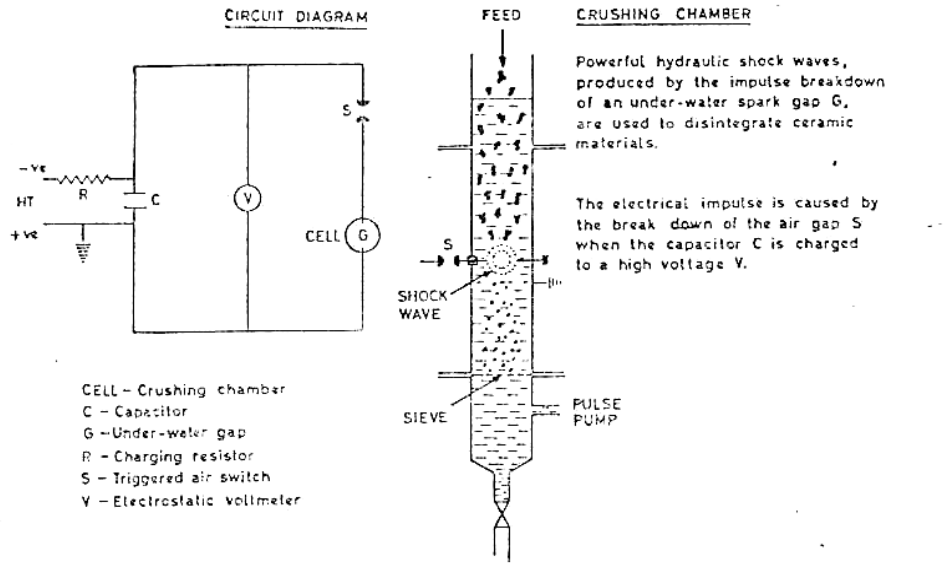


Fig. 1 Electrohydraulic crusher.

Figure -14: Yutkin's underwater crushing (after Maroudas, 1967)

A shock wave is created by the discharge in the water, not through the solid matter. Thus, the efficiency of the shock wave diminishes rapidly with increasing distances from its origin.

Figure -15 shows the crushing chamber of about 50 mm internal diameter, filled with water and rocks. The rocks are supported on a screen. The (+) electrode allows discharge along the centre of the chamber and allows the shock wave to expand radially. The screen ensures that only particles of a certain size report to the undersize section below the screen.

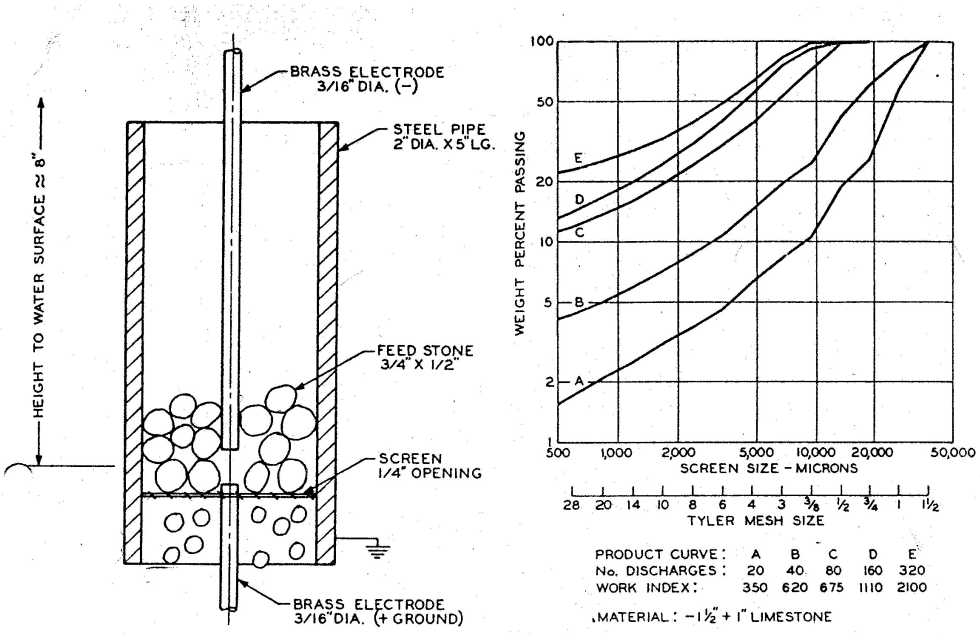


FIG. 5. UNDERWATER ELECTRICAL DISCHARGE of electrohydraulic unit shatters rock near electrodes.

FIG. 6. SCREEN ANALYSIS CHART shows products from an electrohydraulic experiment at A-C laboratories.

Figure -15: Underwater crushing (left) and particle size distributions produced (right) (after Bergstrom, 1961)

This equipment produced, from limestone samples with an initial size of 24 to 36 mm, particles comminuted to various degrees, depending on the number of discharges applied to the sample, which ranged from 20 to 320 to give product curves A and E respectively in Figure -15 above.

The top particle size of the curves shown above suggests that two different screen sizes were used, i.e. about 30 mm for coarse particle size distributions (curves A and B), and about 12 mm for curves C, D and E.

Although energy efficiencies improved with increased voltage, this technique was regarded as extremely inefficient, even when using a Marx generator, configured with series and parallel capacitors.

Since the crushing was done by loading batches of limestone, the gradual destruction of the rocks could be observed. After the first several discharges, no marked change in the appearance of the rock specimens was noticeable.

Andres (1976) suggested the first semi-continuous underwater crusher for the liberation of apatite-nepheline ore, as shown in Figure -16 below.

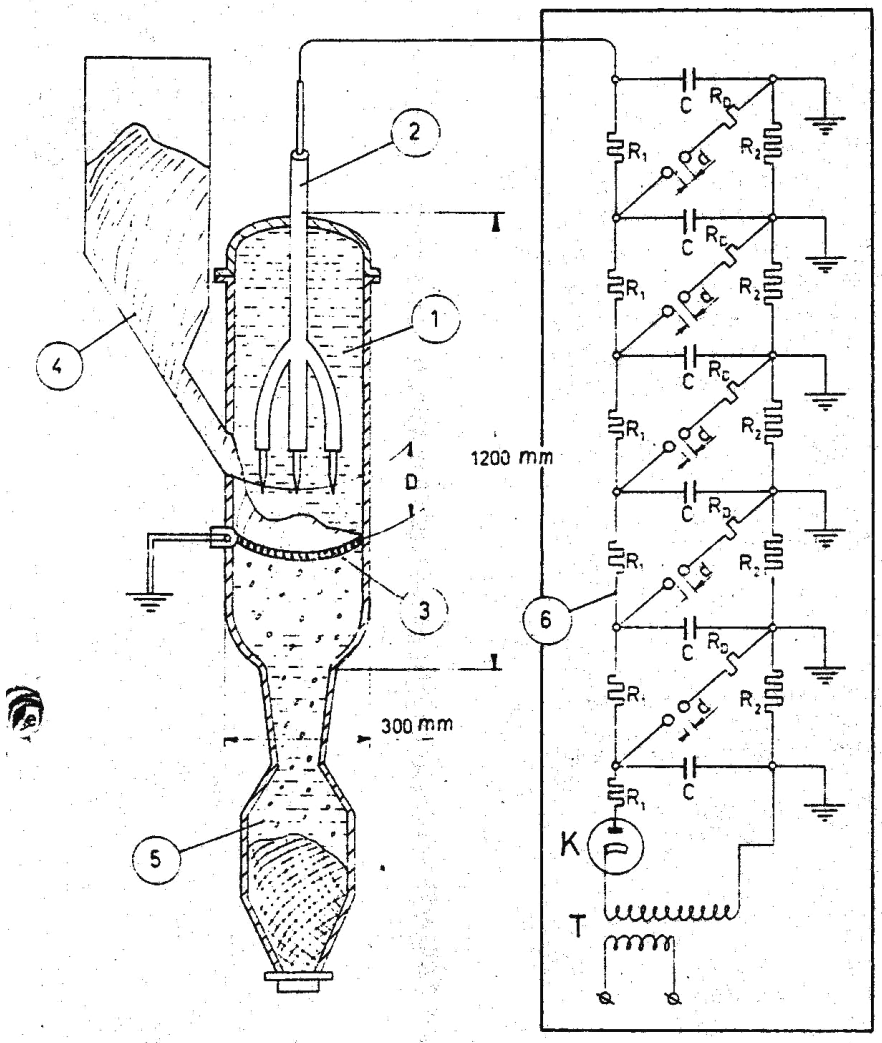


Fig.1. Experimental setup. 1, comminution chamber; 2, chamber discharger; 3, earthed electrode; 4, feed bin; 5, receiver; 6, pulse generator. T, set-up transformer (220/1000 V); K, kenotron rectifier; C, capacitors (0.03 μF each); $R_{1,2}$, charging resistors; R_D, damping resistor.

Figure -16: Underwater continuous crusher (Andres, 1976)

The above figure also shows a five-stage Marx generator used to create the pulsed power. The breakage mechanism appears to be mainly a result of discharge through water, but solid matter may also be in the discharge path, particularly on the left-hand side of the comminution chamber, where the feed chute is connected.

5.6 Power Consumptions

Young (1961) used high-frequency tests with granite material from Butte mine, which can be characterised as quartz monozonite. The energies consumed ranged between 3 000 and 7 000 kWs. Unfortunately, these energies were not related to the newly generated surface area, nor was a particle size distribution of the fractured rock provided. Terms such as 'good cracking' and 'mechanical rupture' are indicative rather than quantitative, thus the energy levels are only useful for appreciating recent advances using modern equipment. Young (1961) estimated that the power requirements for a high-frequency device for treating "several tons" would be in the order of 70 kW. He reported that the El Salvador copper ore broke instantaneously and violently into several pieces as a result of a single-shot discharge of 360 J, using a capacitor bank to drive a DC pulse, after a 2 min heating treatment at 500 kc/s. The parameters of the capacitor bank were 20 mF and a voltage of 6,0 kV, or alternatively 14 mF and a voltage of 14 kV. All tests were conducted in air. Spalling was reported at the contact of the electrode with the rock samples.

Kravchenko (1961) reported that large samples of hard iron ore (up to 15 tons) were broken up into three to four pieces within 3 min. His operating parameters were 250 kc/s with a voltage of 1,0 to 1,2 kV – similar to the ones reported by Young (1961) – possibly due to the higher conductivity of the rock types used. After the formation of the conducting channel (within 10 s), the actual current increased six to eight times to a ceiling of 60 A to 80 A, associated with a voltage drop to about 0,3 to 0,5 kV. Energy consumption was measured to be between 0,1 and 3 kWh, for lump masses of 0,5 tons to 10 tons, and breaking times of 5 to 180 s.

Sarapuu (1973) reported that a Russian rock-breaking machine was designed to operate in air with an electrical load of 100 kVA, a line voltage of 6 kV, and a specific energy of 4,4 kWh/m^3 (15,8 J/cm^3).

5.7 Rock Types Used in Previous Studies

Quartz and other silica minerals have a high electrical resistance and a low inductive capacity, and are thus less affected by magnetic fields. Ferro-magnetic minerals, such as magnetite and hematite, absorb electro-magnetic energy when placed in a rapid changing induced magnetic field. Exposure to high-frequency

excitation will heat these materials intensively and fracture stresses will be created inside the rock.

Kochanowsky (1966) mentioned that when two capacitor plates are used to apply a high-frequency field, heat is generated as a result of the mutual friction between polar molecules as they rotate in the direction of the changing electrical field in the rock. However, the degree of heat and stresses induced depends on the mineralogical composition, the elasticity and the strength of the sample as a whole, and in particular on the grain boundaries and their competence to glue various grain structures together.

The (homogeneous) shale sample used in Young's (1961) experiments broke with explosive violence. The sandstone samples in his experiments broke along grain boundaries.

It is reported that Kravchenko (1961) broke iron ore using a high-frequency method and a capacitor bank. The discharge was through a current-conducting channel that had formed in the rock. The rock types mentioned are ferruginous quartzite, and magnetic and hematite iron ores.

Bergstrom (1961) reported the use of electro-hydraulic crushing techniques to assist with drilling holes into concrete, granite and iron ore. Data on the equipment and performance are unfortunately very limited.

5.8 Black Granite Test Series

The only detailed study was published by Andres (1989). A total 275 South African granite samples were crushed in the UK under variable electrical field and energy conditions. All specimens had an area of 40 by 40 mm, and varied in height from 20 to 60 mm.

Figure -17 shows three areas resulting from all 275 tests, after normalising the height of the various specimens. The points shown in the form of white triangles correspond to pulses causing successful mechanical fragmentation (above line 2), which was the intention of the tests. The points shown in black circles correspond to pulses causing sudden electrical breakdown through the rock, but where mechanical failure is limited to damage within the rock, i.e. the formation of cracks, but no fragmentation (area above line 1). The black triangles

correspond to test parameters (voltage applied per length of sample and energy dissipated per length of sample); no sudden breakdown occurred, but nevertheless the capacitors discharged relatively slowly. All energy was converted into heat only.

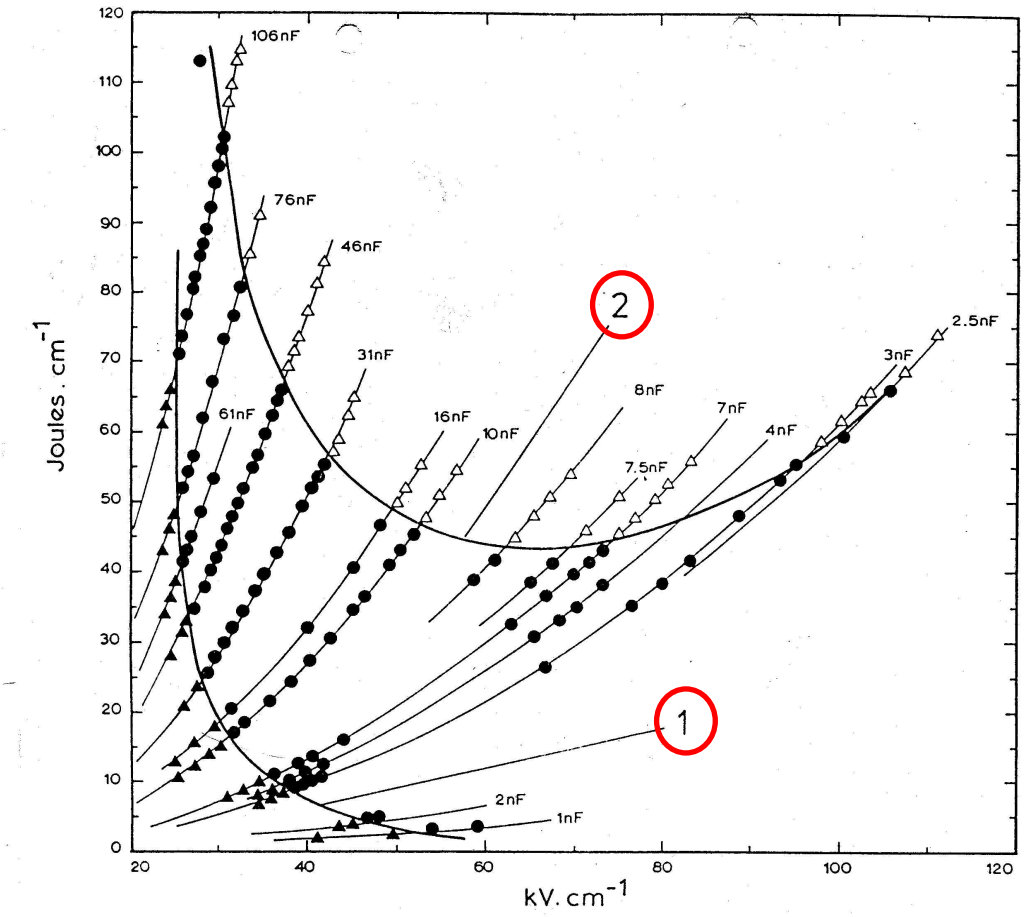


Figure -17: Test results from single shots with fine-grained black South African granite (Andres, 1989)

The distinction between gradual discharge (3) and breakdown through rock (2) can apparently be made from analysis of the voltage and amperage traces on the oscilloscope, as shown in detail in Andres' paper (1989). This chart is the best presentation of a comprehensive test programme with **one** relatively homogeneous rock type.

The possibility of finding an optimum electric circuitry that would produce the minimum energy absorption by granite-type rock at the optimum applied electrical field strength was the basic motivation for test work in South Africa with

different South African rock types. However, in order to find that optimum, a large number of test parameters had to be covered.

The indications from test work are that spalling due to shock waves generated within the rock as a result of electrical breakdown plays a major part in comminution. Of particular interest could be the separation by spalling of the larger, much tougher quartz pebbles from the valuable ore.

5.9 Electric Discharge Paths

In early trials of electric shock wave comminution (ESWC), equipment was developed to generate electric discharges through water (plasma channel), which resulted in shock wave propagation towards the rock. However, most of the energy was reflected at the water/solid interface.

Improvements in the generation and transmission of pulsed power in more recently developed equipment have made it possible to increase not only the strength of the electrical field obtainable between the electrodes, but also the rate of rise of the high-energy pulse.

During the explosive discharge through the rock, extreme temperatures and pressures are obtained, which result in the generation and propagation of shock waves. When reaching the solid-to-water interface, most of the energy is reflected back into the originating medium, i.e. into the rock itself. This reflection provides a second loading, which in turn can cause fracturing at grain boundaries after weakening from the initial shock wave.

In the case of discharge through rock (explosive mode with tensile failure), the majority of the energy remains inside the solid rock. The shock waves initially cause compressive stresses within the rock, which are reflected at the rock-to-water interface, and are returned as tensile expansion waves. Depending on the morphology of the rock, this results in the nucleation of micro-cracks, which weaken the overall tensile strength of the rock.

Final disintegration of the solid rock is achieved by a complex combination of spalling on the outer edges of the rock and tensile failure due to the plasma pressure generated inside the rock in selected channels.

Figure -18 below shows two options for the discharge path. If the discharge passes through the water instead of through the rock, inefficient comminution takes place as only an external shock wave is sent towards the rock.

If, however, the rate of rise of the high-energy pulse is very steep and the electrodes are located favourably close to the rock, the dynamic breakthrough strength of the rock becomes lower than that of the water. For this reason, the preferred discharge path would be through the rock and not through the water. This is referred to as 'direct comminution by explosion'.

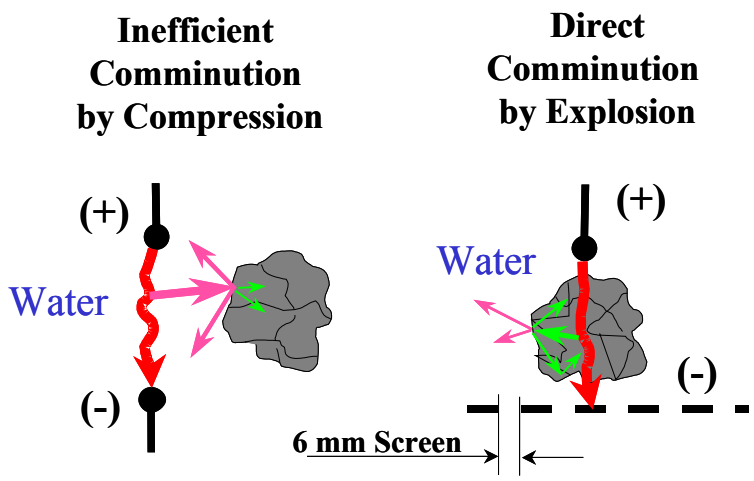


Figure -18: Differences between indirect and direct comminution

The figure also shows a 6-mm-screen used as the cathode. This prevents any oversized particles from gravitating to the next process stage.

The breakdown strength of oil, water, rock and gas depends on the rate of rise of the applied voltage and the breakdown delay, as shown in principle in Figure -19. Naturally, while the electrical field is ramping up, no breakdown occurs. For rock submerged in water, the delay during ramping up is critical as this will determine whether the discharge goes through the water or through the rock.

The water curve in Figure -19 drops at a larger gradient than does the rock curve. The curves cross at a certain breakdown delay time. This delay is in the order of 0,5 µs or shorter (Edinger *et al.*, 1995). Figure -19 below shows that if the rise time is fast enough to reach the electrical field equivalent to the breakdown strength, the discharge must necessarily go through the rock and not

through the water. Fragmentation will therefore take place in the 'explosion' mode and not in the 'compression' mode.

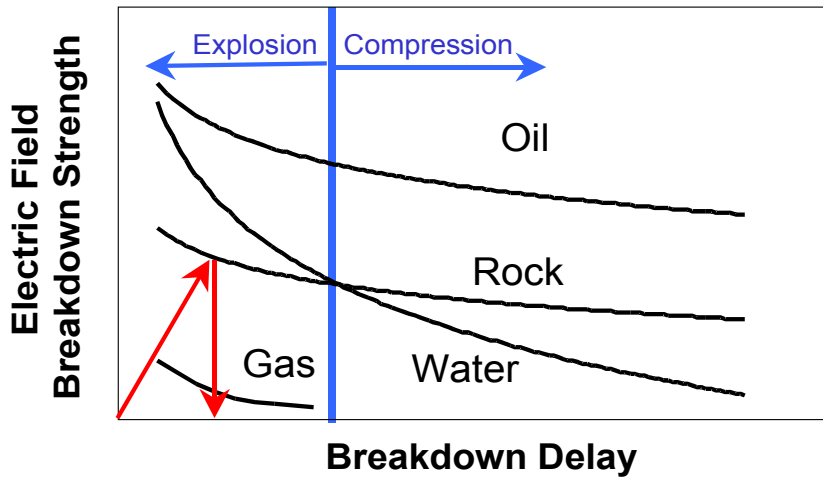


Figure -19: Schematic of breakdown strength vs. delay

Edinger *et al.* (1995) published preliminary data to quantify the range of electrical breakdown strength, as well as typical breakdown delay times. Figure -20 below provides some measured data which show that the steeper the rate of rise, the more likely it is that the discharge path will go through the rock, and not through the water.

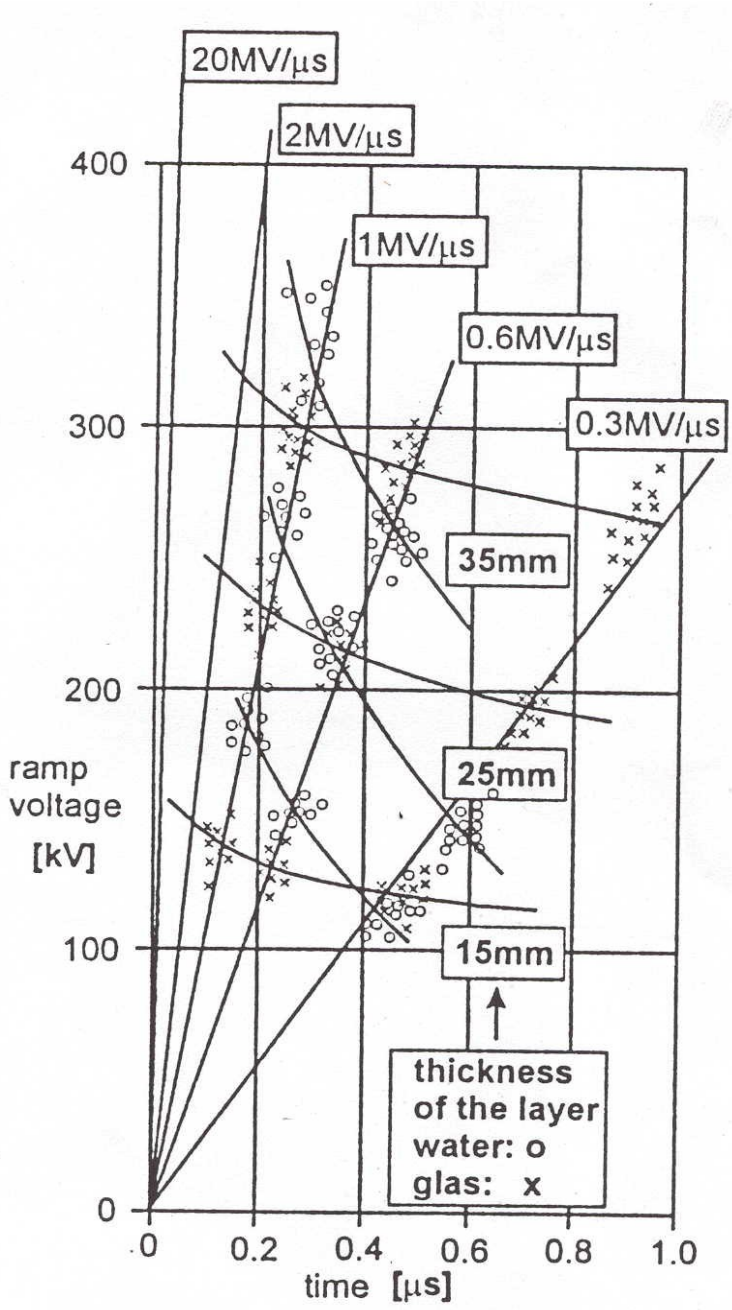


Figure -20: Breakdown curves for water and concrete (Hoppe et al., 1998)

The graph indicates enormous voltages in the order of 500 kV, associated with a 2 MV/ms rate of rise time, for relatively small gaps of only 35 mm.

The implications are that the application of this technology for primary rock breaking will be limited to small-sized broken product produced from the face. For man-less stope technologies, this feature may, however, provide hydraulically

transportable product sizes, directly at the face. This aspect needs to be periodically reviewed as other technologies and concepts are identified.

Table -1 summarises the difference in energy efficiency between comminution by compression and comminution by direct discharge mode.

Table -1: Comparison of operating conditions and energy levels

	Compression (Indirect method) Discharge through water	**Explosion (Direct method) Discharge through rock**
Voltage	20 kV	250 kV
Current	100 kA	6 kA
Pulse duration	1 to 10 μs	0,200 μs
Energy per pulse	6 to 10 kJ	0,2 kJ

The table indicates the benefit of increasing the voltage and reducing the current to achieve an overall reduction in the energy used per pulse for the direct discharge method.

Although discharge through rock is definitely the superior, more energy-efficient mode for comminution, practical solutions have to be found to minimise the water gaps between the electrodes and the rock. **NB:** This technology appears to be very suitable for the disaggregation of concrete (original Russian full-scale application) as mostly rectangular structures provide parallel surfaces with constant distances between the anode and cathode. This allows direct contact of the electrodes with the concrete in such an operation.

5.10 Summary

The electrical breakdown of solid matter was initially studied with the aim of improving insulator performance and reliability. The process of treeing in insulator materials, which takes place over years, can be accelerated if higher voltages are applied for a fraction of a second. This can create explosive fracturing by creating a high-pressure plasma inside the solid matter, i.e. the dielectric rock.

Instead of using air or oils as insulating media around the rock specimen, water is recommended. This bodes well for the hydraulic transportation of broken rock and provides superior insulation properties to those of air or gas.

Marx generators appear to be the most suitable pulsed power source. The most reliable data on breakdown delay times and field strengths, using advanced test equipment, were published by Forschungszentrum Karlsruhe (FZK) in Germany. Another detailed evaluation on black granite rock was published by Andres (1989), who identified power optimums, as well as a quantitative ranking of the extent of fragmentation.

In order to identify suitable, existing rigs for conducting test work with various types of South African rock, an assessment of currently operational test rigs was conducted; this is described in Chapter 6.

6 ASSESSMENT OF POTENTIAL RIGS AND INITIAL TESTS

6.1 Functional Test Rigs Outside South Africa

In the absence of readily available local test facilities for pulsed power rock breaking and in view of published data from overseas test rigs being available, the possibility of using those rigs was assessed. In due course, it transpired that a local rig would be the most desirable option for the test work. This assessment of test rigs therefore also provided pointers on what would be required for a local set-up, as described later on.

6.1.1 TZN, Germany

This company uses compressive shock waves through water to fragment solid matter. Only limited correspondence took place as no further interest from their side was evident. The rig layout is shown below in Figure -21.

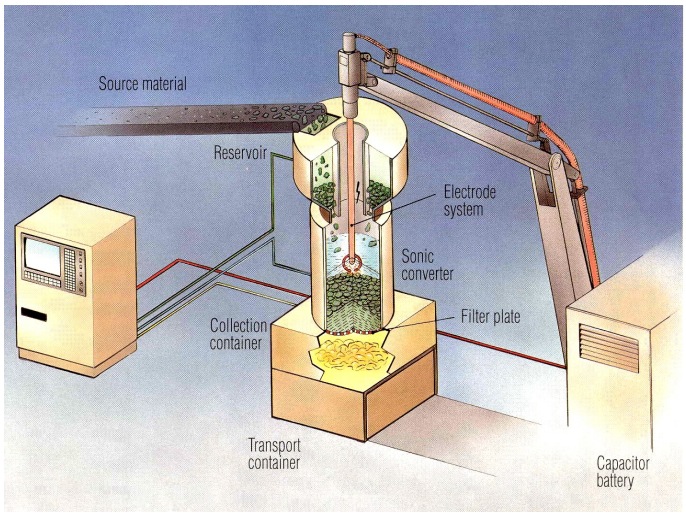
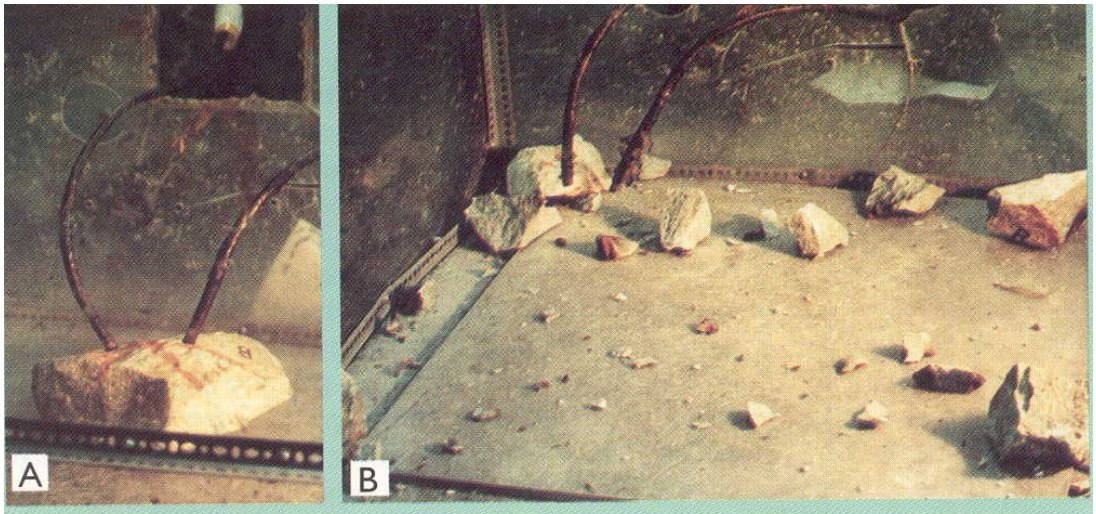


Figure -21: Artist's impression of TZN's comminution rig

It appears that the rig is a small laboratory-based set-up. The operating principle is similar to the ones described later. It is not clear whether or not two stages are involved. It looks as if the upper chamber has a grid interface with the lower chamber, but it is not clear what causes the rock to pass the screen. In the lower chamber, shock wave propagation through water is the method of destruction. The company used to be associated with the development of military equipment and is now tying to earn revenue by selling previously acquired know-how.

6.1.2 IEEE (Switzerland)

Little technical information was found about the preliminary test work on South African rock, commissioned by the Chamber of Mines Research Organization (CoMRO) in the late 1990s. Low energy consumptions were indicated, but not quantified. The following two photos (Figure -22) were published in CoMRO's Annual Report 1990, and show fragmentation by electric discharge.



Electric rockbreaking (pulse of 5 kJ) being tested on a sample of Carbon Leader Reef. a) Before the test. b) After the test.

Figure -22: Fragmentation of Carbon Leader Reef (CLR) (after CoMRO, 1990)

It appears from the photos that the rock was not submerged in water. Surprisingly, the rise time must have been extremely fast to avoid discharge through air. Again, all the details of the test work and the claims with regard to benefits are somewhat clouded with secrecy and by incompletion.

6.1.3 Aerie Partners (USA)

Aerie Partners have developed and built, in collaboration with Physics International, a mobile Electric Pulse Disaggregator (EPD), suitable for batch samples in the kilogram range. It has been successful in the liberation of gemstones. It is claimed in the company pamphlet that the unit concentrates ultra-short, high-power bursts of electrical energy along grain boundaries. The resulting high stresses in the rock cleanly fracture ore along the rock-to-

gemstone boundaries. It is claimed that it creates peak electrical power sufficient to cause electrical breakdown in normally non-conductive rock and yet draws average power comparable to that of conventional crushing and grinding units. A recent Mintek study (Hinde and Joosub, 1998), however, using Aerie equipment, found that with increasing fineness of the product, power consumption increased exponentially to uneconomical levels, and would be significantly higher than for conventional comminution! A schematic of the mobile crusher is shown in Figure -23 below.

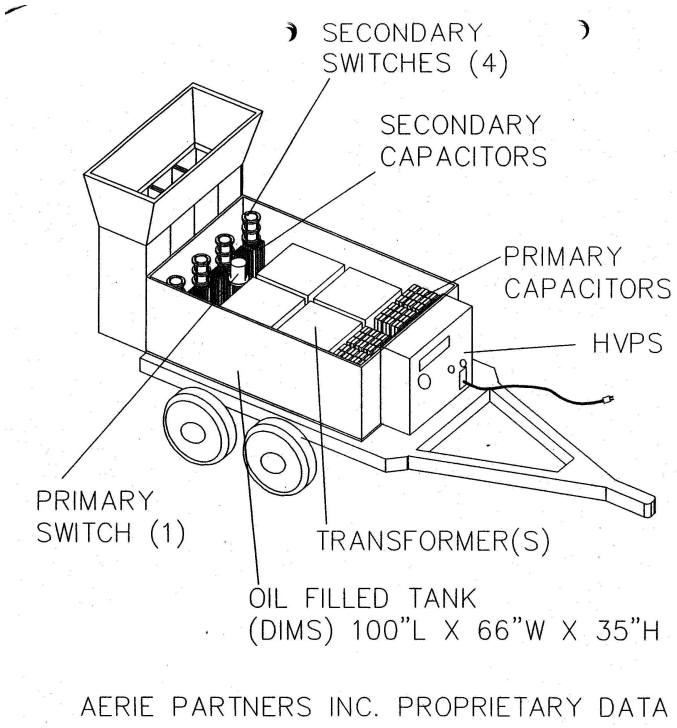


Figure -23: Aerie Partners' mobile rig

The major difference between this technology and the technology used by Euro-Pulse and FZK is that instead of using a focused point-discharge as an electrode, Aerie uses two charged plates, which are rigidly positioned at a fixed angle towards each other. Figure -24 shows the arrangement in principle.

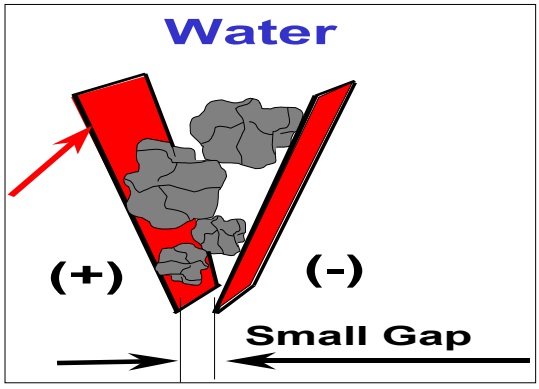


Figure -24: Aerie's rock-breaking chamber

A significant advantage of the plate-based design is the guaranteed elimination of any water gap between the charged electrodes, or plates, and the rocks. The latter will always gravitate until they are wedged in between the plates. However, the reduction ratio is small, and plate wear may be significant.

Like the other institutions, Aerie Partners also claim that breakage occurs between grain boundaries, as shown in Figure -25 below.

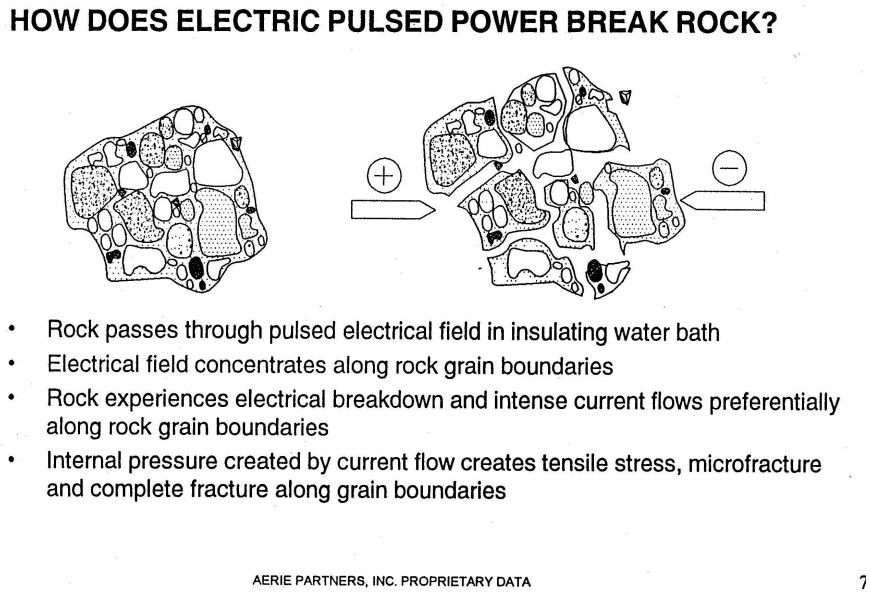


Figure -25: Grain boundary breakage by Aerie EPD unit (Aerie Partners, proprietary data)

A conceptual layout for a production plant is shown in Figure -26.

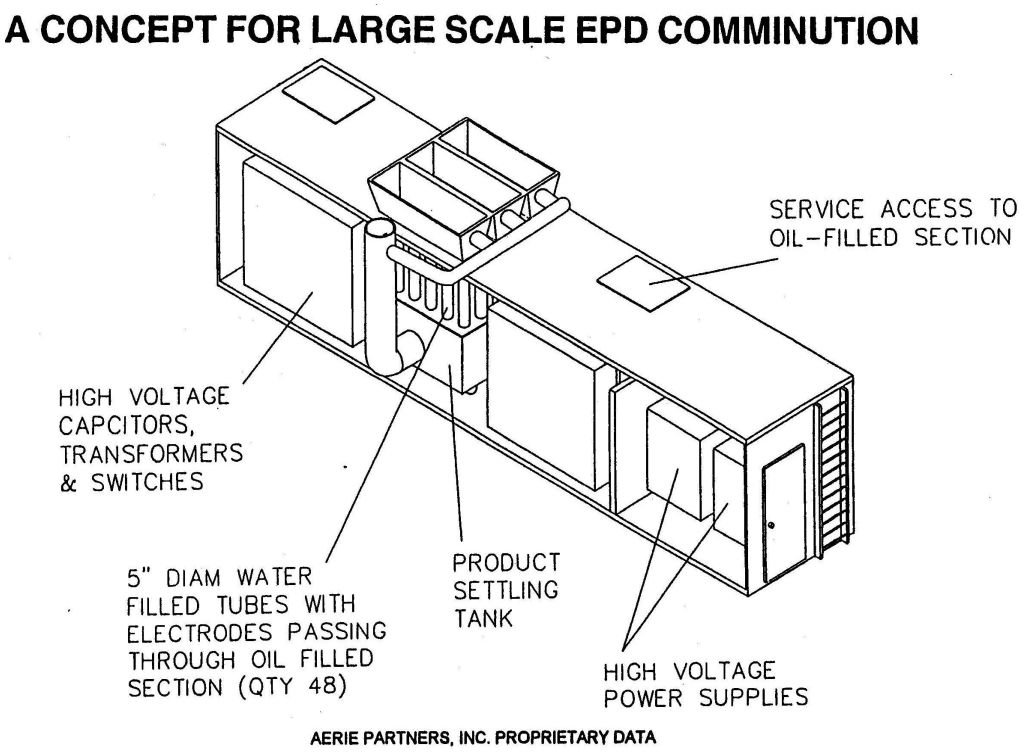


Figure -26: Concept for a large-scale comminution plant (Aerie Partners)

Unfortunately, no convincingly practical industrial plants, able to process a continuous stream of primary crushed materials, have yet been implemented successfully.

The detailed layout of the comminution chamber includes a circulating water system. The conceptual batch discharge of broken rock with water onto a dewatering screen is shown in Figure -27.

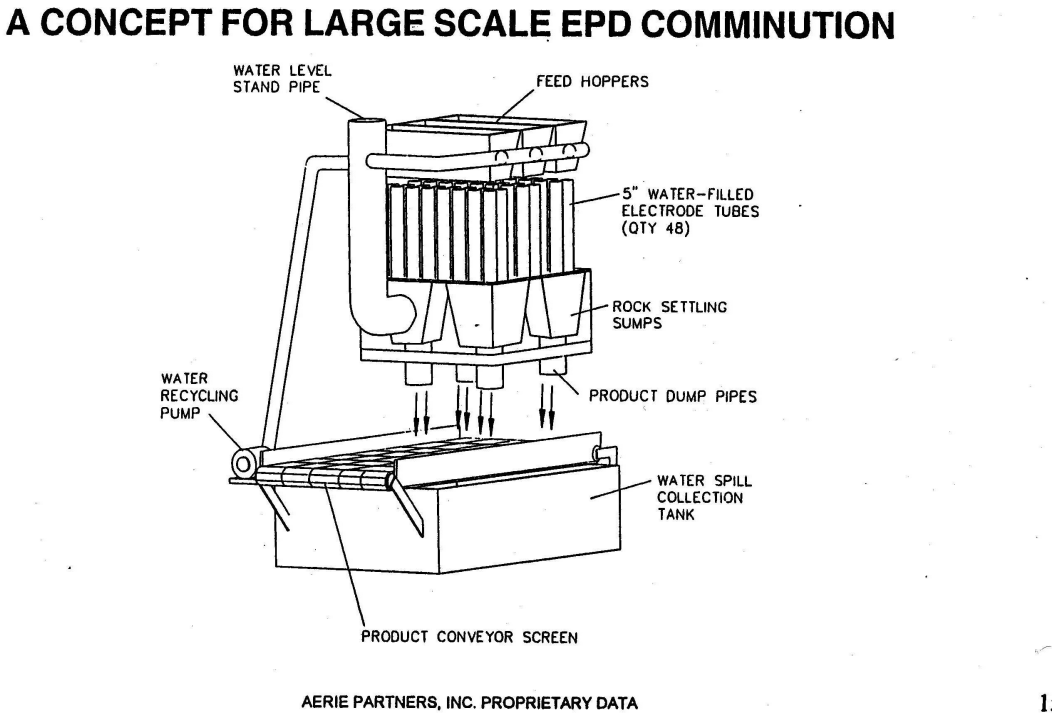


Figure -27: Batch discharge onto screen (Aerie Partners)

The screen size will be problematic: if it is too fine, it will not separate the discharged solids from the water, but if it is too coarse, the ultrafine particles, which supposedly contain all the value, will settle in the water reservoir below. Eliminating the dewatering process altogether, and gravity discharging directly into a Tore® pump vessel, could be considered for underground hydraulic transportation in the future.

For single-shot rock-breaking evaluations, as proposed in this study, the plate-based design is inferior to Euro-Pulse and FZK's rig configurations.

Increased recovery

The EPD test work at Mintek quantified the beneficial effect of the preferential liberation of gold when using Aerie's EPD technology. The various ways in which gold is associated with other matter were provided by Hinde and Joosub (1998) and are shown in Figure -28 by way of illustration.

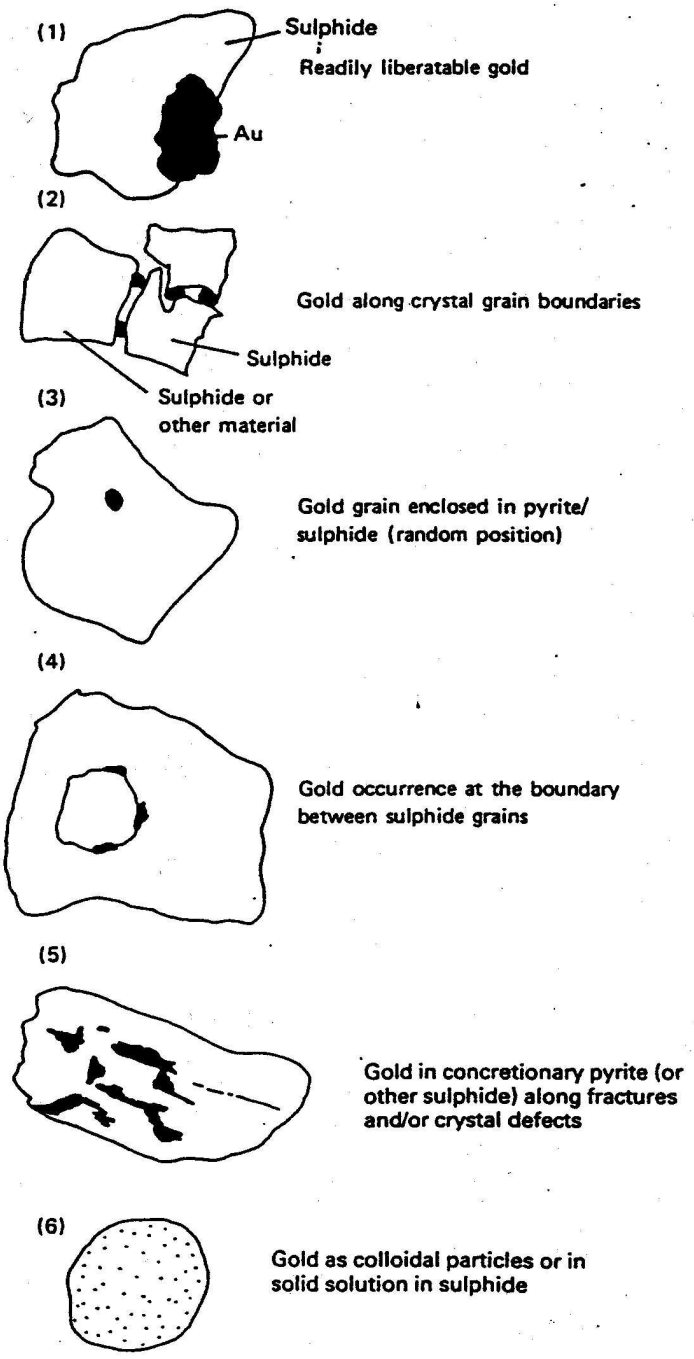


Fig. 2.13 — Gold associations with sulphide minerals.

Figure -28: Various gold associations with host rock

The schematics (4) and (5) in the above figure resemble closely the elliptical flaw shown in Figure -9 and emphasise the potential beneficial effects of electric rock breaking with shock waves.

Table -2 compares electric shock wave comminuted (ESWC) samples with crushed samples of a similar head grade. There appears to be a significant improvement from about 46 to 83 %.

Table -2: Improved recovery with electric rock breaking (after Hinde and Joosub, 1998)

Sample	**PSD %-75 µm**	**Head Calc. g/t**	**Recovery [%] Conc.**
ESWC 1	19,8	5,3	80,0
ESWC 2	19,8	6,2	86,6
Crushed 1	11,7	5,7	44,8
Crushed 2	11,7	5,5	48,0

However, a more realistic comparison of the net benefit would be to compare it with the old recovery after milling, as that would be the typical process. With ESWC treatment, the residence times in the mill may be shorter. It is expected that the large difference in recovery mentioned above will be significantly reduced after both samples have been milled.

6.1.4 Euro-Pulse (UK)

The batch-operated plant at Euro-Pulse (owner: Dr Richard Bialecki, London) provides reasonable voltage and current-recording equipment. This would enable a systematic test programme to be conducted to assess the suitability of different reef and waste types on a relative basis in order to identify the key mineralogical features required for energy-efficient comminution. The equipment is similar to the Franka-0 batch plant (see Subsection 6.2.1) as it can only be operated in single-shot mode. Figure -29 shows the current and voltage signals of a typical discharge though a small rock sample.

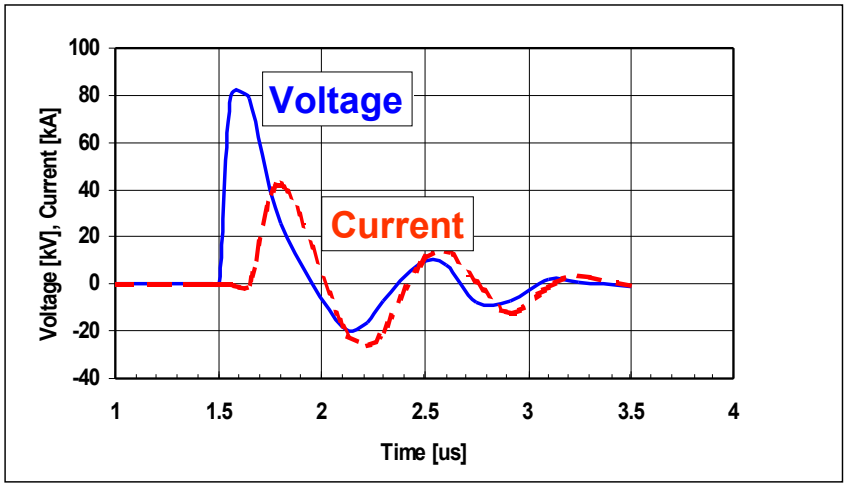


Figure -29: Typical voltage and current signals during discharge (Euro-Pulse set up, after Kramers, 1997)

The graph shows clearly that as soon as the current starts to flow, the voltage breaks down, releasing all stored energy in a single pulse. Based on recent test work at Wits, the above signals are assumed to be smoothed or filtered as they are very idealistic. However, the signal magnitudes were used to specify the expected signals for the local test rig.

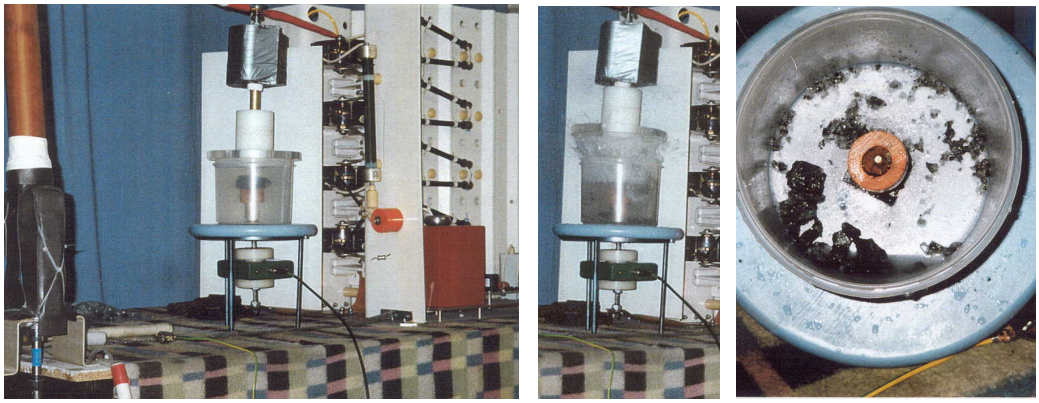


Figure -30: Euro-Pulse: Rock loaded (left), explosive lifting of lid, fragments (right)

The set-up (Figure -30) is very rudimentary, with the Marx generator visible at the back. The scale of the instrumentation appears to be suitable for single shots. It is believed that this instrumentation was used for the various investigations by Andres and Bialecki during 1976 and in the late 1980s (Andres and Bialecki, 1986).

During visits to Euro-Pulse by Kramers, some preliminary test work on reef and waste samples was done. Kramers (1997) stated in his report on the visit to Euro-Pulse that it took about five times more energy to break the waste compared with breaking reef. Unfortunately, the experiment was done with hand-picked rock samples, which were not machined to have a known geometry or mass. Also, the waste or reef types were not specified, neither was the extent of fragmentation.

A general problem with reported electric rock-breaking performances (except Andres, 1989) is the missing link between energy input and extent of fragmentation. To quantify the extent of fragmentation, careful measurements of the new surface areas created by fragmentation, and the strength of the material before fragmentation, would need to be made. Since this quantification is rather difficult and tedious, the technology cannot readily be compared with conventional crushing and milling processes on economic bases and energy consumption.

6.2 Forschungszentrum Karlsruhe (FZK), Germany

Between 1996 and 1999, many CSIR personnel visited FZK in Karlsruhe, Germany, to gain first-hand insight into the progress and development of the electric shock wave comminution equipment. Negotiations to purchase a test rig for South Africa failed due to commercial constraints. However, the insight gained enabled and justified the conceptualisation and performance of test work in South Africa, using local equipment and developing local competence.

Due to substantial contributions by the German Government, and the experience gained in pulsed-power energy applications in general, the FZK-based equipment appears to be the most advanced for technical evaluations and testing.

A strong advantage of FZK is their ability to model the electric circuit, which would enable realistic up-scaling to larger industrial plants, based on performance measurements on a smaller scale.

It is assumed that substantial co-operation on other FZK-based projects requiring pulsed-power technology will be possible in the future.

6.2.1 Batch rig

Based on a Russian prototype design, the Franka-0 batch plant was configured using a Marx generator and conventional capacitors. About 2 kg of rock can be loaded at a time into a water-filled comminution chamber. The rock is supported either on a screen of variable size (1 to 6 mm gap size), or on a blank, closed bottom. The schematic below (Figure -31) shows the batch equipment in principle, with the comminution chamber above the collection sump. Once started, pulses are shot repeatedly at about 5 Hz until the load is fragmented.

The two most significant disadvantages of this batch equipment are (i) that it is not configured to be operated in single-shot mode, and (ii) that only limited instrumentation is available to monitor the actual power consumption and pulse energies. FZK was not prepared to improve the instrumentation of this equipment.

Any pulse discharge (through water or rock) may blow the rock samples away from the electrode and, as a result, any subsequent discharge will be uncontrolled and accidental, and may, or may not, go through the rock sample. However, if the sample is exposed for a sufficiently long time in the chamber, the entire rock sample will be completely comminuted and can be analysed for mineral-liberation potential, particle size distribution and particle shape. Thus, the equipment is only suitable for limited, indicative test work.

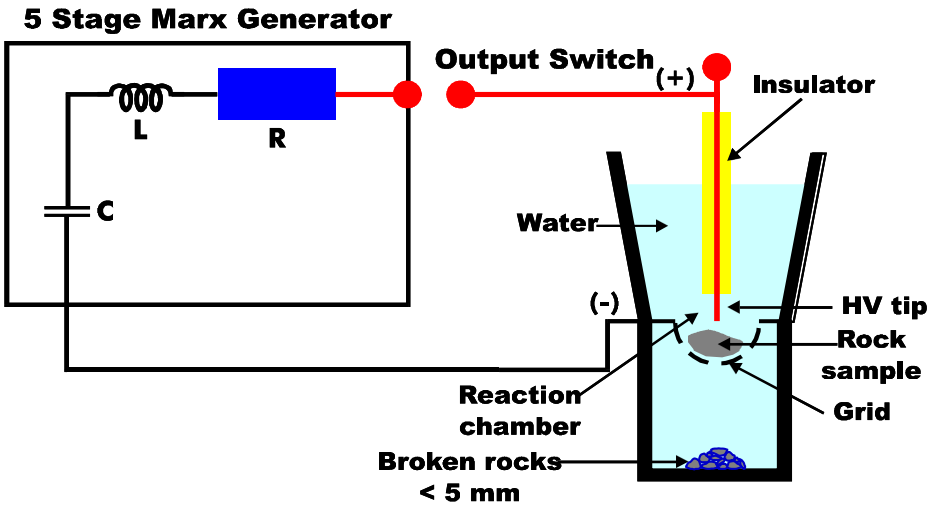


Figure -31: Schematic of batch rig at FZK, 'Franka-0'

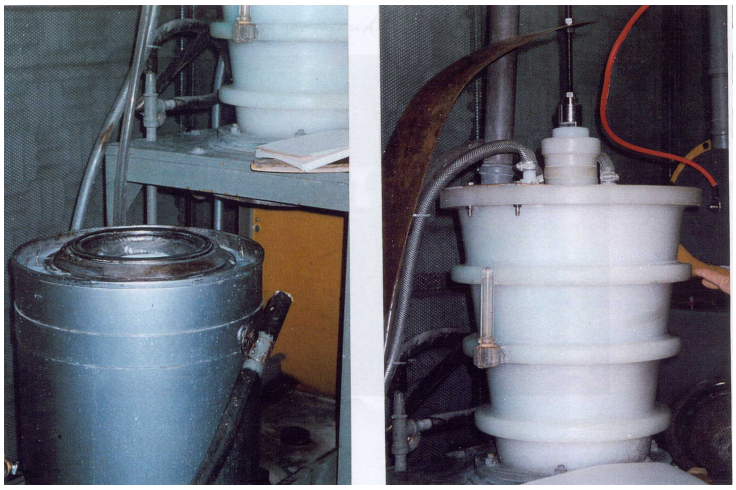


Figure -32: Collector base with screen on top (left) and conical comminution chamber (right)

The comminution chamber (Figure -32) has an external water-level indicator, which seems to be necessary to avoid overfilling. The collector base can be removed to extract fragmented items; this technology can be used not only for rocks, but also for recycling of small, commercial appliances, such as electric shavers, according to FZK.

Like Euro–Pulse, FZK also uses Marx-generator-based pulsed power. The spark gaps are located in a sealed, horizontal chamber, as shown in Figure -33 below, where the gaseous environment, within which the sparkover is triggered, can be modified to allow higher charges than in normal air.

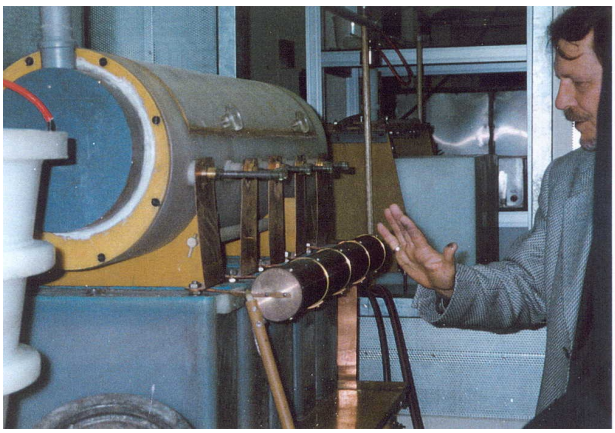


Figure -33: FZK's Franka-0 Marx generator

The Wits Marx generator was not encapsulated – thus humidity in the air may have affected the charge and sparkover voltage per Marx stage on any given test day.

6.2.2 Continuous rig

Using the insight gained by operating the Franka-0 batch equipment, FZK developed and built the Franka-Stein plant (Figure -34), which is used for the disaggregation of industrial waste concrete on a semi-industrial scale. The plant is designed to operate with a continuous feed stream at about 1 t/h.

It conforms to the stringent industrial safety standards associated with high voltages and high levels of potential radiation. A schematic is shown in Figure -34 below.

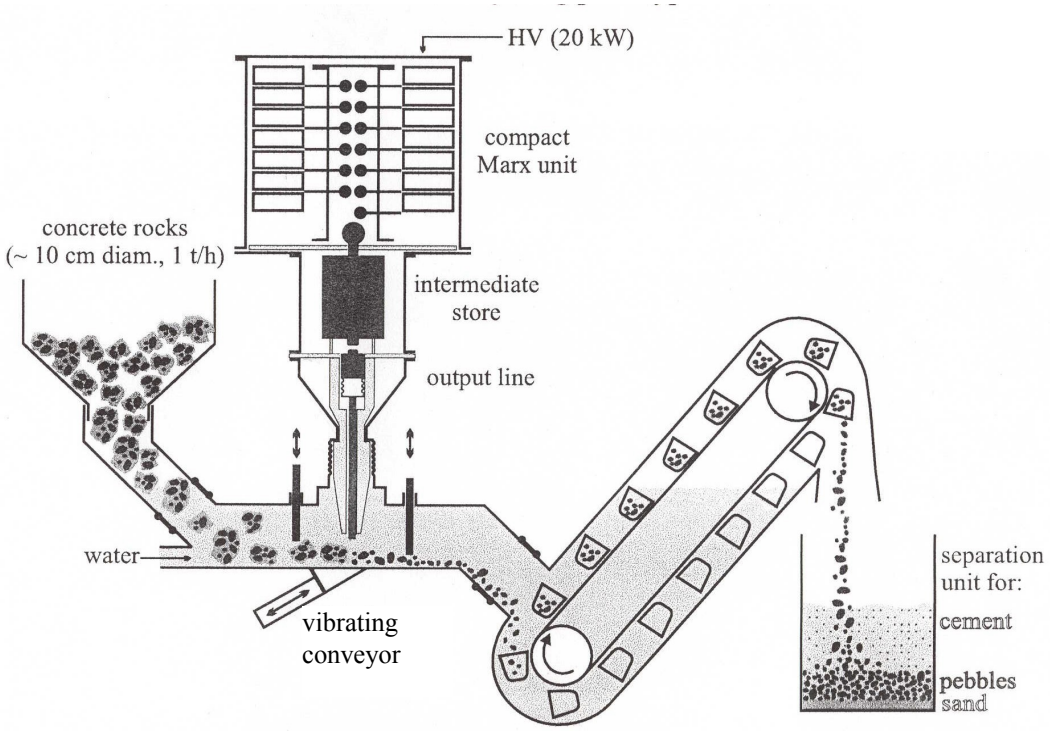


Figure -34: Schematic of FZK's 'Franka-Stein' continuous rig (Hoppe et al., 1998)

Potential for steady-state rock comminution

The generation of pulsed power for this pilot plant is also based on the Marx generator principle, but a continuous rock storage, rock feed and rock discharge

system has been added. This allows the processing of pre-crushed concrete (top size of about 100 mm) to recover the original constituents, i.e. ultrafine cement, medium-sized sand and coarse gravel.

The power pack with the Marx generator in seven parallel stages is shown for size comparison in Figure -35 below.



Figure -35: Marx generator for continuous rig

Instrumentation

The entire electric circuit is linked to a data-acquisition system to capture all the relevant operating parameters. The gas medium and gas pressure in the switch tower can be varied to trigger the initial spark at various loading voltages. The actual current is recorded using a self-integrating Rogowski coil, calibrated by using a 42 kA/μs pulse generator.

Circuit modelling and performance analysis

The entire electrical system was put on the P-Spice software code. The dynamic behaviour of the electrical system could thus be simulated for different breakdown voltages. Initially conducted discharges through a liquid resistor, with known resistance, confirmed the predicted and actual measured performance. This was a pre-requirement before the loading was increased up to 500 kV. The

signals recorded by the system are used to correlate the actual performance with theoretical predictions.

6.2.3 Challenges for continuous rock-breaking plant

An important criterion for an industrial comminution plant would be that sufficient current must be able to flow as a result of high voltages, thus providing a 'boost' after the initiation of the initial path.

6.3 Evaluation of Rock Specimens Fractured at FZK

6.3.1 Macroscopic and microscopic analyses before fragmentation

All samples were macroscopically analysed for constituent minerals and their volume percentage was estimated. This work was supervised by Dr Thomas Wallmach and executed by a Miningtek Intern, Philamon Moseme, both geologists.

The microscopic analysis was done with a polarising microscope. The polished samples were mounted on a glass slab and ground to a thickness of 0,025 mm to prepare standard thin sections. The thin section that was most representative of the entire core was analysed for each rock type.

The minerals were then identified systematically by their optical properties. The properties of colour, relief, cleavage-extinction angle, orientation and twinning are observed under crossed polars. This method aids in the analysis of mineral phases and in the semi-quantitative analysis of the minerals present in the core sample.

Thin sections were prepared of the specimens to provide complementary information to the XRD (X-ray diffraction) and XRF (X-ray fluorescence) analyses. When appropriate, photographs were taken to document the condition of the samples prior to comminution. Unfortunately, no suitable pictures could be taken after electric discharge to compare directly with the pictures taken before.

XRD analysis was applied in order to determine the mineral phases, but mostly to distinguish *between* the mineral phases, which are optically similar. XRD

analysis showed that quartz is the dominant mineral in the Ventersdorp Contact Reef (VCR) sample and muscovite and chlorite occur in accessory amounts.

The lava is dominated by plagioclase, both the sodium-rich end-member (albite) and the potassium-rich end-member (microcline). Amphibole occurs as one of the dominant minerals.

The Spotted Dyke sample consists of anorthite, hornblende, stilpnomelane and muscovite. The chemical analysis is consistent with the microscopic analysis.

Table -3 and Table -4 provide an overview of the results of the XRD and XRF analyses of the samples.

Table -3: XRD analyses

%	VCR	Lava	Spotted Dyke
SiO_2	73,73	47,65	49,20
TiO_2	0,45	1,00	1,49
Al_2O_3	7,84	12,70	10,47
Fe_2O_3	8,90	14,86	15,50
MnO	0,06	0,21	0,22
MgO	2,12	4,74	5,04
CaO	0,10	8,87	7,59
Na_2O	0,04	4,63	4,42
K_2O	1,68	1,62	2,48
P_2O_5	0,01	0,09	0,19
CR_2O_3	0,07	<0,01	0,04
NiO	0,02	0,02	0,02
V_2O_5	<0,01	0,04	0,02
ZrO_2	0,02	0,02	0,02
CuO	0,02	<0,01	0,03
LOI	2,83	1,56	1,41
Total	97,99	98,02	98,13

The major element concentrations of the comminuted samples are given in Table -5. This analysis supports the microscopic investigations. The high SiO_2 content in the VCR reflects the abundance of conglomerate in the rock composition. The Fe_2O_3 reflects the presence of pyrite and chlorite. The Al_2O_3 is bound in clay minerals and the K_2O in sericite.

The Lava is relatively poor in quartz compared with VCR and Spotted Dyke and the quartz is not bound in conglomerate or in a single mineral. It is nevertheless

rich in clay minerals (high Al_2O_3), some microcline (K_2O) and albite (Na_2O). All the Fe_2O_3 in the Lava is bound in the chlorite and amphibole.

The Spotted Dyke is also relatively poor in quartz and very rich in clay chlorite (high Fe_2O_3) and other clay minerals (high Al_2O_3), with some muscovite (K_2O) and albite (Na_20). Table 6-3 provides the data.

Table -4: XRF analyses

Ppm	VCR	Lava	Spotted Dyke
CU	109	60	250
GA	13	18	19
MO	14	1	1
NB	8	3	13
NI	261	130	142
PB	11	3	3
RB	48	25	63
SR	6	440	445
TH	9	5	5
U	3	3	3
Y	17	19	18
ZN	54	95	126
ZR	277	113	138

XRD analysis showed that quartz is the dominant mineral in the VCR sample and muscovite and chlorite occur in accessory amounts.

The lava is dominated by plagioclase, both the sodium-rich end-member (albite) and the potassium-rich end-member (microcline). Amphibole occurs as one of the dominant minerals.

The Spotted Dyke consists of anorthite, hornblende, stilpnomelane and muscovite. The chemical analysis is consistent with the microscopic analysis.

Table -5: Summary of geological assessment

			Macroscopic Description			Microscopic Investigation				
No.	**Rock Name**	**Rock Type**	**Mineral (Estimate Vol. %)**	**Grain Size**	**Texture**	**Mineral (Estimated Vol. %)**	**Shape**	**Grain Size**	**Colour**	**Texture**
1/8/6	Spotted Dyke	Dolerite	Quartz 40 % Chlorite 30 % Plagioclase 30 %	Coarse (>5 mm)	Phaneritic	Amphibole 50 % Ortho-plagioclase 20% Chlorite 10 % Pyroxene 10 % Epidote 5 % Magnetite 3 % Quartz 2 %				
3/8/6	Western-Areas Lava	Lava	Chlorite 50 % Clay minerals 50 %		Veins of chlorite	Amphibole 25 % Chlorite 25 % Quartz 20 % Plagioclase 15 % Epidote 15 %		Fine	Green Colour-less Colour-less	
4/86	VCR	Conglo-merate	Quartz 60 % Clay minerals 35 % Sulphides 5 %	Coarse (>5 mm)	Angular grains, poorly sorted, matrix supported. Pyrite is randomly distributed.	Quartz 70 % Clay minerals 25 % Pyrite 5 %	Rounded	Coarse	Colour-less Black	Oligomictic, matrix supported.
5/8/6	Vein quartz	Vein quartz	Quartz 99 % Other 1 %	Medium (1 mm)	Granular	Quartz 100 %	Angular	Coarse	Colour-less	

6.3.2 Initial tests at FZK, Germany

The various visits by FZK and CSIR personnel to develop and negotiate future collaboration led to a favourable atmosphere for conducting rudimentary but indicative comminution tests. The following three sections and the section for the VCR sample describe the first four rock types tested by the author at FZK.

Lava

The core sample of amygdaloidal lava from the Ventersdorp Supergroup belongs to the Westonaria Formation, which overlies unconformably the Ventersdorp Contact Reef (VCR).

The very homogeneous lava core sample was comminuted by FZK. Due to the uncontrolled loading of the batch plant and the inability to conduct single-pulse discharges, the extent of comminution of each core sample depended on whether it happened to be positioned below the electrode. However, the indications are that the lava sample was more difficult to comminute as the following photograph (Figure -36) shows an almost undestroyed core sample.

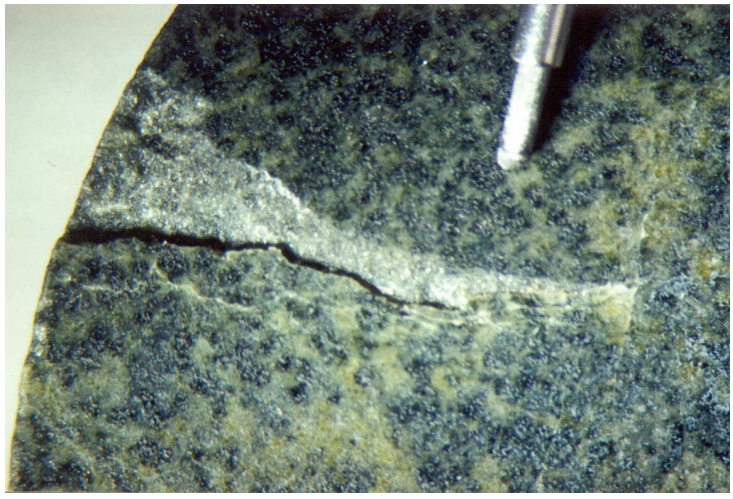


Figure -36: Lava: Initial, small chip from core sample

As with the VCR sample, the lava sample also shows cracking close to the edges, as shown in the photograph in Figure -37.

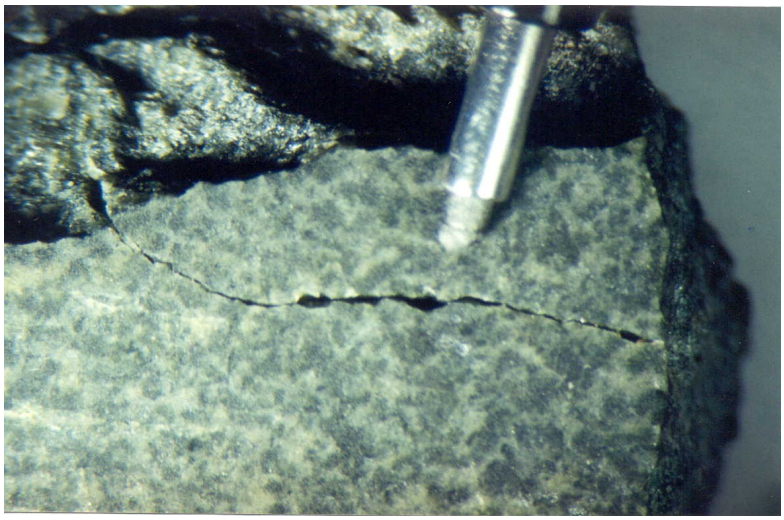


Figure -37: Lava: Chipping and cracking near edge of core sample (pencil tip with lead provides a relative scale)

Although the same number of pulses (about 50) was allowed for all samples, the lava sample showed the least amount of new surface area produced, which would indicate its lesser suitability for ESWC.

The electrically treated sample of the lava was also analysed. Along the fractured surfaces it had a whitish khaki colour. The grains of this whitish part were analysed microscopically and glass was found (Figure -38).

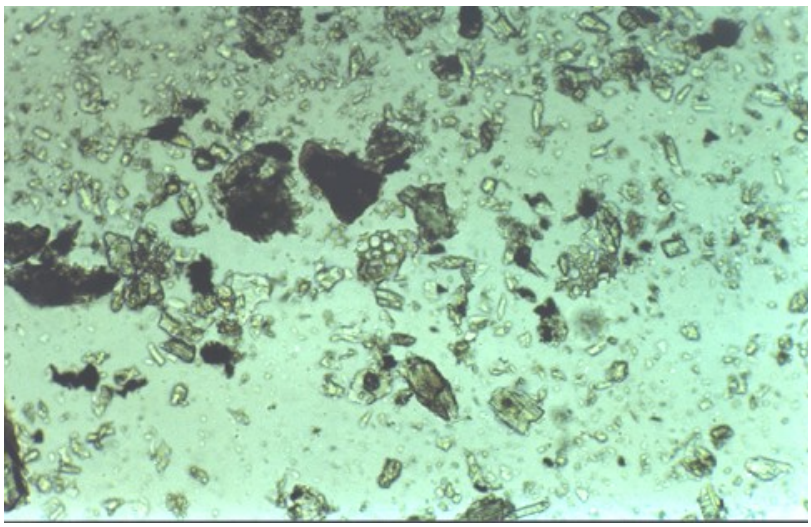


Figure -38: Evidence of glass particles in the discharge path

The only plausible explanation for this is that the rock melted and cooled very rapidly during the electric treatment. There was insufficient time for recrystallisation.

Spotted Dyke

The Spotted Dyke is one of the dykes that intrude into the Upper Jeppestown Subgroup of the Witwatersrand Supergroup in the West Driefontein mine as a network of dykes. This dyke is stratigraphically found below the Carbon Leader Reef. The rocks have a dull, mottled appearance with large grains of plagioclase.

During the indicative tests, the Spotted Dyke specimens also appeared to be difficult to comminute. However, this could have been a result of the uncontrolled 'hit-and-miss' positioning of the sample inside the comminution chamber.

The following photograph (Figure -39) shows how cracks developed along the polished flat side of the core sample after comminution.



Figure -39: Spotted Dyke: Cracks along the surface of the polished sample

In the next photograph (Figure -40), showing the fractured side view of the core sample, the polished area is visible at the upper end of the photograph.

The effects of comminution can be classified as chemical and structural. The chemical effect is the process of glass forming on the lava. The electrical current causes a high temperature increase and melts certain minerals, but this occurs very rapidly and the melt has no time to recrystallise as it cools. The pyrite, at this high temperature, reacts to form phyrhotite and sulphur. Yellow sulphur stains were observed on the cracks of the treated samples, as shown in Figure -40.

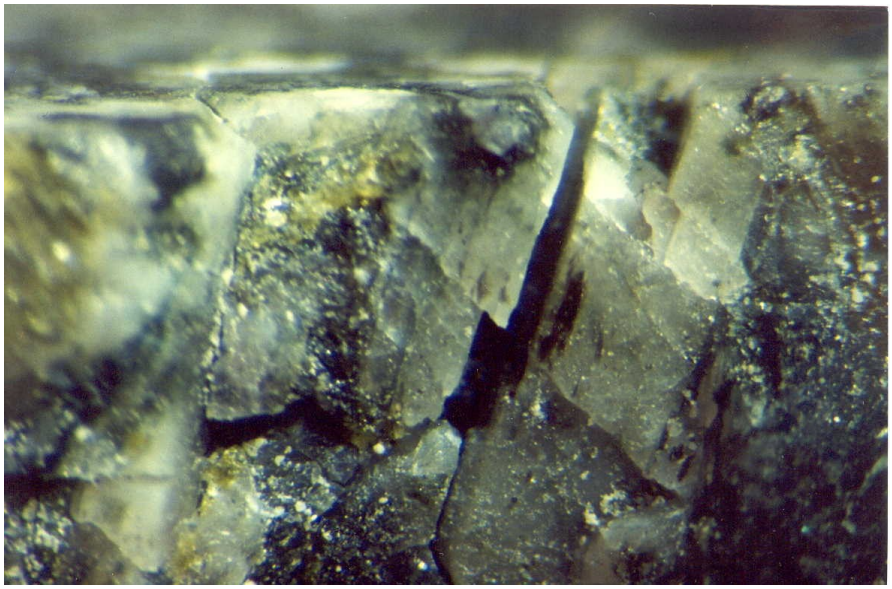


Figure -40: Sulphur staining along the cracks of the crushed Spotted Dyke sample, and fracturing along the grain boundaries

Quartz

Mylonites, pseudotachyllite and irregular development of vein quartz were reported at the base of the green bar. The vein quartz and the pseudotachyllite were present in the samples collected. These features are the result of bedding plane faulting confined to the base of the green bar. The vein quartz is monomineralic with granoblastic grains of quartz.

The following photograph (Figure -41) shows a quartz particle after crushing. The structurally damaging effect of comminution is shown in the multi-striated jointing in the vein quartz. This is caused by high pressures, as was noticed for

the geological structure known as South African Vredefort Crater due to the impact of a large meteorite (Wallmach, 2001).



Figure -41: Multi-striated jointing in vein quartz

The following platinum samples were tested during another visit by Pat Willis to FZK.

UG2 and Merensky samples

Small core samples of UG2 and Merensky reef were comminuted during the January 1999 visit to FZK by Mr Pat Willis from the CSIR. Both samples proved to be suitable for comminution as the operating time was reported to be very short. Unfortunately, the CSIR received no further technical information.

The comminuted samples were returned to Miningtek for optical and particle size distribution analysis. Figure -42 below shows the combined particle size distribution obtained below the screen, as well as the particle size distribution remaining above the screen, after five seconds of crushing.

The controlled top size and the few fines generated in the products makes this technology very suitable for combining with coarse hydraulic transportation technology, using Tore® pumps for hydrohoisting.

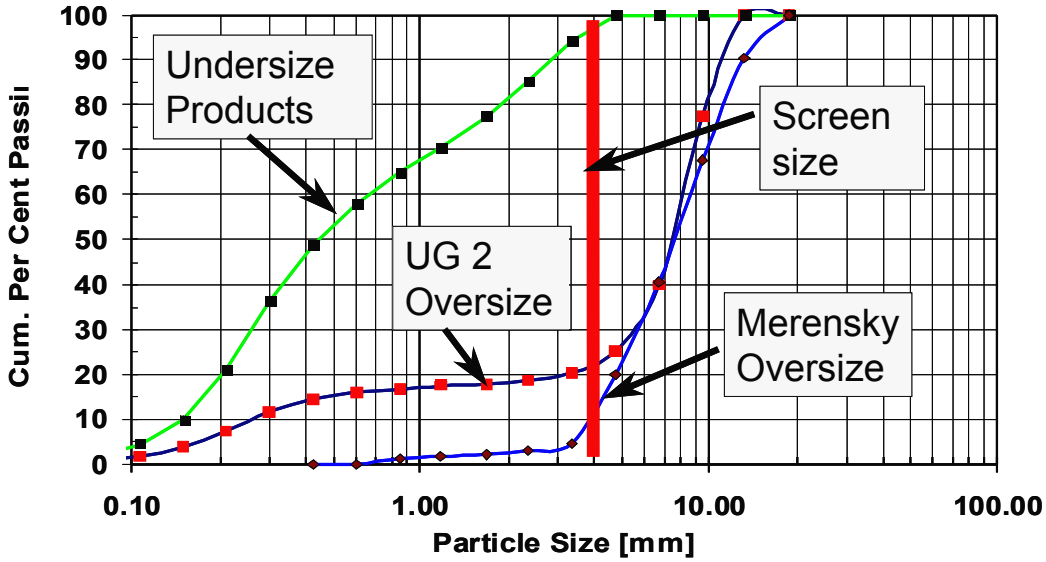


Figure -42: Indicative platinum PSDs from FZK's batch rig

From the literature, the indications were that mineralised specimens, particularly from gold bearing reefs, would offer preferential paths for dielectric breakdown. The VCR sample was therefore analysed in detail, and is discussed below.

VCR

This is an oligomictic conglomerate with angular grains of vein quartz. It is poorly sorted, with pyrite grains randomly distributed. The quartz grains are 5 mm in diameter. This is one of the highly mineralised economic reefs in the Witwatersrand Basin.

The VCR consists of rounded to angular pebbles of quartz in a matrix of pyrite and clay minerals (muscovite, chlorite, sericite and phyrophyllite). Some pyrite grains can also be observed. Most of the pyrite grains occur as rounded grains and are therefore of detrital origin.

Cubic pyrite grains are also found and these are indicative of the action of hydrothermal fluids, which help the detrital pyrite to recrystallise. The action of hydrothermal fluids is also seen in the VCR sample from the veins filled with pyrite, seamed by chlorite Figure -43.

The VCR sample, obtained from West Driefontein, was electrically comminuted. (Another VCR sample from Western deep Levels (WDL) was electrically

comminuted in 1997 by Euro-Pulse, and was also given to Anglo American Research Laboratories (AARL) for analysis and to promote possible further collaboration or a financial contribution. Unfortunately, the technology supporter left AARL before any results were obtained.)

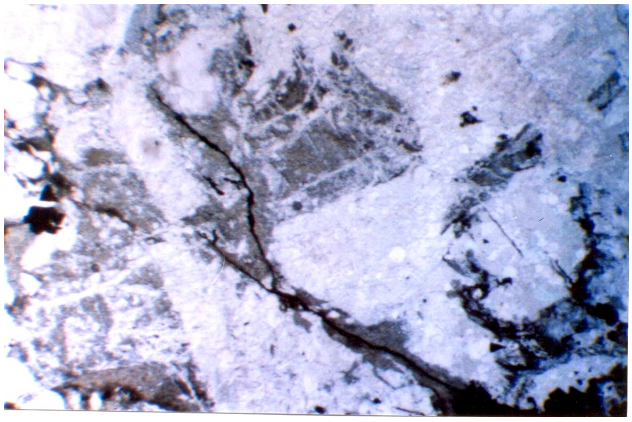


Figure -43: VCR: Pyrite seamed by chlorite

The indications are that the thin pyrite vein would be the potential path for electric discharge. Figure -44 shows the polished flat face of an 8-mm-thick core sample after ESWC by FZK, with indications of spallation and preferential cracking in general.

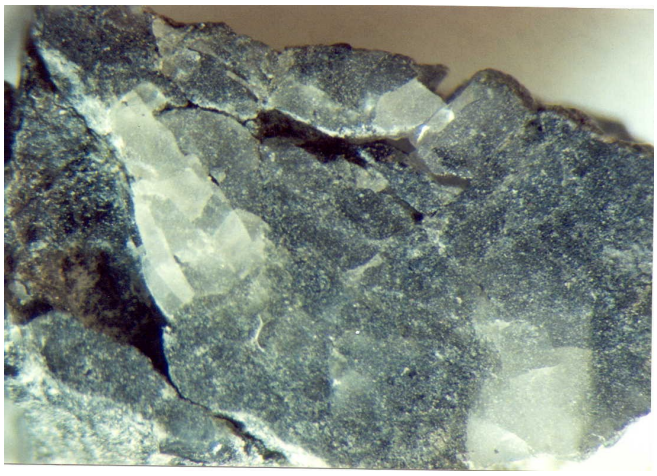


Figure -44: VCR: Indications of spalling at the edge of the sample

6.3.3 Particle size distributions (PSDs)

The particle size distributions of gold-mine-related rock types were analysed at CSIR Miningtek and are given in Figure -45.

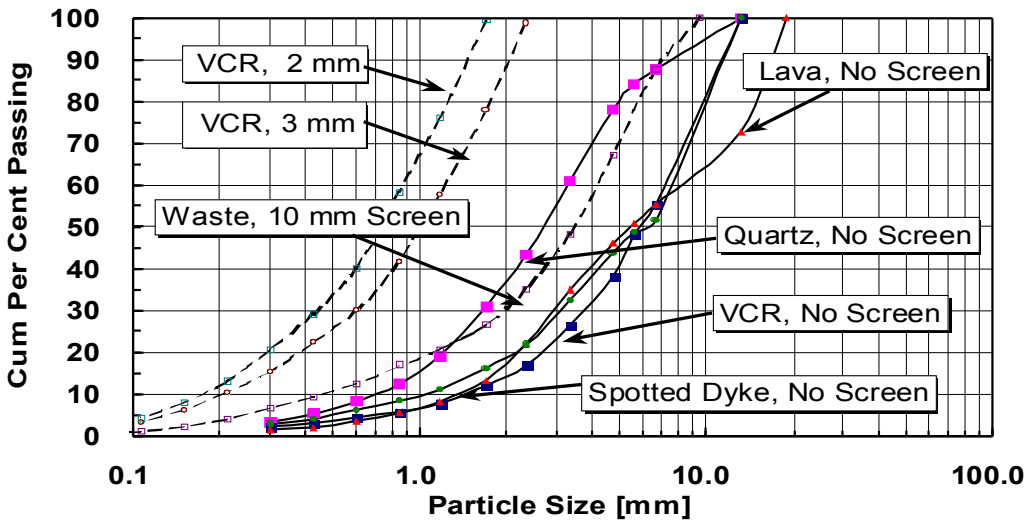


Figure -45: Gold-mine-related particle size distributions – FZK batch rig

As with the Pt products mentioned above, the coarseness of these PSDs makes these products ideal for Tore® pump technology.

It is evident that the electrically crushed samples are more cubical that the flaky-shaped conventionally crushed samples. For this reason, particle sphericity measurements on conventionally and electrically crushed samples were also done at CSIR Miningtek. The more cubical particle shape would improve the hydraulic transportation behaviour, which is the major motivator at present for underground pulsed-power comminution.

6.3.4 Particle shape definitions

To determine the particle size and shape of fragmented rock specimens, their mass could be converted to an equivalent sphere. The sphere diameter could then be referred to as the 'nominal' particle diameter. However, the settling velocity of irregular particles in water depends on their individual shapes.

The extreme, generic shapes of rectangular particles were classified by Pettijohn (1949). The concept and measurements of three principal axes (a, b, and c), which are perpendicular to each other, is shown in Figure -46 below.

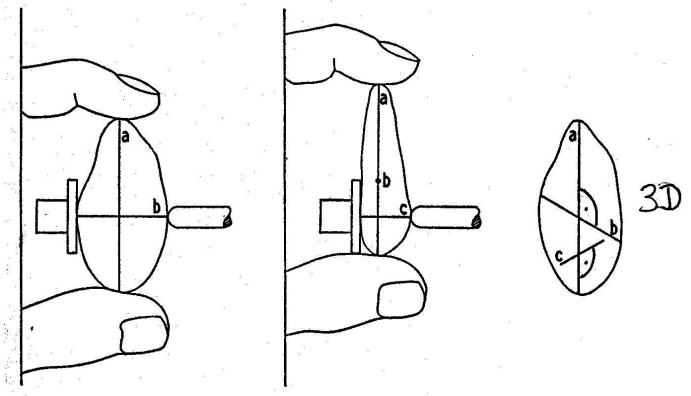


Figure -46: Three principal axes for fragment size determination (after Pettijohn, 1949)

Once the three axes have been determined, fragments can be classified within the four options shown in Figure -47 below.

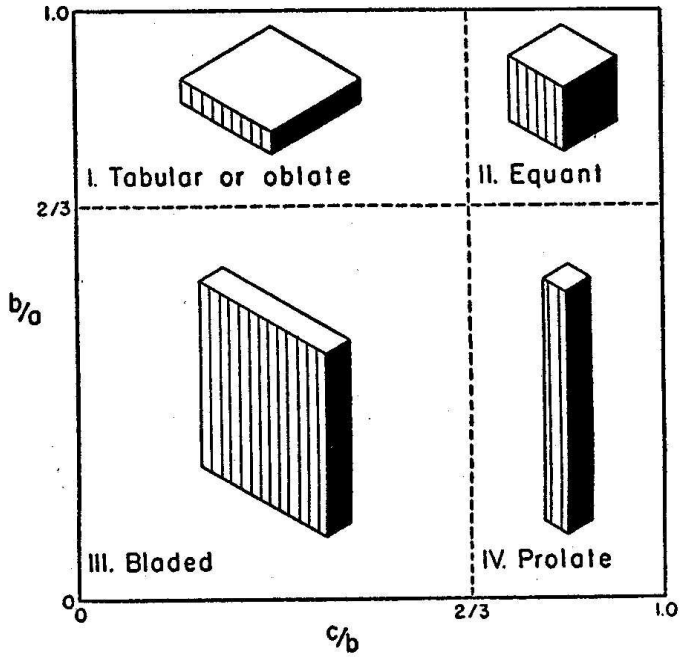


FIG. 25. Zingg's classification of pebble shapes. Note that although the representative solids shown (rectangular parallelopipeds) have the same roundness (o), they have different shapes.

Figure -47: Particle shape definitions (after Pettijohn, 1949)

Optical comparison indicated a more ‘bladed’, flaky shape for the impact-crushed particles, whereas the electric shock wave comminuted (ESWC) particles showed a more ‘equant’, cubical shape.

6.3.5 Comparisons of settling velocities

The settling behaviour of fragmented particles is important for the successful operation of the Tore® pump, which relies on the particles to settle in the zone of influence, where the swirling water stream picks up the solids for hydraulic transportation by pipeline.

Fundamental work on the effects of various shapes on the settling velocity was published by McNown and Malaika (1950) from the Iowa Institute of Hydraulic Research, USA. A number of representative axisymmetrical shapes were evaluated. A correction factor, K, was defined by McNown and Malaika to take various test conditions and particle properties into account. The results of the comprehensive test matrix are shown in Figure -48 below.

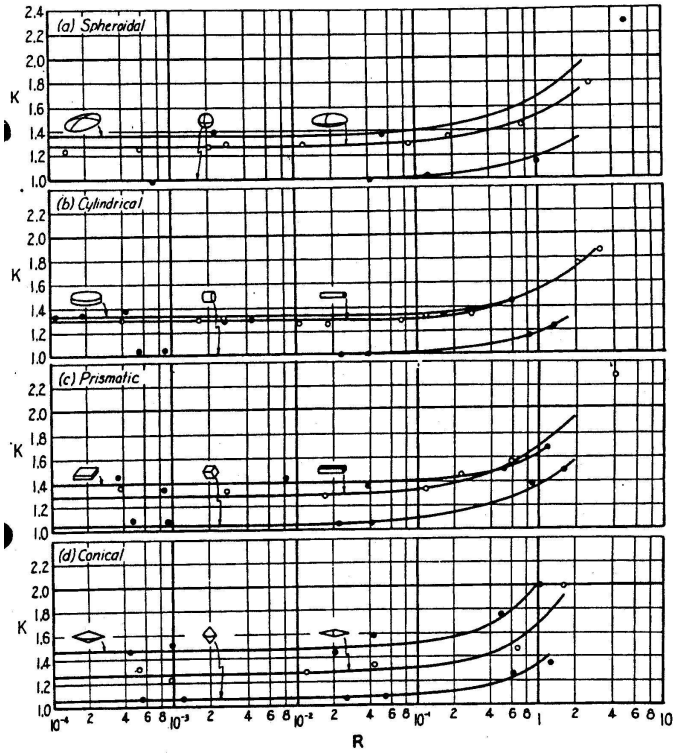


Figure -48: Correction factors for non-spherical particles (after McNown and Malaika, 1950)

The above results led to the conclusion that the ratio of the principal axis lengths was by far the most significant factor. The surface roughness and the roundness of smaller corners were less significant.

Based on McNown and Malaika's findings, rock specimens fragmented by both methods (electrically and by mechanical impact) were measured to determine their nominal diameter (d) if they were spherical. Their longest single length (D) was also measured (see measurement 'a' in Figure -46) to calculate each particle's sphericity S = d/D. The results are shown in Figure -49.

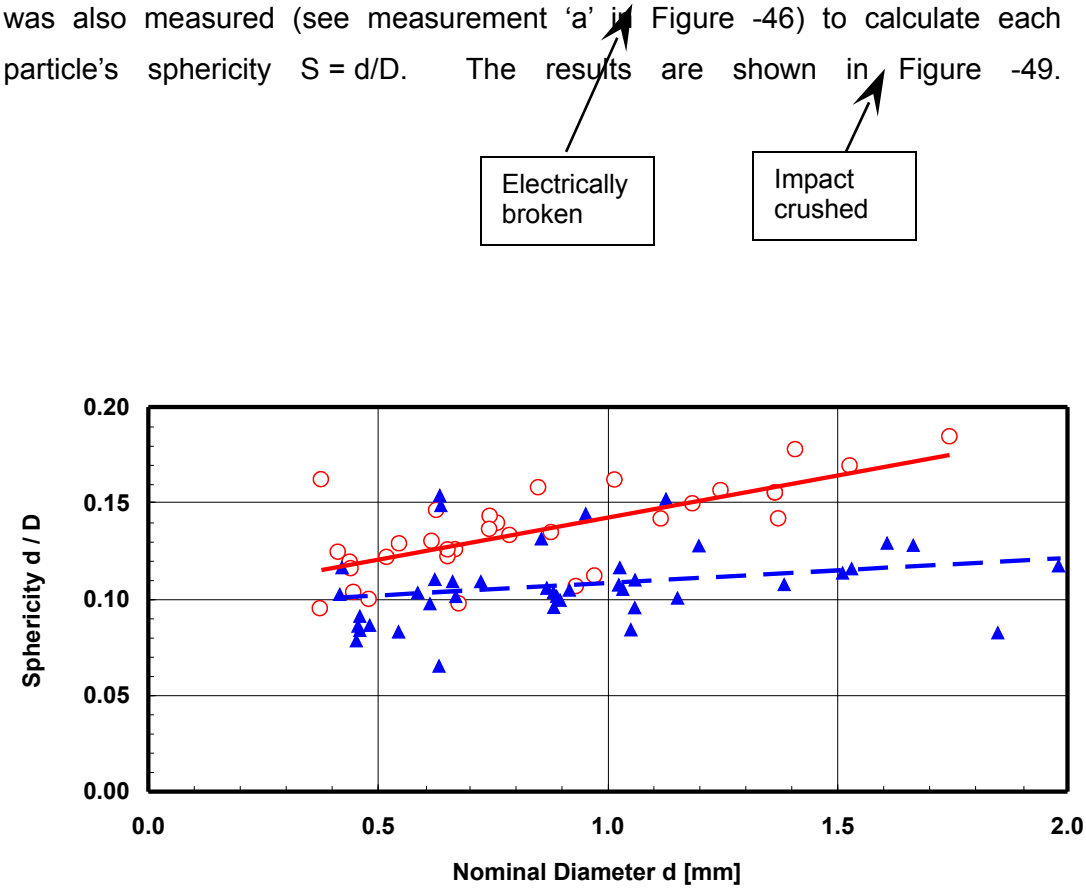


Figure -49: Sphericities of ESWC-crushed and impact-crushed particles

The figure reveals that both particle types are significantly non-spherical, as their sphericity values are low, between 0,1 and 0,2. However, a trend is evident, namely that the electrically broken fragments are more spherical than the impact-crushed fragments. The larger the nominal diameter of the fragments, the bigger is the difference in their sphericity.

In order to quantify the settling velocity, as this would be required to determine cycle times for loading the batch-operated Tore® pump vessel, terminal settling

velocities were measured at CSIR Miningtek in clear water at 25 °C. After the initial acceleration phase, particles reached terminal velocities in the water-filled, transparent settling tube, which was 2 m high. Each test was conducted with 10 particles, which were taken from a dry screening process. The results are shown in Figure -50 for a range of size classes up to 12 mm, which would be the expected top particle size for hydraulic transportation.

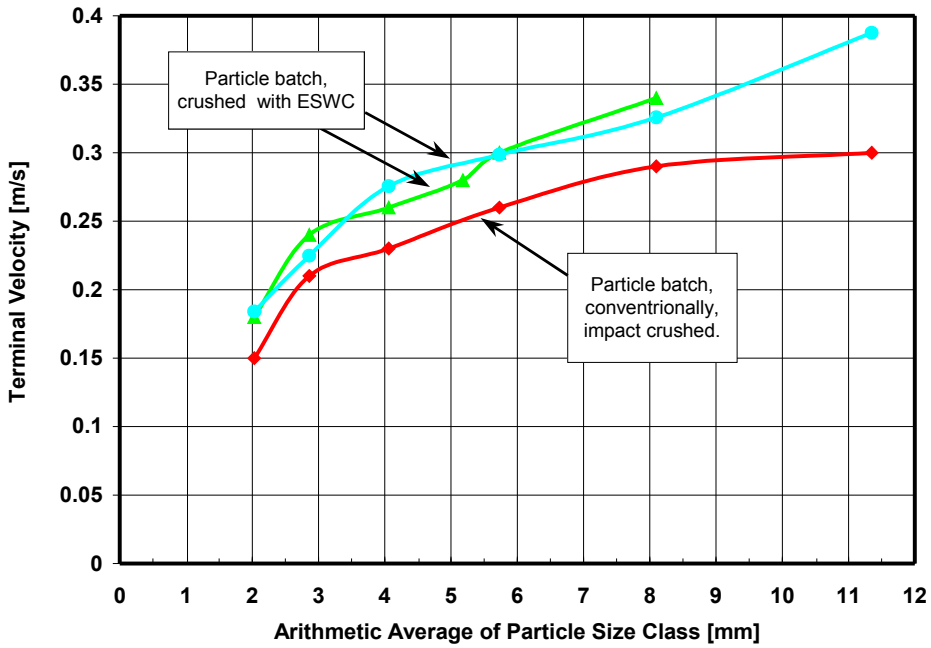


Figure -50: Settling velocities for fragments

The measurements indicate that the terminal settling velocities for electrically broken fragments were about 0,5 m/s faster.

In conclusion, particle sphericity and settling tests have confirmed that electrically broken rocks are more spherical in shape and therefore settle a bit faster that the more flaky-shaped, impact-crushed particles. Although the differences are only marginal, they would render the electrically broken rocks more suitable for the Tore® pump technology. Previous Tore® pump tests with particles sized from 5 to 10 mm, which were conventionally impact crushed, had already demonstrated the excellent behaviour of these particles in the Tore® test set–up.

6.4 Success Criteria for Electric Rock-Breaking Tests

6.4.1 Importance of voltage rise time

All research reported in the literature, particularly the results published by FZK, indicates that it is not only the maximum voltage applied across the rock that is vital, but also the voltage rise times. Energy storage in Marx generators, which is a fairly old technology, still appears to be the most favoured technology, as opposed to capacitor banks. FZK reported that typical Maxwell capacitor banks, as used by Physics International, and – according to the technical schematic – also in the Aeries equipment, do not have sufficient life-time for the frequent load changes associated with pulsed power applications.

The transmitting length between the Marx generator and the rock-breaking chamber must be short to reduce any losses and not to create any undesired capacitance or inductance, which could decrease the sharpness of the high-voltage pulse.

6.4.2 Submergence in water

In order to increase the field strength across rocks, they should be surrounded with water. This leads naturally to the hydraulic transportation of fragmented rocks, and eliminates any dust problems associated with conventional impact crushing. The effects of electric discharge on the water quality should be determined at a later stage in more detail, once the primary functionality of electric rock breaking has been proved to be practical.

6.4.3 Single shots for investigations into the breakage of various rock types

In the absence of any data for the various South African reefs and rock types, some fundamental test work should be done to determine which rock types are the most suitable for this technology. The loading of either single samples or a fistful of loose material (as was done at FZK) does not provide comparable data or insight into the fragmentation potential of the rock types. Continuous discharges at, say, 5 Hz will also create compressive shock waves from discharges through the water. The less homogeneous the rock specimen is, the

more variable the measurements will be. For this reason, more test samples should be prepared for use as inhomogeneous specimens.

6.4.4 Electrical instrumentation

Ideally, energy consumption should be determined from voltage and current traces to enable the power requirements to be specified for a continuous plant. The single shots should have a trigger mechanism and should enable the voltage charge applied per stage of the Marx generator to be varied.

The instrumentation must not decrease the voltage rise times or affect the current circuit to create undesired side-effects, e.g. superimposing frequencies that are not related to the pulsed voltage rise and the resultant current flow. High-speed data logging of the relevant signals is essential for analysis.

6.4.5 Clamping of rock samples

The specimens should be machined to provide good mechanical contact between the electrodes and the rock samples. Point loading with an electrode tip or area loading via a flat plate (as shown in Figure -24), or a hybrid between the two (say a 5-mm-diameter flat electrode tip) should be considered, which can be applied to all specimens in the same way.

For very uneven samples, like the VCR samples, a plate contact would be preferable, since that would enable the discharge to find its path easily through the mineralised veins. However, if the diameter of the electrode plate approaches that of the specimen, flashovers beside the specimen are more likely (see Figure -9).

6.4.6 Sampling facility

A sampling device should be placed below the comminution chamber to collect all the fragments after a single discharge in order to determine the extent of fragmentation.

If a bulk sample of loose rock is being fragmented with repetitive (single) discharges, but without rearranging or clamping the specimens between a fixed

arrangement of electrodes, the entire fragmented sample should be collectable. The set-up should be similar to those shown in Figure -16 and Figure -32 above.

6.5 Summary

CSIR Miningtek's intention was to evaluate the breakage behaviour of different rock types by means of single-shot tests, using small core samples obtained from various development waste and reef types, prior to sending rock samples of approximately 1 ton to FZK. In continuous operation, the comminution performance and 'average' power consumption of the ESWC technology would then have been assessed. A copy of the draft agreement between the CSIR and FZK is provided in Appendix A for reference.

Table -6 summarises the features and limitations of the two ESWC equipment types operational at FZK.

Table -6: Features and limitations of the FZK ESWC equipment

	Franka-0	**Franka-Stein**
Feed mode	Batch feed	Continuous feed
Electrode gap settings	20 mm	0 to 100 mm
Sample mass	2 kg	1 t/h
Feed top size	20 mm	100 mm
Instrumentation	Limited	Comprehensive
Circuit modelling	No	Yes
Pulse control	10 Hz	Single shot, and 5 to 10 Hz
Variable breakdown voltage	No	Yes
Maximum pulse energy	750 J	1 500 J
Energy consumption for concrete	-	10 kWh/t

The table shows the significant advances that have been made by FZK in developing and building the continuous rig. This rig provides the potential for sophisticated systematic research into the technical feasibility of electric shock wave comminution, but it cannot be used for clamping individual specimens between two electrodes to conduct single shots in order to evaluate the correlation between rock properties and applied electrical pulsed power.

Unfortunately, it was not possible to finalise a co-operation agreement between CSIR Miningtek and FZK on acceptable financial terms. It was therefore decided to assess available local equipment and to build up local expertise, based on the

observations and analyses conducted with the overseas equipment and from tests so far.

7 RIG CONFIGURATION USED FOR LOCAL TEST WORK

7.1 Requirements for Local Test Equipment

A local test set-up had to comply as far as possible with the requirements identified in Section 6.4 above. From an operating point of view, personnel familiar with the existing equipment had to be available to assist during the tests and to make modifications in order to maximise the utilisation of the rig and its output.

7.2 Identification of State-of-the-Art, Local Equipment

7.2.1 Apollo

NETFA (National Electricity Testing Facility) is a division of the South African Bureau of Standards (SABS) and they offered to conduct indicative single-shot discharges using either of their two Marx generators. This set-up would discharge a high-energy pulse directly onto the rock sample, which would be in a water-filled bucket. No intermediary energy storage, such as the inductive storage built by FZK, was available. Peak currents could be up to about 80 kA; the rise time was not known and would have to be determined during the tests.

The size and details of the 18-stage Marx generator are shown in Figure -51.



Figure -51: NETFA's 18-stage Marx generator, control room, concrete tower and capacitor banks

The energy-storage capacity was greater than the anticipated energy requirements for single shots through rock specimens of a few centimetres in

thickness. A smaller, eight-stage Marx generator could also have been made available, but additional instrumentation for recording and varying the voltage and current was not available at this site. The eight-stage Marx generator and its control panel are shown in Figure -52.

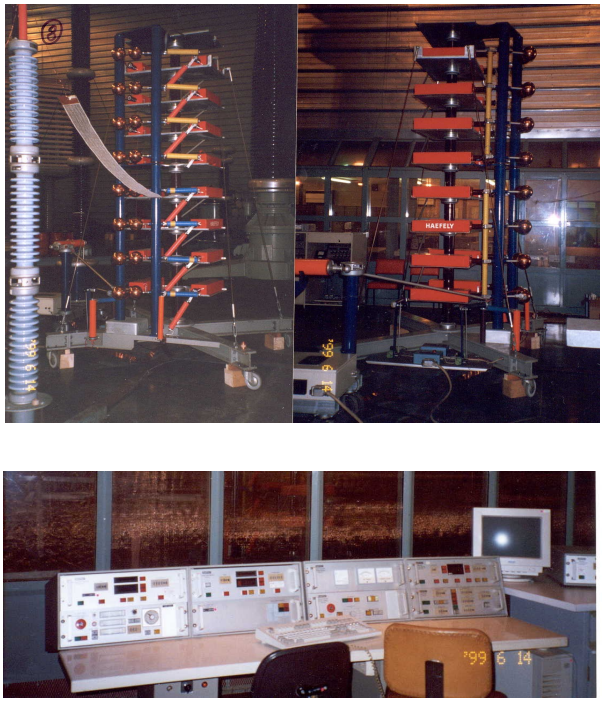


Figure -52: NETFA's eight-stage Marx generator with control panel

The hiring costs for these customised tests would have been far in excess of the available budget, and the flexibility of the site and the equipment appeared to be limited (Kroninger, 1999). Therefore, the idea of testing at this site was not further pursued.

7.2.2 Potchefstroom University

Pulsed power is used at Potchefstroom University at very low energy levels. Its main application is for the sterilisation of the viruses that circulate in air-conditioning systems. Pulses are not created with Marx generators, but with alternative electric circuits. The voltage and amperage levels, as well as their rise times, would not be sufficient to discharge through rocks (Swart, 1999).

7.2.3 Atomic Energy Corporation

The Atomic Energy Corporation (AEC) also has a unit that could be used for testing the electric breakdown of rocks. This unit provides inductive energy storage downstream of the capacitor-based storage unit. This would increase the peak current obtainable. However, the water-filled comminution chamber (bucket) must be interfaced directly with the inductive energy storage to be effective. Figure -53 is a schematic showing how a single rock could be fragmented.

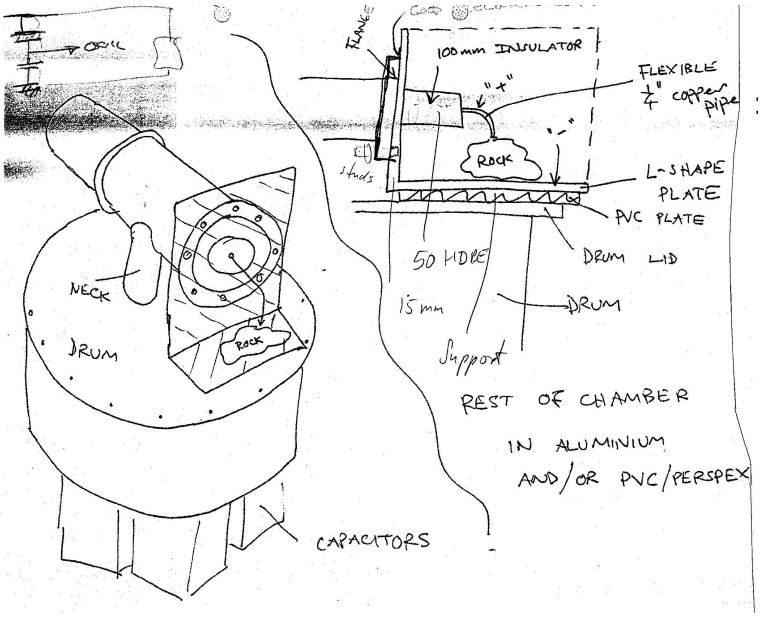


Figure -53: AEC's potential test set-up (after Turner, 1999)

Everything in the above figure, with the exception of the L-shaped plate for holding the rock specimen, is already available. However, the equipment was in intermittent use, and AEC did not intend to engage in water-submerged rock-breaking experiments. If a large research project could be created as a joint venture between the CSIR and AEC, which should include primary rock breaking at the face, the chances of successful collaboration would increase significantly.

7.2.4 High-Voltage Laboratory at the University of the Witwatersrand

The University of the Witwatersrand (Wits) conducts a lot of contract research for Eskom in the field of high-voltage experiments and dielectric breakdown. A ten-stage Marx generator is available, which can easily be detuned to a six- or four-stage circuitry to suit the electrical energy requirements. Each stage can be charged up to about 40 kV. Postgraduate students could assist with the set-up and in conducting the test work, which has to comply with strict safety regulations.

Most important, however, was Wits' positive attitude towards investigating an unquantified phenomenon such as electric rock breaking – this was the decisive factor in the selection of this facility to conduct the test work. The test work had to be scheduled to fit in with student projects to minimise unnecessary commissioning and decommissioning work. Accessories such as a high-voltage divider and passive Pierson coils were also available to provide suitable instrumentation for the study of electric rock breaking.

7.2.5 Comparisons of equipment

The most significant technical difference between the equipment assessed is the available energy per discharge. A comparison in given in Table -7 below.

Table -7: Comparison between the energy per pulse of potential test rigs

FZK Franka-0, 5 stages	**FZK** Franka-Stein, 7 stages	**NETFA** Small unit, 8 stages	**NETFA** Large unit, 24 stages	**AEC** Small unit, Capacitors	**AEC** Large unit, Capacitors	**Wits** High voltage, 10 stages
0,75 kJ	1,5 kJ	24 kJ	380 kJ	0,2 kJ	10 kJ	1,4 kJ

Except for AEC's test rig, which uses capacitors only, all the others operate with pulsed power generated by multiple stages of Marx generators.

7.3 Test Rig for Electric Rock Breaking

7.3.1 High-voltage circuit

Various high-voltage components were configured at the Wits' High-Voltage Laboratory to provide a test rig that would satisfy the rig requirements identified. On the basis of initial estimates of requirements, four stages of the ten-stage Marx generator were initially converted to match the other rig components. A manual trigger box was installed, which was used to trigger the high-voltage pulse manually. This was convenient as photographic and data-acquisition systems had to be started just before discharge took place. The Marx generator was charged via a variable, but conventional, 220 V AC power supply, which was rectified to provide a high voltage – up to 40 kV DC per stage. For the final test series, six stages were configured to accommodate the thicker rock specimens.

A high-voltage resistor divider (1 MV, 13 kΩ) was coupled in parallel across the comminution chamber to measure the voltage signal across the specimen during each test. A passive Pierson coil was placed in series into the discharge circuit to measure the current. The wire connecting the electrode was as thin as a human hair, since the discharge event was too short to warm up the wire, even though the instantaneous current was very high. Voltage and current were logged on an oscilloscope, and a separate multimeter was used to measure the actual voltage across a single stage to avoid over-charging of the relatively aged Marx generator.

A schematic layout of the overall electrical configuration is shown in Figure -54 below.

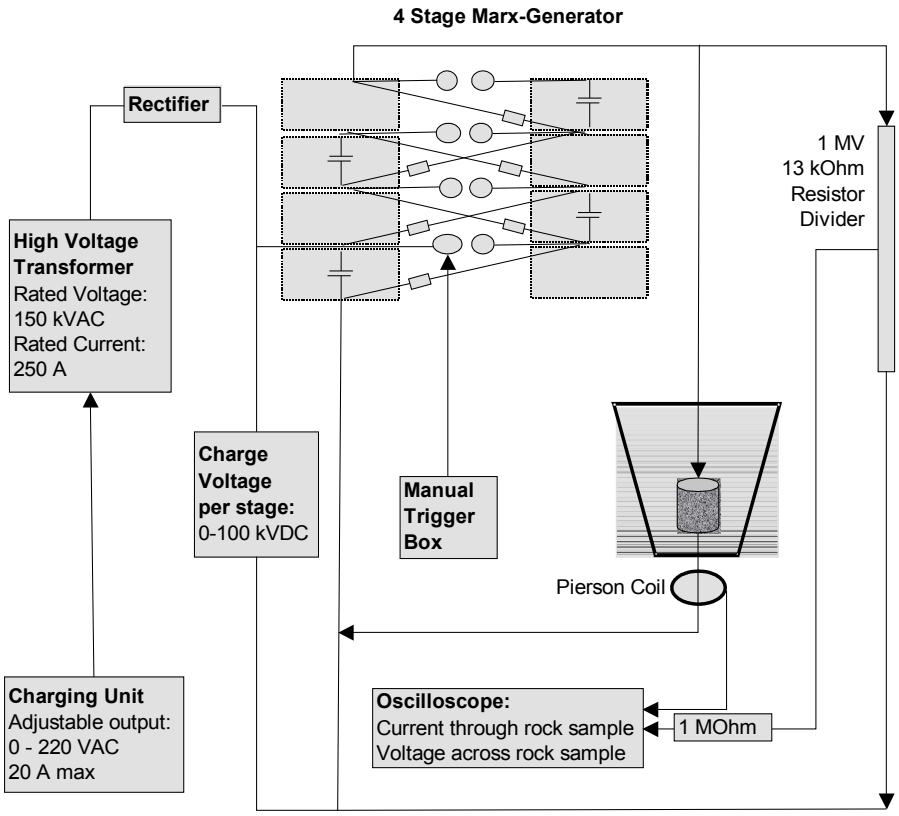


Figure -54: Test rig – Electrical layout

The impressive ten-stage Marx generator with the high-voltage transformer is shown in Figure -55 below.



Figure -55: Wits' Marx generator and high-voltage transformer

Earthing of the set-up prior to entering the test area was essential to prevent injury to the personnel. The electronic equipment was placed about 4 m away from the test set-up, and was covered with aluminium foil as much as possible while still maintaining accessibility and functionality (Figure -56).

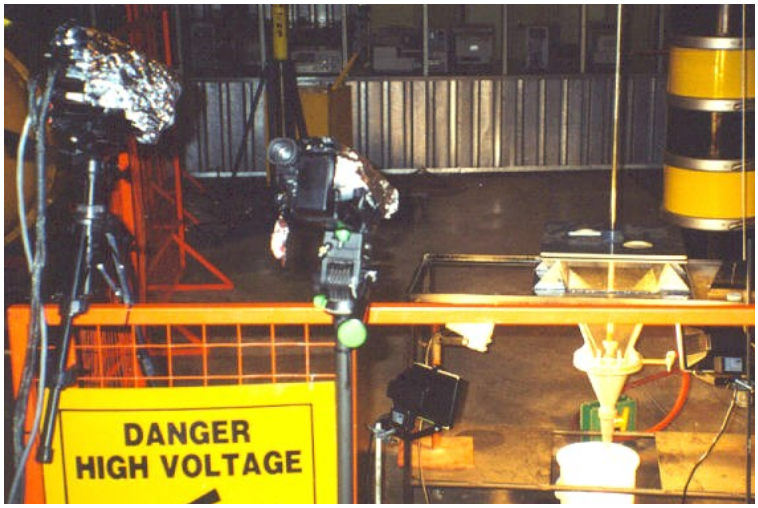


Figure -56: Shielded cameras, FlashCam (left) and Sony (right)

In some instances, the video cameras stalled due to the high electrical fields present.

The resistors of the Marx stages were changed to match the test requirements. In initial tests conducted with a gap setting of 10 to 15 mm between the Marx-generator capacitors, it was not possible to increase the breakthrough voltage to the threshold levels at which rock fragmentation would be induced. Instead, water flashovers were observed, and there was little damage to the rock. The gap between the capacitors was therefore increased to enable a higher-charge voltage to be applied. In addition, a fifth capacitor stage was included in the configuration. The gap between the polished spark balls, shown in Figure -13, was carefully adjusted to 18 mm.



Figure 7-7: Spark trigger unit and spark caps

The high-voltage divider, the Pierson coil and the multimeter to indicate actual charge voltage per stage are shown in Figure 7.8 below.

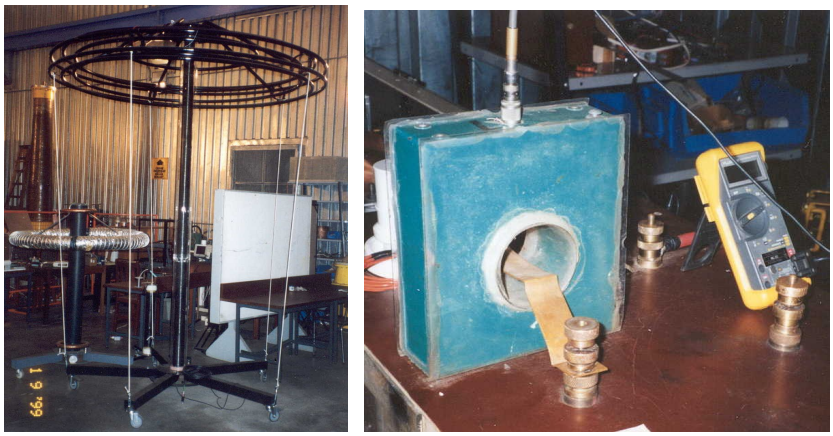


Figure -8: High-voltage divider and Pierson coil

The test configuration had to be dismantled a few times for other projects and student demonstrations. It was noted that the dynamic behaviour of the pulsed power circuit differed between the individual set-ups. This was evident during the standard 20-mm water-gap test from the amount of 'ringing', i.e. the phenomenon of ultra-high frequencies superimposed on the typical circuit frequency.

7.3.2 Rock-breaking chamber

The explosive fracturing of submerged rock causes significant shock waves, as was evident with the lifting of the lid at Euro–Pulse (Figure -30). For this reason a conical chamber was considered. This shape would also dissipate lateral shock waves and thus reduce mechanical stresses on the chamber. For the photographic (video) capturing of discharges and rock fragmentation, transparent side walls were required.

The distance between the electrodes had to be variable, and a metallic grid was necessary as a cathode closing the electric circuit. Sampling facilities and a circulating pump were considered to return the water after the solids with water had been dropped into the sampling box. Above the pinch valve was an intermediary storage area into which the smaller fragments that had passed through the metal sieve could settle (Figure 7.9).

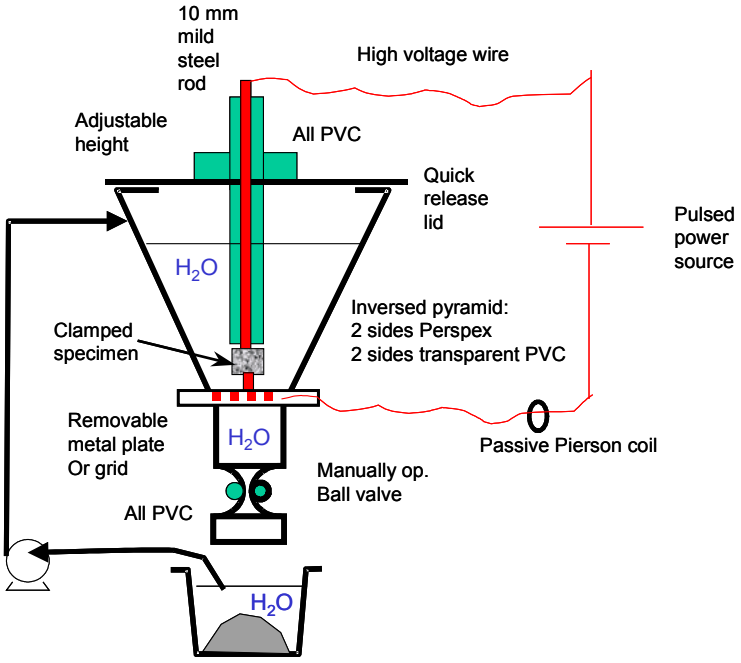


Figure -9: Test rig – Mechanical layout

Except for flashovers towards the end of the test programme, the initial use of metal bolts for the flange, and limited perforation damage of the insulation of the electrode, the mechanical design of the chamber fulfilled its purpose.

To obtain good colour video recordings, a light source with a total of total of 3 000 W was installed near the chamber. This heated up not only the water inside the chamber, but also the plastic construction.

To maximise photographic contrast during the rock-breaking process, either black or white plastic sheets were inserted into the chamber behind the rock specimen. The white background proved beneficial when working with black UG2 samples, and the black background provided the necessary contrast for the bright flashovers.

The water-filled rig with the Marx generator in the background is shown in Figure -9 below.



Figure -9: Water-filled comminution chamber and flashover, visible far above the clamped specimen and at the bottom left

The photo on the right above shows an unwanted flashover, while the specimen, 42 mm in diameter and 20 mm high, remains undamaged.

7.3.3 Signal conversions

The voltage signal was divided by means of a high-voltage divider to obtain low voltage levels suitable for oscilloscope input. The current signal was converted with a passive Pierson coil to provide an independent secondary circuit. The calibration factors are provided in Table -8 below.

Table -8: Calibration factors for oscilloscope

Signal	1 V on oscilloscope equals:
Voltage across the rock specimen	18 200 V until 18-11-2001
	46 500 V from 19-11-2001
Current through the rock	100 A prior to 15-3-2001 1 000 A on and after 15-3-2001

All oscilloscope signals for voltage and current, some of which are given in the relevant sections later, required conversion using the above factors to obtain the actual values.

7.3.4 Cameras and lighting settings

The effectiveness of four different cameras was evaluated at various stages of the study to document the discharge and fragmentation processes:

1) Black-and-white digital high-speed camera with nearly 2 000 frames per triggered event
2) Sony Hi 8 video camera in ‘golf’ and ‘moon’ modes, with 10 optical and 28 times digital zoom
3) Black-and-white FlashCam digital high-speed camera, seven events on one frame at 1/1 000 000 s, triggered by the oscilloscope
4) Canon AE1 photo camera with either 200 or 400 mm optical zoom, operated in ‘B’ mode.

Digital camera with 2 000 frames per event

The first approach was to use a camera that could handle a total of 2 000 frames, at a frame rate of 1 000 per s. The distance to the comminution chamber had to be increased to protect the electronic equipment inside the camera from the high-voltage fields. The electronic trigger box for synchronising the camera with the breakdown voltage, which crushed the rock, did not operate satisfactorily. Manual triggering therefore had to be used which required a time-consuming search for the relevant frames – among the 2 000 recorded frames – immediately after each shot to enable the minimum number of frames to be saved, thus freeing the memory. Even with a dedicated cameraman, this procedure was not practical and hindered the progress of the tests significantly. The images recorded were of disappointing quality, even when using a 300 mm zoom lens and 3 000 W of lighting.

This video camera was abandoned after a few initial trials. Each image was composed of four quadratic sub-images (Figure 7-10).

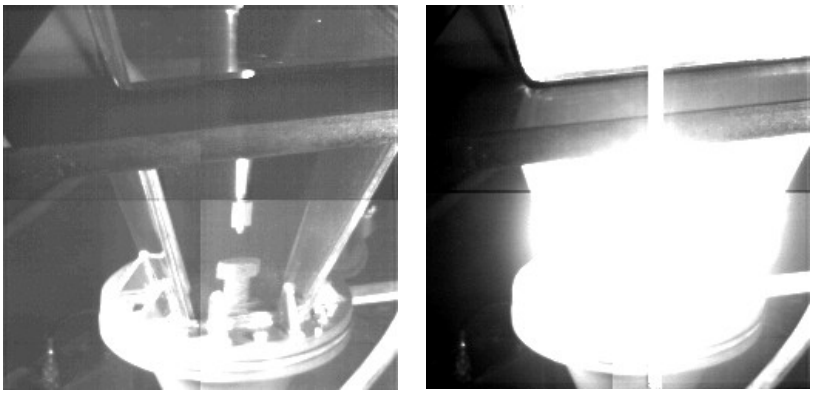


Figure -10: Digital images composed of four frames each, and over-exposure

The bottom right quadrant in the left-hand frame above is exposed slightly more than the other three. The apparent optical distortion of the electrode is due to the angle of the camera in relation to the chamber. The lower part of the electrode was seen through the inclined side-window, whereas the upper part of the electrode was seen through the transparent lid, separated by the angle iron. The photo on the right is a typical example of either over-exposure or incorrect timing in relation to the event.

The mechanical, electronic or optical set-up of the camera did not function satisfactorily and subsequently the other three cameras were used. However, this camera was able to capture a water leakage from the chamber, which originated during discharge at the right-hand corner of the vessel, as shown in Figure 7-11 below.

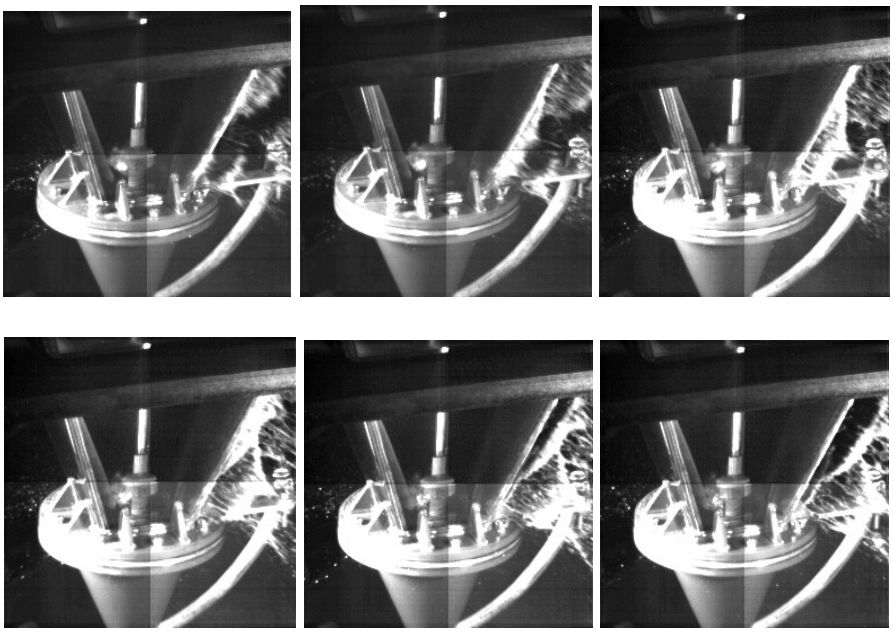


Figure -11: Frames showing water leakage on the right

Since no discharge flash is evident in the sequence, it is assumed that the above sequence was captured after the shock wave had been created by the discharge. The shock wave opened up an existing, fine crack in the corner of the chamber and forced a limited amount of water, like a single wave, through the crack.

Sony Hi 8 colour video camera

To complement the single-shot images of the high-speed camera taken at 1 µs, a Sony Hi 8 camera was installed to record the much slower process of rock fragmentation after the electrical breakdown had taken place. The frames in the sequence below (Figure 7-12) were created by interlaced subsequent frames to

maintain a certain reference with regard to the tip of the electrode and the occurrence of the bright flash.

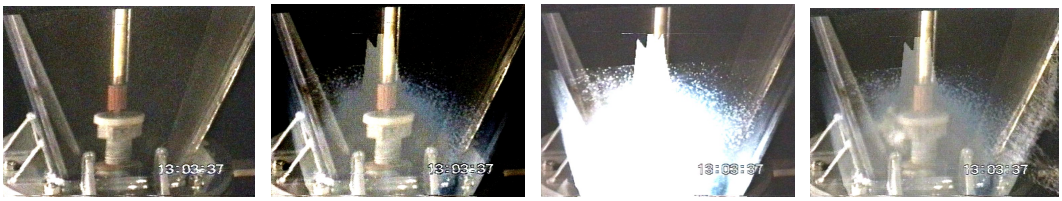


Figure -12: Interlaced frames from Sony Hi 8 camera

The fourth frame in the figure above also shows the discharge of water from the right-hand corner of the chamber as a result of the shock wave created by the flashover. The rock specimen was not damaged in this test. The top peak of the flash has a similar erratic shape to that captured with the FlashCam camera shown in Figure 7-17, bottom right.

Various discharges through the water were recorded with the Sony camera. Initially, the shutter times were set to 'golf' mode (1/4000 s) to capture a very sharp image. However, the number of frames per second that the camera could take was fixed. The time between the frames was therefore extremely long when compared with the event to be captured. This is illustrated in Figure 7.13 below.

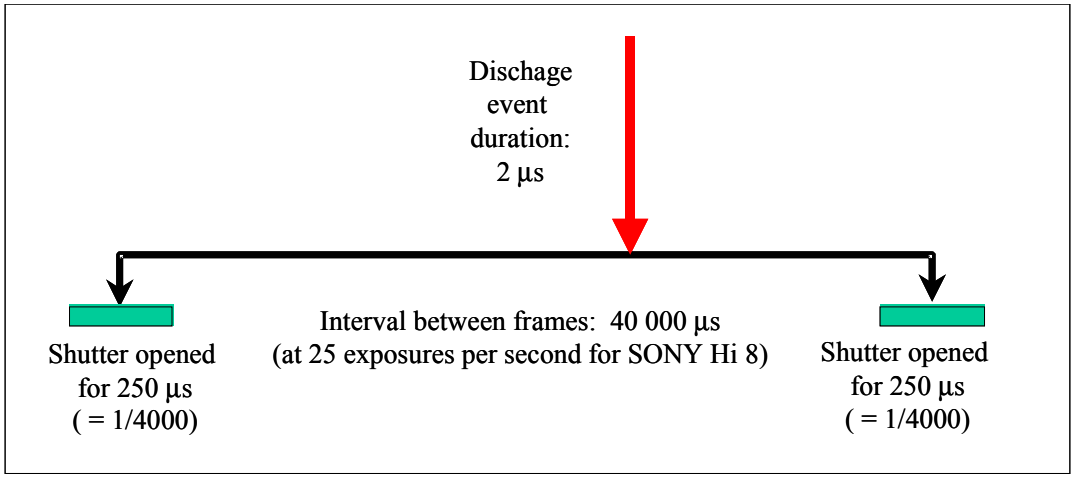


Figure -13: Shutter speed (SONY 'golf' mode) and event duration

When the camera's recording mode was changed to 'moon', the exposure time per frame was increased to 1/50 of a second. Up to five frames per explosive event could be captured, although at a reduced resolution.

FlashCam digital black-and-white camera

A FlashCam camera was provided by Wits which can take up to ten frames per sequence but, since all the frames are superimposed, the result is a single combined photo. Although this camera can capture up to ten frames at a shutter speed of 1/1 000 000 s (i.e. 1 μs width), all these frames would be downloaded in one picture. This camera would be best suited to capturing the bouncing of a white ball in front of a black background: in this case, seven white balls at different positions would be seen. The delay between the individual exposures would determine the distance that the ball would have moved, e.g. if the ball images overlapped partially, the delay times would be too short.

This camera is equipped with a simple facility for downloading the single frame after each shot.

Canon AE1 spool camera

A 400 ASA film was used to obtain sufficient exposure. The mechanical shutter was operated in 'B' mode and the light from the self-illuminated discharge was captured. It was found that if the shutter remained open for about 5 min, the surrounding set-up could also be captured on the same negative.

This camera provided very sharp pictures which provided evidence of the flashover through the comminution chamber – this is shown as a parallel spark in Figure 7-14. Only single images were recorded with this camera, but no fragmentation sequence.

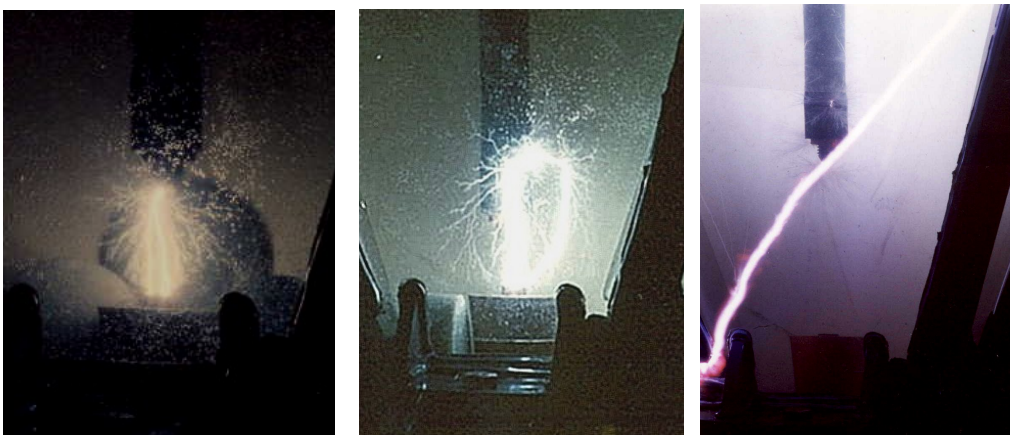


Figure -14: Unpredictable flashovers through water (taken with Canon AE1 spool camera)

The photos on the left show the double spark between the tip of the electrode and the base. The middle picture shows that the flash initiated on the right side of the electrode, about 20 mm above the tip, due to failing insulation. The photo on the right shows a flash across the comminution chamber, ending on a bolt of the outside flange. Its upper point of origin was not captured. The same discharge event triggered some branches treeing from both the electrode tip and the failing electrode insulation. The unfortunate effects of these flashovers were that they affected the monitored voltage and current signals and that additional energy was consumed during single-shot rock-fracturing tests. For any future test work, photographic evidence of each shot could be complemented by high-speed acoustic signal evaluations. They may be able to distinguish between and document a good discharge through rock only, or any other form of discharge through both rock and water.

7.3.5 Photographic settings for discharges through water

Two different images were captured of discharges through water, as shown below in Figure 7.15. The photo on the left reveals a treeing formation at the bottom of the flash, and that the centre of the flash is not in the middle of the discharge path. The vertical bright line next to the discharge path in the photo on the right is assumed to be a reflection of the spark on the Perspex window.

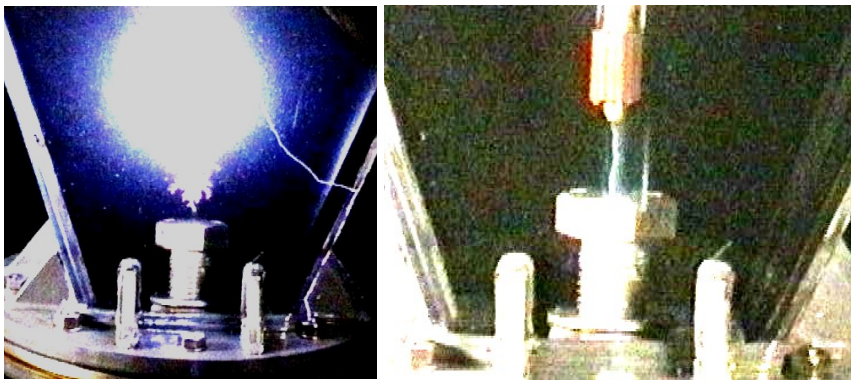
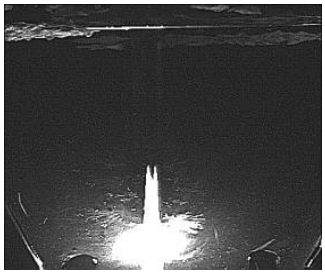


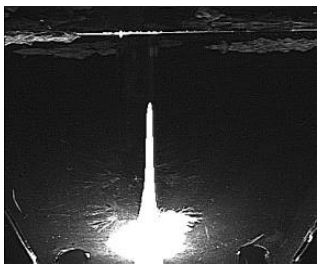
Figure 7-15: Comparison of water discharge pictures (Sony)

Various camera settings on the FlashCam camera were evaluated for capturing the discharge flash. The effect of the camera shutter exposure width, i.e. the shutter speed, is shown in Figure 7-16 below. The camera was tilted downwards at about 30 degrees. In Figure 7-17, the camera was placed horizontally to capture the height and width of the discharge flash.

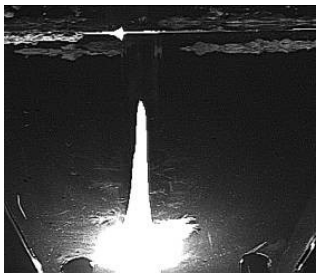
A page break has been inserted here to keep the following four pictures on one page for better illustration.



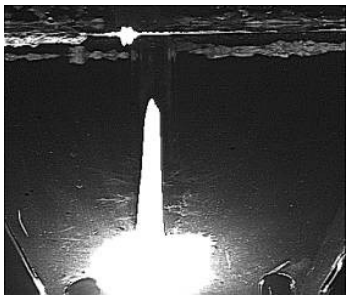
Camera shutter exposure width: 1 µs



Camera shutter exposure width: 2 µs



Camera shutter exposure width: 3 µs



Camera shutter exposure width: 4 µs

Figure -16: Effect of shutter exposure width on flash capture

It appears that a longer exposure width captures a longer discharge path, and that the light originates at the base plate, not at the electrode.

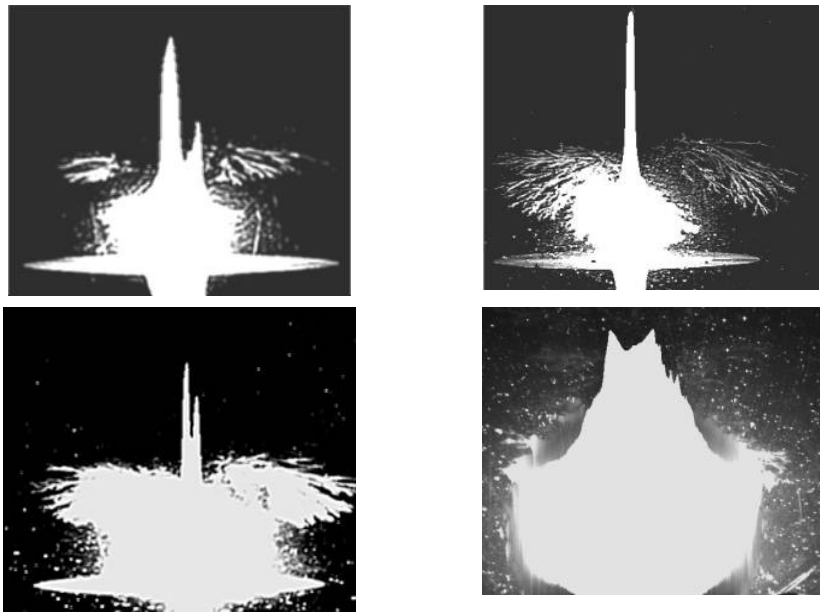


Figure -17: Four individual water discharges, all at 1 µs exposure

The discharges were electrically triggered by the oscilloscope, which monitored the voltage signal across the electrodes. The top right-hand photo in Figure 7-17 shows beautifully the treeing of bright channels, as are reported in the literature. If the timing is not optimal, as for the bottom right-hand photo, overexposure and glare eliminate any detail.

7.3.6 Photographic settings for rock-breaking sequences

The sequence below (Figure 7-18) shows single frames extracted from the Sony recording for each event.

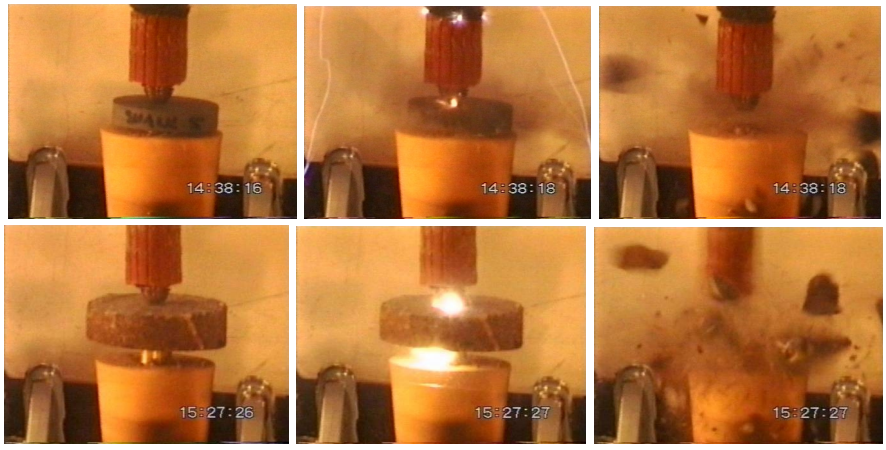


Figure -18: Rock-breaking sequence (Sony video camcorder)

Although faulty insulation was evident in the top middle picture, sufficient energy was deployed to fracture the 8-mm-thick specimen. Bright flashes of light were recorded with the FlashCam camera, as shown below in Figure 7-19.

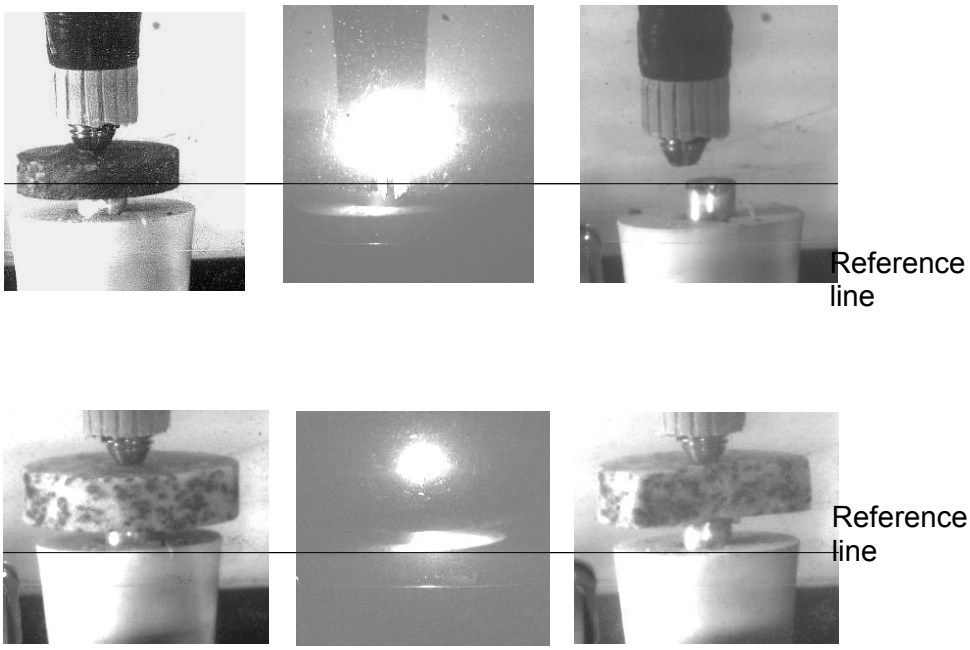


Figure -19: Sequence for rock breaking (FlashCam camera)

The three photos per row above were aligned vertically to the horizontal line for reference. The lower sequence shows the splitting of a 12-mm-thick 'molten rock' type into two fragments, with the larger fragment remaining clamped between the electrodes. The fragmentation of a 20-mm-thick gold-bearing Western Areas Reef specimen was captured on both cameras (Sony and FlashCam), as shown below in Figure7-20.

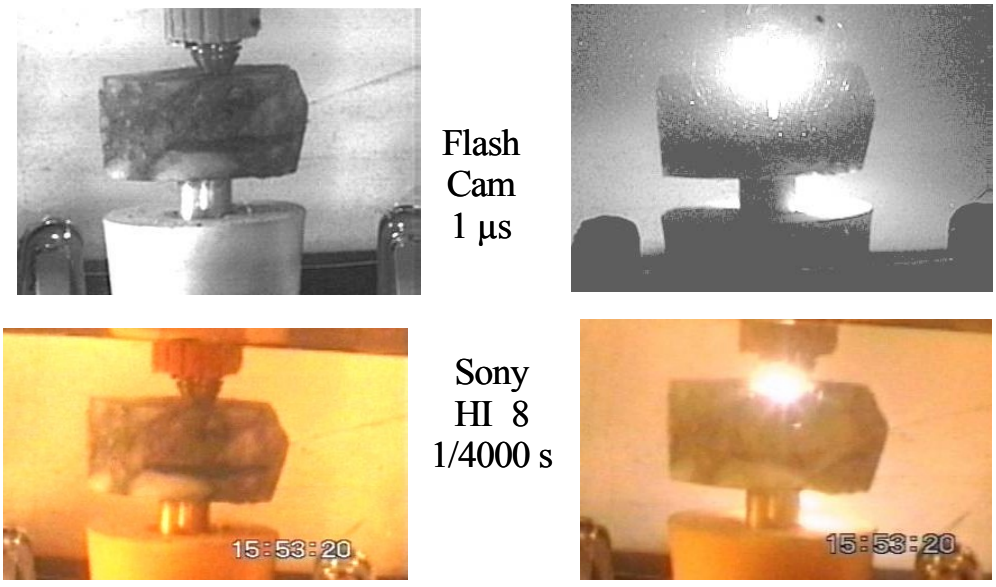


Figure 7-20: Comparison of different cameras for identical discharge through 20 mm gold reef specimen

Considering the long interval during which the shutter is supposedly closed, it is surprising that the flashes were recorded with relatively conventional equipment in the high-speed shutter (i.e. 'golf') mode. It is possible that although the discharge event is very short, the duration of the decay of the heated gas is much longer.

7.4 Quantification of the effect of the water gap on breakdown delays

Initially, discharges through the water were conducted to provide a reference performance for comparison with discharges through various rock types.

7.4.1 Voltage rise times and strength level

Figure 7-21 shows the voltage signals for increasing the water gap. Due to different trigger settings on the various test days and dynamic delays, the voltage signals were shifted in Excel by a few fractions of microseconds on the time scale to show the similarity of the ramp-up patterns. This is the reason why they are so close to each other and aligned, as shown below.

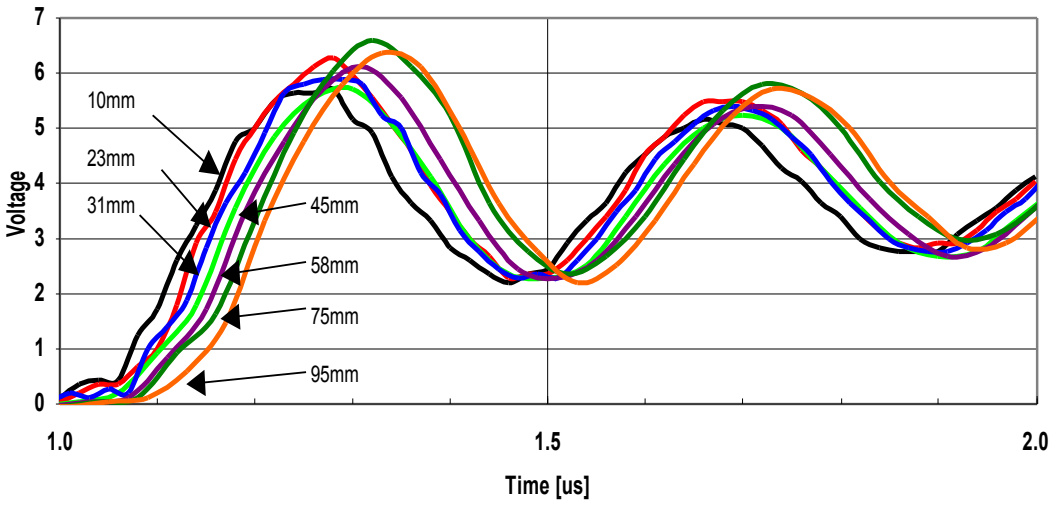


Figure -21: Ramp-up voltages for water tests with different water gap sizes

The figure shows the voltages recorded with the oscilloscope which could be converted into the actual voltages across the specimen. However, the rate of

rise and the repeatability of the ramp-up times are of interest here. It is evident that the entire voltage can be applied across the specimen in 0,2 µs, which is within the rise time required to break rock submerged in water. The exposure time of the high–speed, single-shot FlashCam camera is as long as the entire x-axis in the above graph (1 µs).

7.4.2 Discharge delay with applied high voltage

The gap between the two electrodes was varied between 10 and 57 mm to quantify its effect during direct water discharge without a rock specimen placed between the electrodes. The larger the gap, the longer the delay time. The maximum applied voltage was the same for each test, but with increasing gap distance, the delay before discharge increased, as shown in Figure 7-22.

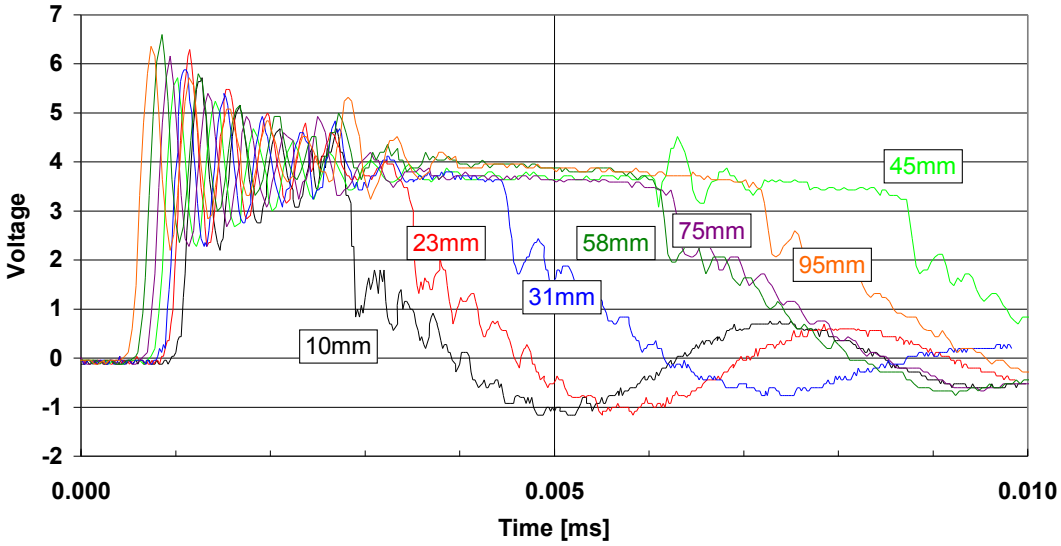


Figure -22: Discharge delay through water

As mentioned before, the time scales were shifted horizontally by fractions of microseconds to show an almost similar ramp-up point. The final ramp-up level was always the same voltage per Marx stage. The significance of the above figure is the increasing delay with increasing gap size.

It is evident that after the sharp rise, which is equivalent to the charge voltage of the Marx generator, the voltage oscillates around a constant value. This effect was typical for the configured rig set-up.

7.4.3 Current wave-form during discharge

Maintaining the same shift of the x-axis as in Figure 7-22 above, Figure 7-23 below shows the corresponding current wave forms. As with the voltage signal, the 10 mm gap setting had the shortest, and the 45 mm gap setting the longest delay time between ramping up and final breakdown.

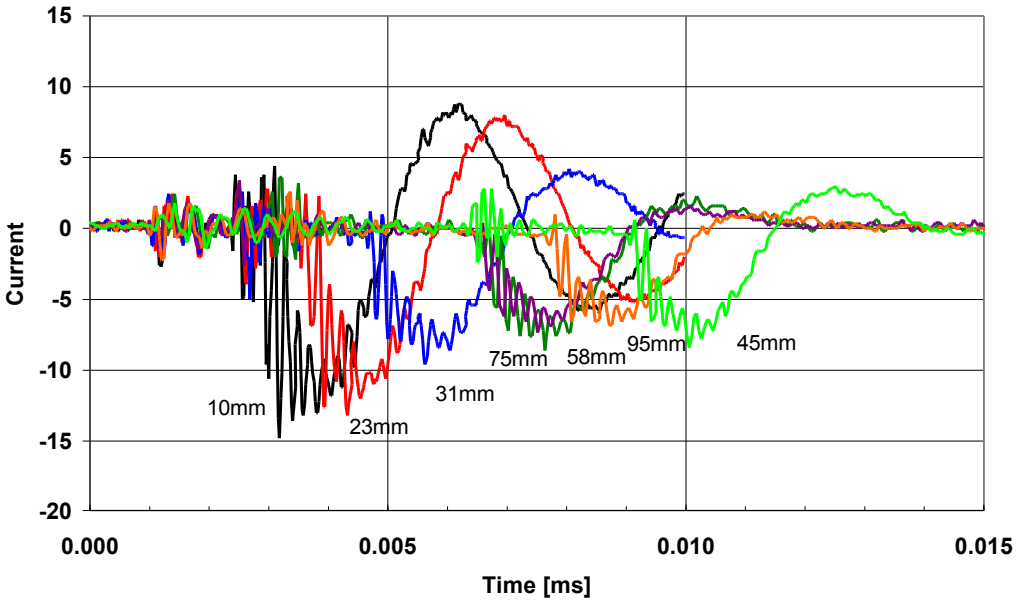


Figure -23: Currents for water discharges (moving average 2)

It can be seen that only at discharge does the current start to flow. By increasing the moving average from 2 to 10, the wave-form pattern becomes clear and distinct, as shown in Figure 7-24.

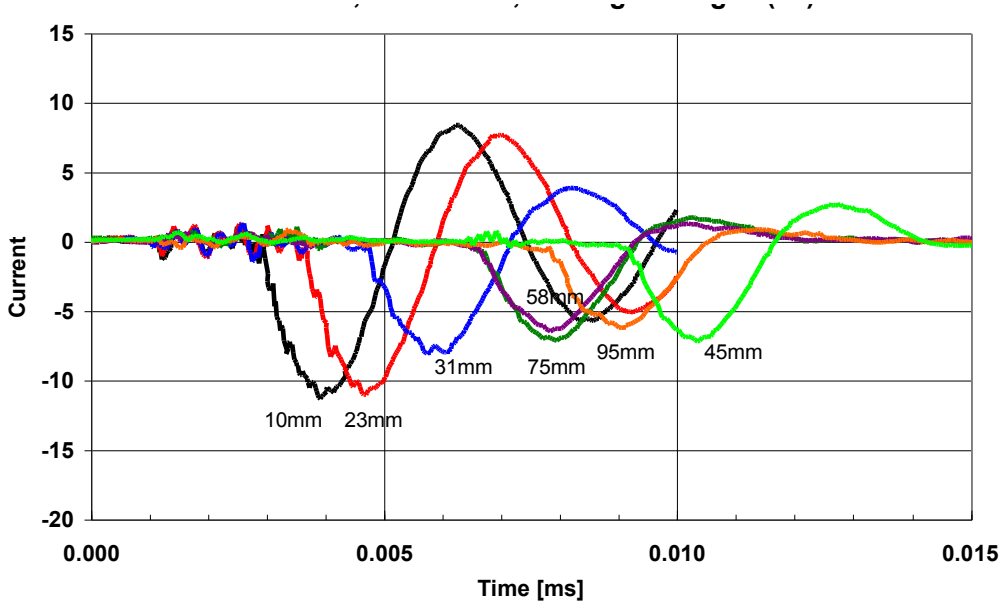


Figure -24: Currents for water discharges (moving average 10)

The 'out of order' result with 45 mm water gap is discussed in more detail later.

Figure 7-25 shows the voltage breakdowns for the tests with clear water at various gap sizes. All signals were shifted horizontally to provide an overlap at the relevant breakdown times. This allows a visual comparison of the various patterns to be made.

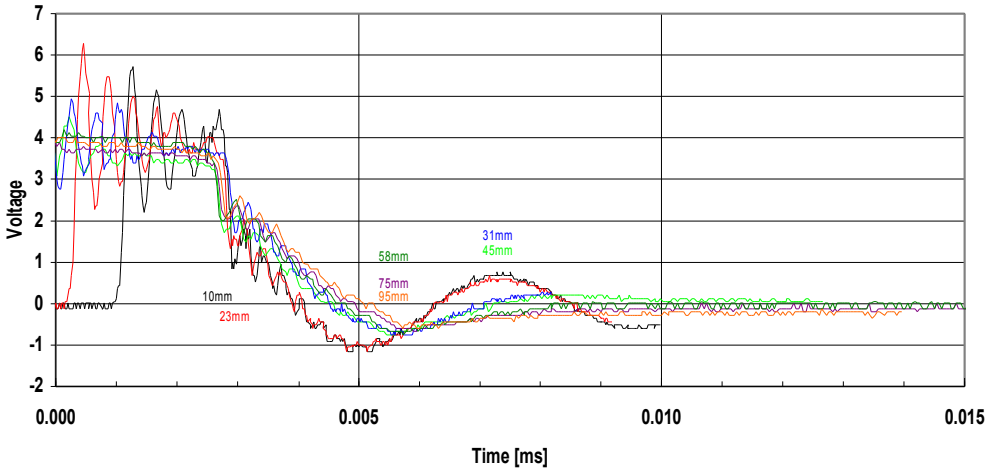


Figure -25: Water discharges, aligned to voltage breakdown event

Only the discharges through small water gaps of 10 and 23 mm displayed a meaningful second wave form, climbing back to about 20 % of the original value. Not the entire charge is released into the water. This means that excess energy remained in the electrical system. The remaining energy oscillates forwards and backwards within the electrical components.

7.4.4 Breakdown delays through water

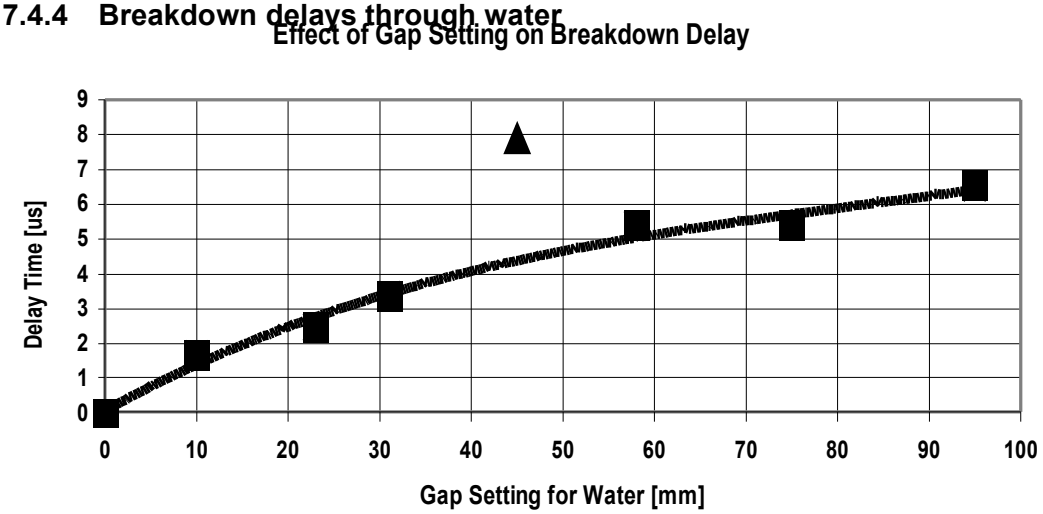


Figure -26: Effect of water gap on breakdown delay

The breakdown peak voltages were the same (Figure 7-26). The phenomenon of delay is due to the polarisation required of the water molecules to initiate the development of a suitable breakdown path.

The wave form for the test with 45 mm gap setting was assessed in more detail to see if something unusual occurred. While the 'normal' delay took place at high voltage, the voltage signal displayed a spike, associated with oscillation of the current. This event was set to trigger the data logging of the oscilloscope. When triggered, the oscilloscope also stored data before the trigger event, in an overriding, temporary memory. From the trigger event (time = zero), the time scale is positive, as shown in Figure 7-27 below.

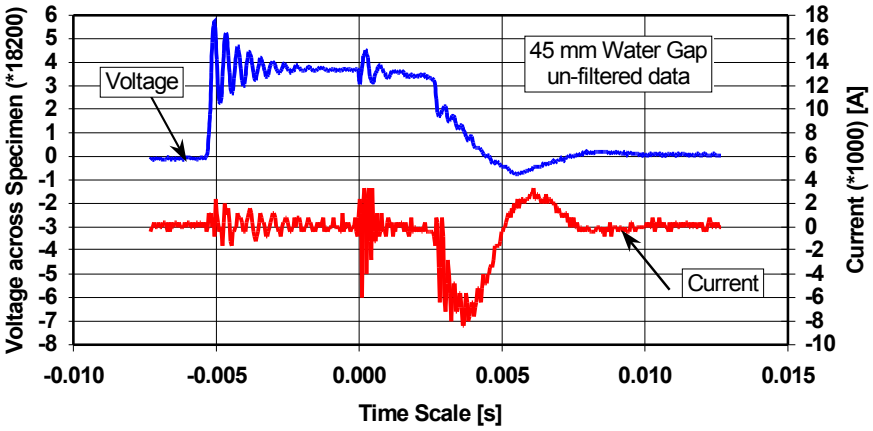


Figure -27: Traces for the 45 mm water gap test

It remained unclear why the discharge delay took so much longer for this gap setting than was expected in relation to the other delays. (**N.B.** Future test work must include sufficient time to allow repetitive tests for confirmation.)

The signal noise in the traces in Figure 7-27 was reduced by applying the Median function in Excel as a filter over 10 values. The pattern in Figure 7-28 shows a small increase in voltage, as well as a temporary flow of current in the opposite direction from the direction during normal discharge, but without triggering the discharge event.

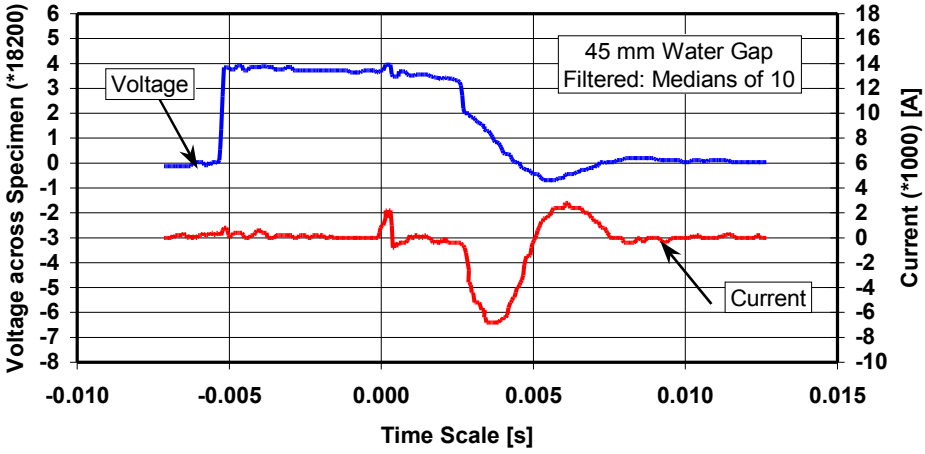


Figure -28: Median of 10 for the 45 mm water gap test

It remains unclear why the discharge was delayed for so long, and why the current reversed temporarily. It may be attributed to the dynamic interactions associated with high-voltage tests and charged components.

7.5 Summary

Based on the literature review and FZK's experience, a high-voltage rock breaking test rig was established at Wits, which proved to be the most feasible location for conducting systematic research work.

Various photographic means were tested in terms of resolution, shutter speed and successful trigger mechanism. The light created during the discharge had to be balanced with the ambient light to illuminate the specimens and the fragments themselves. Unfortunately, it was not possible to track and record in detail the individual discharge paths through the rock due to the violent and bright nature of the event, and due to the minimum distance that the electronic equipment had to be placed away from the intensive fields around the comminution chamber.

Rock clamping, power supply, voltage rise rate and maximum voltage level, as well as voltage and current recording equipment, were configured successfully in this first test rig for electric rock breaking in South Africa to match the reported overseas performances.

The water test results varied slightly from day to day, but this variation was less than the differences in rock breaking. The rig was suitable for conducting a systematic test programme with various geometries of different types of rock and reefs.

8 ELECTRIC ROCK BREAKING TEST WORK

8.1 Geometries of Various Rock Types

The rock types varied from gold-bearing reef and waste to UG2 and Merensky. Dykes and shales were also included, as well as quartz, which was expected to be a control sample. The available core samples varied in diameter and thus it was difficult to obtain exact matches of specimen geometry in terms of sample diameter and thickness.

The limited stock of core samples with diameters of 32 and 16 mm were cut into discs of heights 16 and 8 mm. Samples with diameters of 46 mm were cut into disks of 6, 12, 24 and 46 mm in thickness. The largest-diameter core samples in the collection have a diameter of 66 mm and were cut into cylinders with heights of 66 and 33 mm. Some UG2 samples were prepared with thicknesses of up to 80 mm, but it was not possible to test them using the six-stage configuration at Wits.

8.2 Evaluation of Electric Rock Breaking Signals

The initial fragmentation tests were conducted with a high power output to ensure fragmentation and the creation of discharge paths for analysis. The settings of the oscilloscope were varied to determine the best settings for triggering the FlashCam camera with a TTL circuit. Detailed understanding of the events that occurred with each discharge only emanated a few days after each test day. Thus, a series of tests was conducted as planned and any discovery or fault was only discovered after the tests. The video images had to be analysed frame by frame so that they could be studied in detail. The time scale for the oscilloscope was long in order to capture the dampening after the discharge. The detailed voltage and current traces for the ramp-up pattern and electric discharge had to be exported to Excel for detailed analysis and interpretation.

Many results were not really usable because the first discharge passed through the water, which led to some compression of the specimen and may have conditioned the rock electrically prior to the next single discharge with a higher charge voltage. Some discharges were very violent, as evidenced by the loud accompanying sound. (It felt like shooting ants with canons, and then trying to

determine in which order the ants' legs had been broken!) Other discharges threw the specimens undamaged off the clamping arrangement with the electrodes; some were reused at higher voltages in an effort to create fragmentation nonetheless, but the electrical and mechanical properties may have been altered during the first discharge. Unfortunately, many of the prepared specimens were lost without meaningful results being obtained.

It was decided to improve the sensitivity of the charge-up procedure, as well as the ability to obtain an immediate indication of the effectiveness of the breakdown. A decision could then be made either to select a thicker specimen from the same rock type, or to increase or decrease the Marx generator's cap setting.

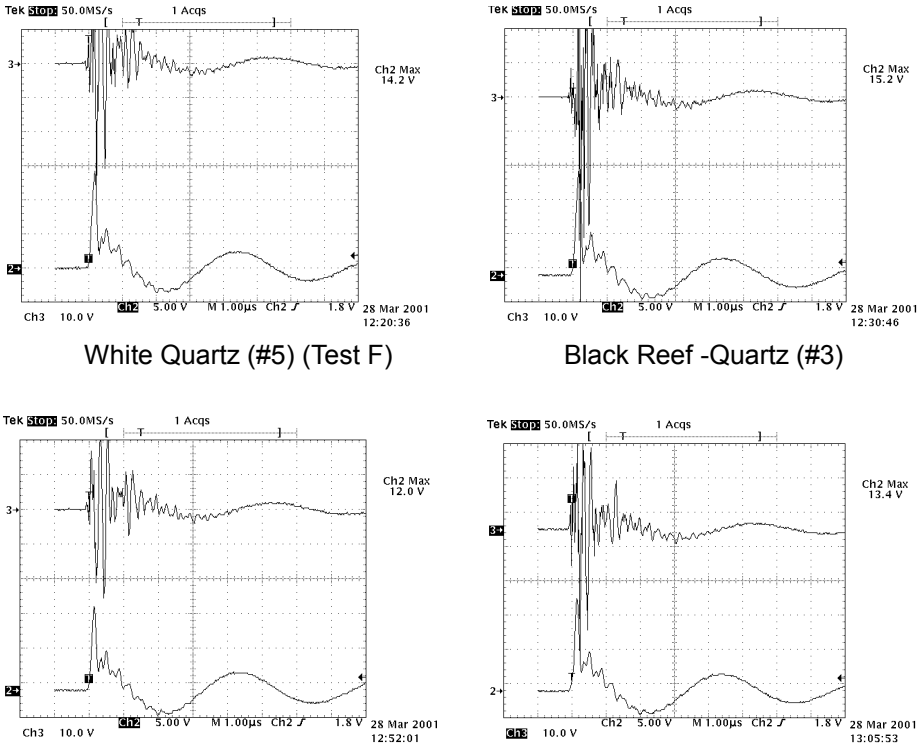
Thus, in addition to each visual inspection of the fragmented rock, the peak voltage at which discharge took place was included in the oscilloscope's display of every discharge. The current signal was too noisy to be meaningful, but it was decided not to filter it prior to logging in order to enable possible future analysis.

The manual trigger box was not reliable for inducing discharge. The caps of the Marx generator were therefore set to the highest possible setting of 20 mm. This enabled the Marx generator to be charged gradually – it was controlled manually for a few minutes each time. The gap setting of the cap for the lowest stage was set slightly smaller to initiate the first flashover, which mobilised the entire discharge.

After the rig configuration had been fine-tuned, including the setting of the scope, a systematic test series was conducted with same-sized specimens, with a diameter-to-thickness ratio of four, i.e. a 32 mm disc diameter and an 8 mm specimen thickness. These specimens were initially tested for their electro-dynamic resistivity, as shown later in Figure -65 .

The original oscilloscope traces of the discharges for the various specimens are shown below in Figure -57. Channel 2, i.e. the curve at the bottom of the scope chart, refers to the breakdown voltage, after it had been reduced by the high-voltage divider and a 1 MΩ resistor. The oscilloscope voltage therefore needs to be multiplied according to the factors given in Table -1 to calculate the actual voltage across the specimen, if required.

Three different VCR and two different quartz specimens were tested to provide a typical average for these inhomogeneous rock types.



White Quartz (#5) (Test F)

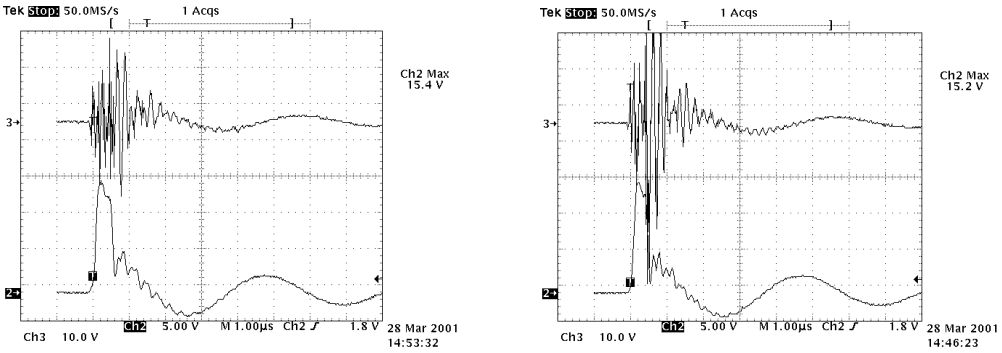
Black Reef -Quartz (#3)

VCR (#3) (Test J) more evenly sized grains than VCR (#5) & (#4)

VCR (#4) (Test I)

Figure -57: Oscilloscope traces for VCR and quartz specimens

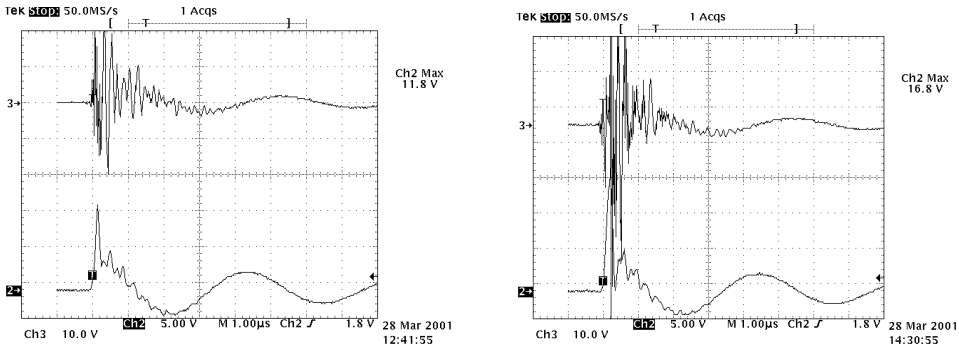
The oscilloscope traces above show almost identical voltage patterns for the quartz and VCR specimens, with a sharp drop to about 50 % of the initial voltage immediately after breakdown. The noise and amplitude in the current signal of the Black Reef Quartz specimen was significantly higher than in the VCR (#5) specimen, due to the higher peak voltage of 15,2 V in the Black Reef Quartz compared with 11,8 V for the VCR. The voltage breakdown was delayed after ramping up for the Kudu Dyke and Lava specimens, as shown in the oscilloscope traces in Figure -58 below.



Kudu Dyke (#5) (Test M) Lava (#5) (Test N)

Figure -58: Oscilloscope traces with delayed breakdown for Kudu Dyke and Lava

A direct comparison of the lowest and highest voltages recorded, for the VCR (#5) specimen and the Square Pebble Marker (#5) respectively, is given in Figure -59 below using the same scale factors for the scope display.



VCR (#5) (Test H) Spare Pebble Marker (#5)

Figure -59: Oscilloscope trace comparison: VCR Spare Pebble Marker

8.2.1 Breakdown through reef

The oscilloscope traces were exported to Excel to provide multiple charts for direct comparison of the voltage patterns. The more interesting discharges are shown in Figure -60 below for comparisons between reef and footwall (F/W) samples from tests A, B, C and D.

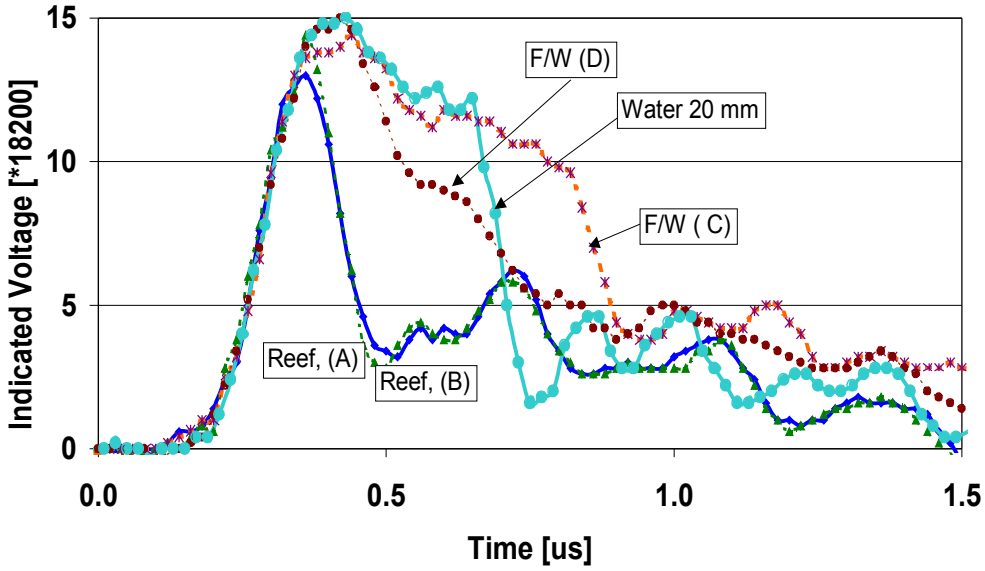


Figure -60: Preferential discharge through reef types, 20 mm thick

The non-reef types show clearly a significant delay between ramping up and eventual breakdown.

Based on the scatter of rock results, which seemed to be generated by a variety of unappreciated effects, it was decided to conduct standard water tests more frequently as a means of referencing and calibration, especially when components were temporarily removed from the circuit for other users. Reconnecting them might have affected the quality of the contacts for components such as: charge transformer, scope connectors, Pierson coil, trigger box, etc. Water quality decay may have occurred during the tests, and there may have been changes in the atmospheric moisture content, which affected the air immediately above the water in the comminution chamber and the condition of the air between the Marx generator caps. (FZK used a gas-filled chamber to house the Marx generator caps.)

Even with additional precautions and trying to maintain similarity as much as possible, it was found that the water test results were scattered. The 20 mm water gap results shown in Figure -60 above are therefore not from the initial water test series, but from a water test conducted on the same day as the rock tests. This scattering would require more detailed testing, including water quality analysis after each discharge.

8.2.2 Unsuitable rock types – unwanted discharge through water

Figure -61 confirms with different types of specimens, but with the same specimen geometry of 8 mm thickness and 32 mm diameter, that mineralised reef specimens are significantly more susceptible to electric breakdown than non-reef rock types.

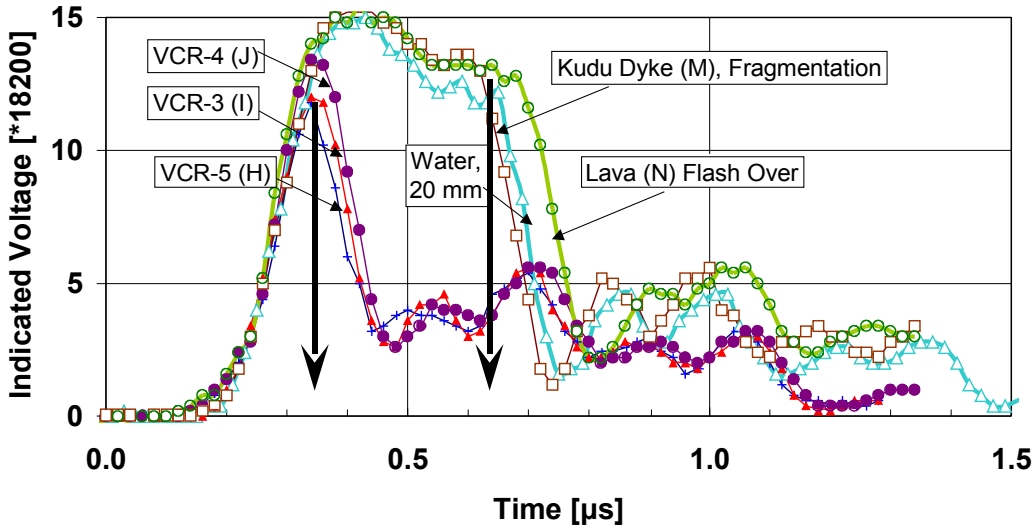


Figure -61: Discharge through VCR, Kudu Dyke and Lava, 8 mm thick

The data were imported into Excel from the oscilloscope traces. It is clearly shown that the three VCR samples facilitated a sudden breakdown while the voltage was ramping up. The Kudu and Lava specimens either fragmented or resulted in flashover through the water, thus bypassing the rock.

8.3 Associated Currents to Above-Voltage Signals

The current signal was recorded with the oscilloscope unfiltered to avoid losing any potentially interesting wave form patterns. It was not known at the time how to design such high-frequency signal filters, which could eliminate circuit-specific electrical noise, but maintain the features of electrical breakdown through rock or water.

Aries Partners (Hinde and Joosub, 1998), Bialecki (Kramers, 1997), see Figure 6-9, and Andres (1989) reported very smooth current wave forms. These might have been processed to eliminate any noise and to illustrate the principle rather than providing accuracy. Appendix D provides the voltage and current traces

from Aries Partners, which were part of a technical appendix in the report from Hinde and Joosub, and published images from oscilloscope traces from Andres (1989). Their test rig set-ups had matured over many years, whereas the test rig at Wits was in its infancy. During the author's visit to FZK in Germany in 1998, FZK hinted that they were investigating suitable filters for their continuously operating Franka-Stein Plant.

The approach to data analysis during the exploratory fragmentation work for this dissertation was to use Excel functions (e.g. Moving Average or Median) in preference to filters to avoid losing data on unique breakage tests which could, by their nature, never be repeated with rock specimens having the identical properties.

The following two figures show current traces grouped together for similar rock types. The breakdown through the VCR specimens occurred at 0,35 µs (Figure -61) and the associated current traces are given below (Figure -62).

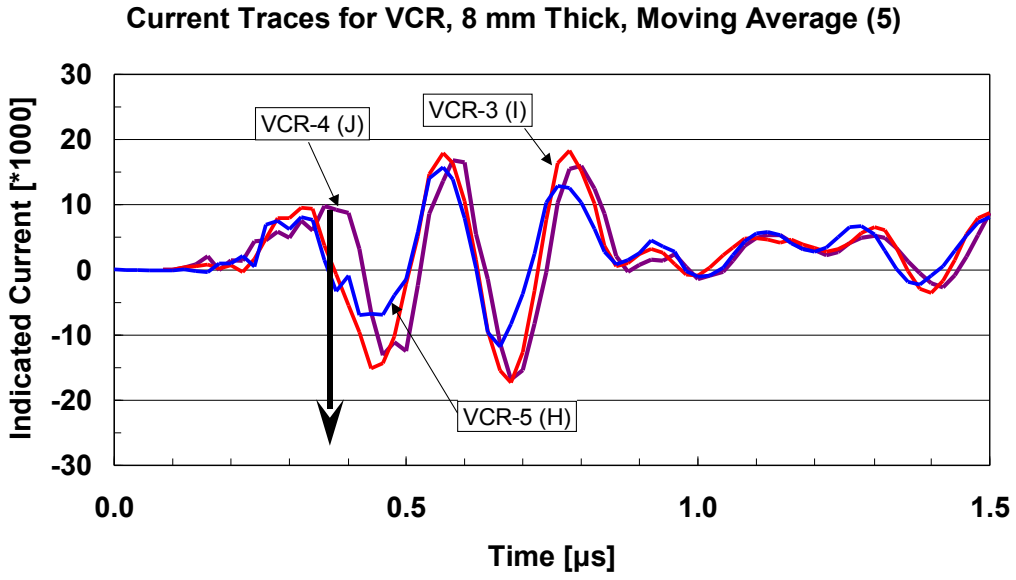


Figure -62: Current traces through VCR, 8 mm thick, moving average of 5

The figure above shows the traces smoothed with a moving average of 5, which provided the best data interpretation. All three events were very similar in terms of the initiation time of the currents, their direction (positive in this case), the inherent system frequency, the magnitude and the duration after the breakdown. However, it is unsatisfactory that the current oscillates around zero. This makes it difficult to calculate a reasonable energy consumption.

Less similarity was evident for the Kudu Dyke and Lava specimens of equal geometry, as shown in Figure -63 below.

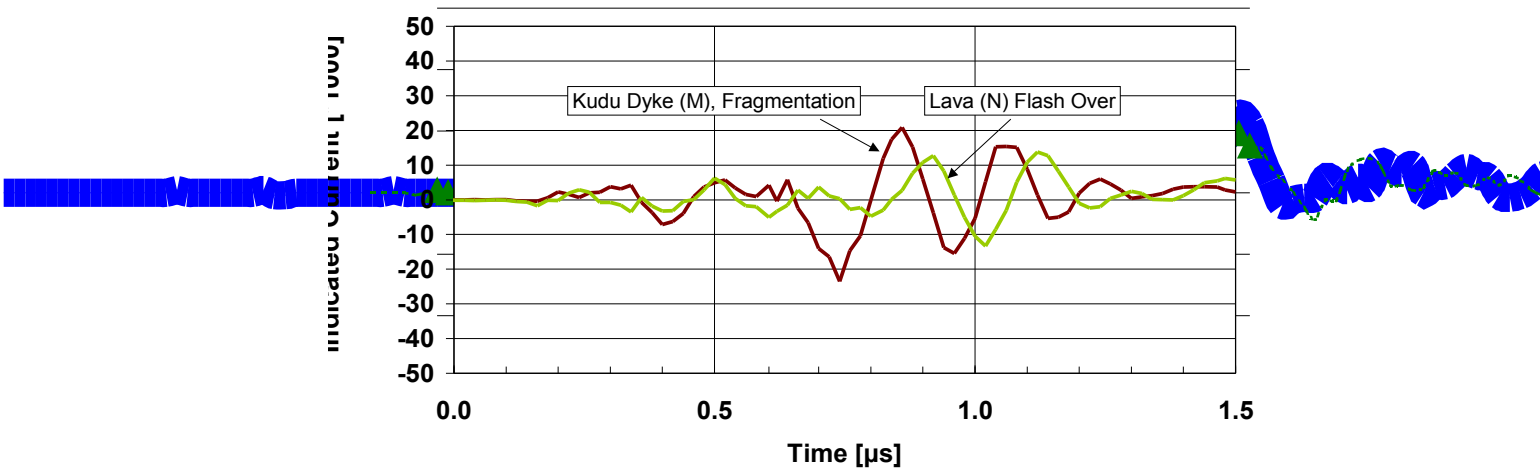


Figure -63: Current traces for Kudu Dyke and Lava, 8 mm thick

The time scale in the above figure relates directly to the time scale for the applicable voltage traces shown in Figure -61. At voltage breakdown across the specimen, at approximately 0,7 µs for both Kudu Dyke and Lava, only the current of the Kudu Dyke sample shows an appreciative increase after the initial noise during ramp-up. This selected response created some doubt about the competence and repeatability of the available components of the circuit.

8.4 Energy Consumption

In order to estimate any meaningful energy consumption, it was hoped that voltage and current signals could be used to calculate the energy consumption associated only with the fragmentation. The phase angle between the two signals seems to shift during the sudden discharge. No meaningful results were obtainable.

It was difficult to identify the transition from useful energy transfer into the rock to create fragmentation, and the subsequent 'useless' energy consumption due to oscillating energy. It appears that the electric system induced some form of energy oscillation forwards and backwards within a short period of time. This alone consumed part of the overall energy. In practice, any post-fracture power consumption would be part of the overall system efficiency, which appears to be rather low.

8.5 Electrical Rock Properties

The core diameters varied from site to site and the samples were cut into cylinders and discs of different thicknesses to produce width-to-height ratios ranging from 1 for the cylinders (18 by 18 mm) to 4 for the thin discs (8 mm thick and 32 mm diameter). The decision about the geometry depended on whether sufficient sample length was available, and on the natural grain size distribution and homogeneity of the samples. This was done to ensure geometrical symmetry during the measurements of electrical properties, as well as for the intended application of single-shot electric discharges perpendicular to the parallel faces of the core samples.

All rocks have complex structures, which will affect their overall electrical properties, namely resistance, and inductive and capacitive properties, as shown in Figure -64 below.

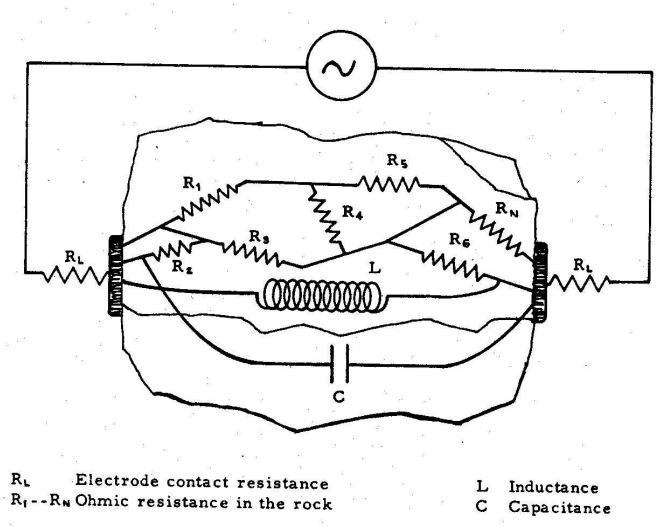


Figure -64: Complex electrical properties of rock (Sarapuu, 1973)

Resistivity and dielectric constant measurements were performed using the thinnest discs, which were 8 mm thick. To ensure good electrical contact for the current electrodes, a strip of tin foil was used. The ends of the sample were dipped in soft solder. The electrical properties were measured using a Hewlett Packard RF vector impedance meter.

The dielectric constant and resistivity were measured at room temperature at a frequency of 16 MHz. Figure -65 below shows the results of two samples taken

from the same core for each rock type. Unfortunately, no UG2, Merensky or Kimberlite samples could be prepared and tested with this small geometry of 8 by 32 mm. Larger geometries would have created different side and end-effects, making any quantitative comparisons doubtful.

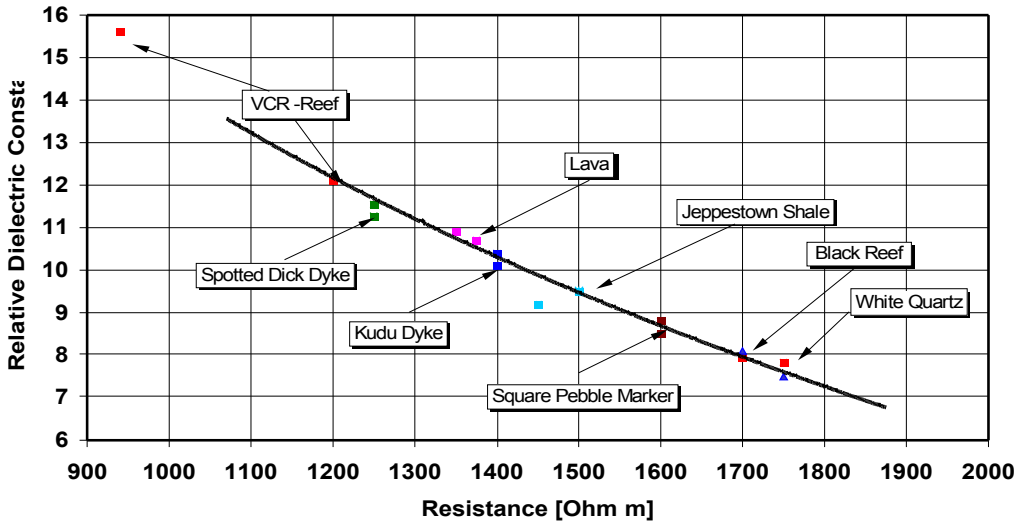


Figure -65: Electro-dynamic rock properties

As expected, good correlation was obtained between the two physically related rock properties. The ranking of the materials was intended to provide an indicative order in terms of the samples' potential for electric comminution. The graph indicates that the VCR samples have a lower resistance than the non-gold-bearing materials, but also a much wider scatter.

8.6 Correlation of Electrical Rock Properties and Breakdown Voltage

The breakdown field strengths for the 8 mm thick and 32 mm diameter specimens were calculated from the voltages across the specimens and the specimen thickness, and are shown in Figure -66 below, sorted by increasing value.

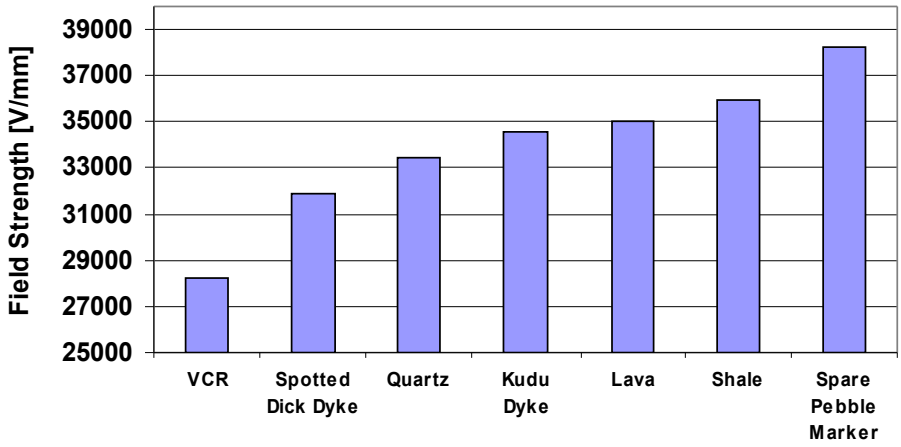


Figure -66: Breakdown field strengths for various rock types

8.7 Correlation between dynamic resistivity and breakdown field strength

In order to determine whether there was a correlation between the relative resistivity property measured while applying a 16 MHz frequency (Figure -65), and to determine the field strength at which discharge took place (Figure -66), averages for the two quartz and the three VCR samples were calculated. The VCR samples had the lowest resistance and the lowest field strength requirements at discharge.

The correlations between resistance and breakdown voltage are given in Figure -67 below. The quartz specimens had a high resistance, but discharge took place at a low field strength. Thus, after the exponential trend line had been fitted, a poor correlation coefficient of 0,46 was evident, as shown below.

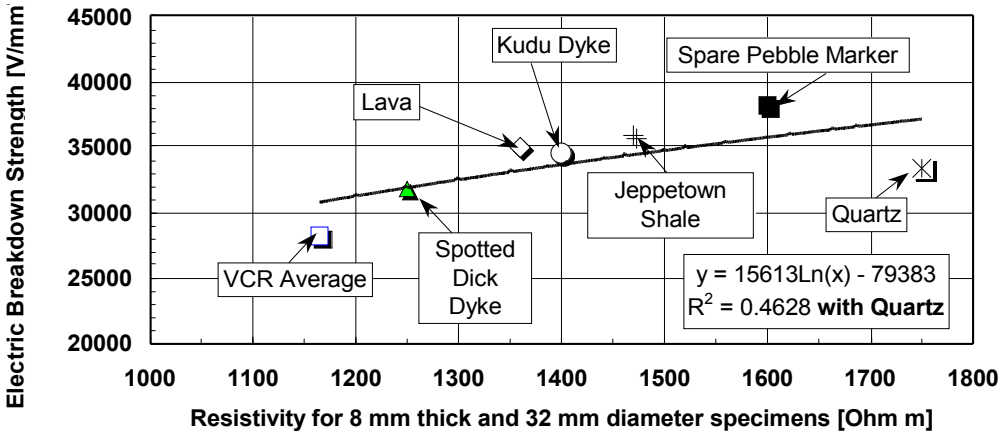


Figure -67: Correlation <u>with</u> quartz results

Because the quartz specimens were only intended as a control rock type, without the variety and complexity of the mineralised samples, the correlation coefficient, R^2, **without the quartz specimens** shows a dramatic improvement to 0,95. The results are shown in Figure -68 below.

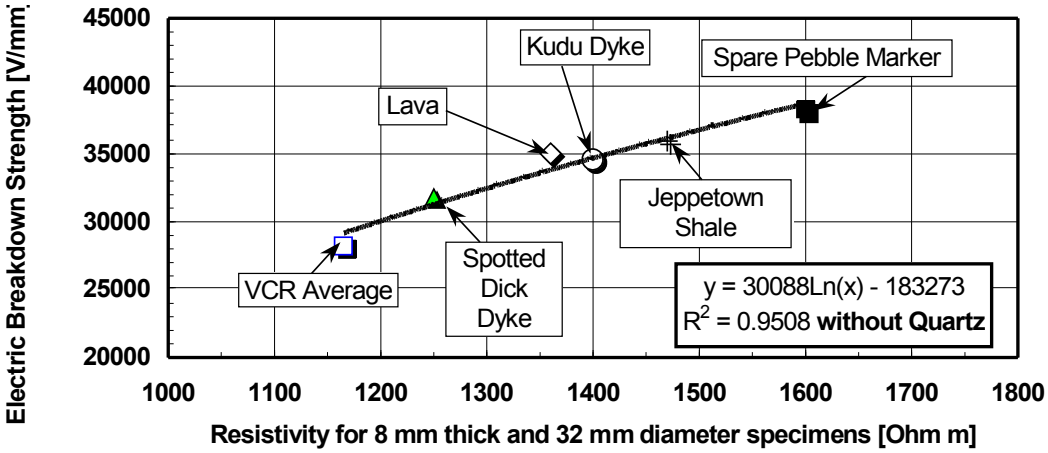


Figure -68: Correlation <u>without</u> quartz results

It is therefore concluded that it should be possible to estimate breakdown field strengths for various reef types on the basis of dynamic resistivity tests at 16 MHz.

8.8 Assessment of Reef Type, Fragments and Specimen Thickness

The following observations are indicative for the different rock types. Even duplicate specimens of the same core samples can vary considerably, and a large matrix of tests would be required to determine this effect, similar to the 275 tests conducted by Andres (1989) on **one** type of specimen.

Figure -69 shows the fragmentation of Carbon Leader Reef specimens. The specimen in the left-hand photo was 8 mm thick and had a diameter of 16 mm, and the specimen in the right-hand photo was 8 mm thick and 32 mm in diameter. The single discharge shattered the rock into large fragments without the creation of fines.

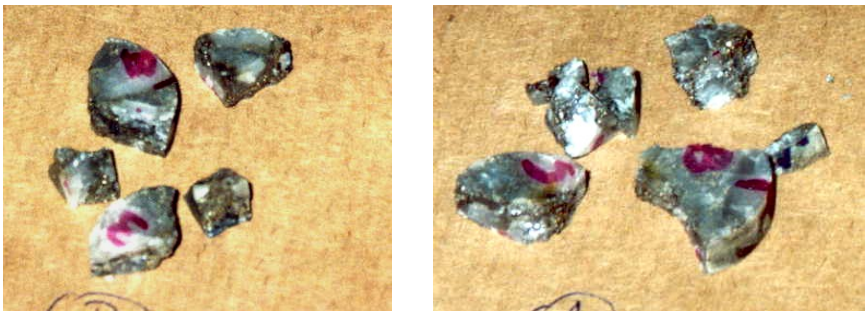


Figure -69: Carbon Leader Reef, no fines creation

The UG2 specimens shown in Figure -70 below had different thicknesses, but the same diameter (40 mm). The thinner specimen on the left-hand photo broke into largely pie-shaped fragments, whereas the thicker specimen shattered into various shapes of different sizes. Also, a lot of very fine particles in the sub-millimetre range were produced from the thicker sample.

There was insufficient evidence as to whether the amount of fines was proportional to the thickness of the specimen. If there *was* a relation, it could be argued that with the thicker sample and multiple fragments, significantly more new surface areas were created, which would mean a more efficient fragmentation process.



Figure -70: UG2 specimens, 8 mm thick (left) and 40 mm thick (right)

The Elsburg Formation gold reef test specimens, which are very mineralised with large grain sizes, were found in every test series to be very suitable for dielectric breakdown comminution, as every test resulted in successful fragmentation. Although no sound wave patterns were recorded for analysis during this study, each discharge through this reef type created a subjectively 'stronger' sound, which was a combination of the sparks created at the large capacitor balls at the

Marx generator, as well as the discharge shock wave created in the comminution chamber. The fragments from some larger test specimens are shown in Figure -71 below.

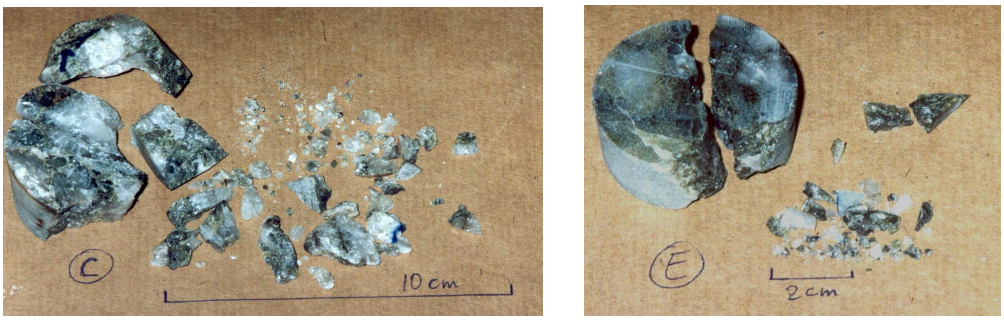


Figure -71: Gold reef, Elsburg Formation, sample fragments

There was no evidence of any remaining plasma in the discharge paths.

The largest Kimberlite sample tested had a diameter of 50 mm and a thickness of 56 mm. It was broken simply into two half-moon-shaped fragments, without any fines creation. This broken specimen is shown in Figure -82 with the whitish area that was occupied by the plasma.

According to the theory of growing channels, the plasma trace would have been initially a thin channel between the electrodes, which widened during the explosive phase. As the channel became wider, the remaining area, still keeping the specimen together, reduced proportionately. The pressure created tensile stresses in the surrounding rock, which eventually exceeded the tensile strength of the Kimberlite material and the specimen broke in half.

The smaller Kimberlite specimens broke into multiple pie-shaped samples, like the thinner UG2 specimen.

8.9 Effect of specimen thickness on breakdown voltage

After the test rig had been fine-tuned and the systematic tests with 8-mm-thick specimens had been completed, the effect of the thickness of selected rock types was tested for three different reef types up to 56 mm in thickness. The results are shown in Figure -72 below.

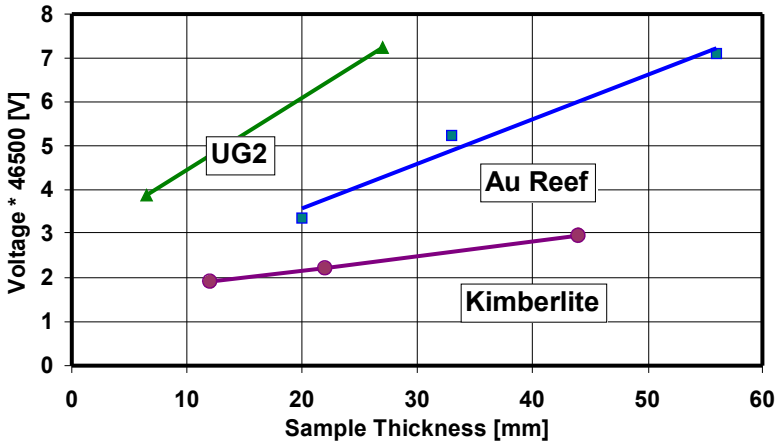


Figure -72: Effect of specimen thickness on breakdown voltages

The voltage across the specimens appears to increase linearly within the thickness range tested for each reef type. This is significant and shows that the test rig was able to identify certain trends for electric rock breaking.

The correction factor (on the y-axis in the figure above) from the voltage divider was changed for these test series from 18 200 to 46 500 to accommodate the higher breakdown voltage, as detailed in Table -8.

Figure -73, Figure -74 and Figure -75 show exact voltage patterns for the three different reef types (Kimberlite, Elsburg Formation, and UG2) at various specimen thicknesses. The vertical axis shows the actual voltage across the specimens during initial ramp-up and subsequent breakdown. (**NB:** The three Kimberlite specimens used in these tests were Kimberlite types available at the CSIR from another project, and thus were randomly labelled A, B and C for reference.)

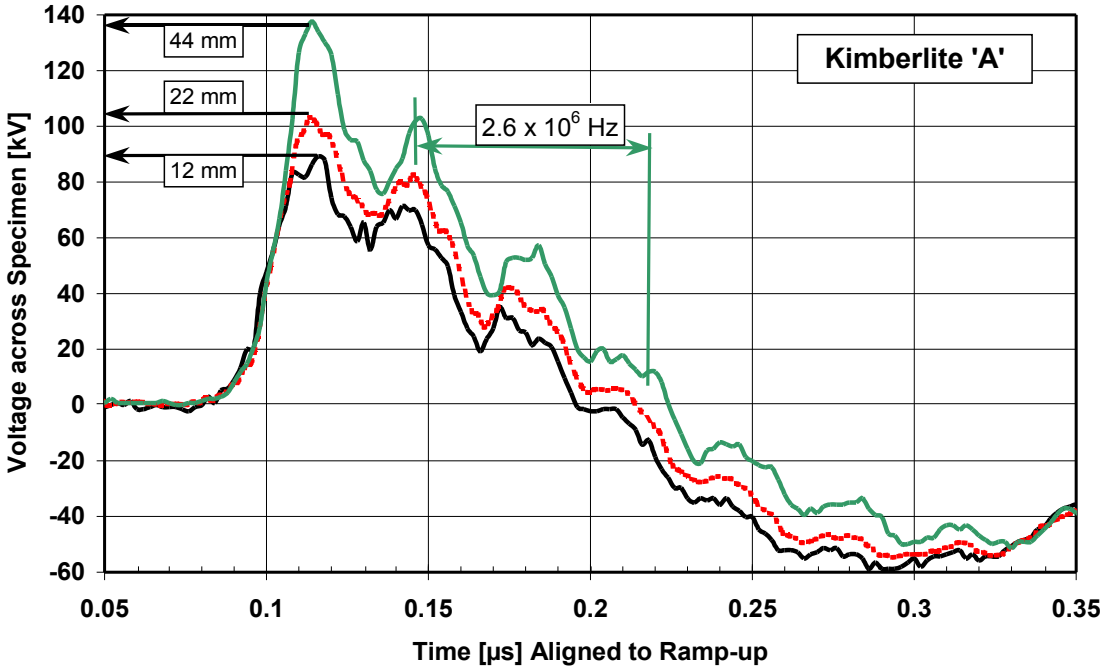


Figure -73: Voltage breakdown patterns for Kimberlite 'A' specimens

Figure -73 shows that immediately after breakdown (i.e. during discharge), all three voltage signals show a very similar pattern of oscillation and voltage decay. The time for two sinusoidal cycles was used to better identify the wave pattern and to calculate the oscillation frequency. As confirmed in Figure -74 and Figure -75, this frequency of about 2,6 x 10^6 Hz was constant for the different rock types, as well as for water. Thus, it is assumed that this is a dynamic system characteristic, which may also affect the phase angle of the oscillating energy after discharge.

The above figure also shows that with increasing specimen thickness from 12 to 44 mm, the voltage across the specimen rose to higher levels for the thicker specimen. Although the voltage increased, the electrical field strength in [kV/mm] across the specimen prior to breakdown decreased. This is shown in the summary Figure -76 later.

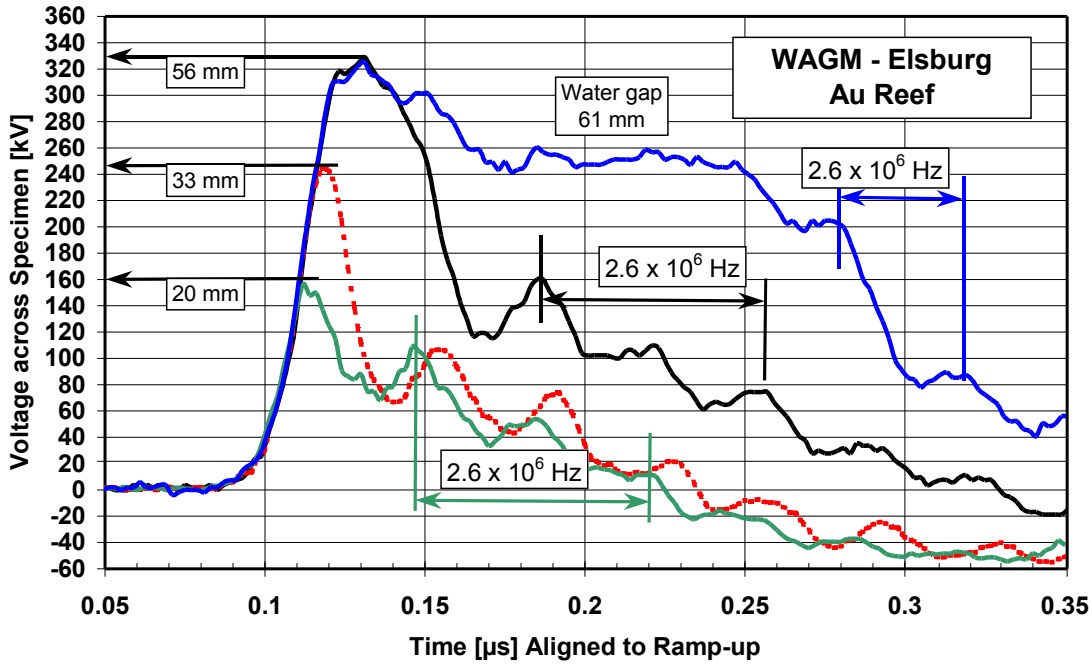


Figure -74: Voltage breakdown patterns for gold reef specimens

The discharge through a water gap (with the nearest comparable distance of 61 mm) is also shown for reference. All curves were aligned on the time scale to their ramp-up shape to enable comparisons to be made. The rate of rise was identical for all specimens, as all voltage signals overlapped exactly.

Only two UG2 specimens (thicknesses of 6,5 and 27 mm) were successfully fragmented in this test series. Two further specimens (thicknesses of 28 and 56 mm) displayed a large crack due to the discharge, but no fragmentation. This phenomenon could relate to partial discharge through the rock and partial discharge through the water, as discussed in the photographic section above. The two failed UG2 tests are included in the summary Figure -76 for reference. They are connected with a dotted line to provide insight into an overall trend. The voltage breakdowns for successful fragmentation of UG2 are shown in Figure -75 below.

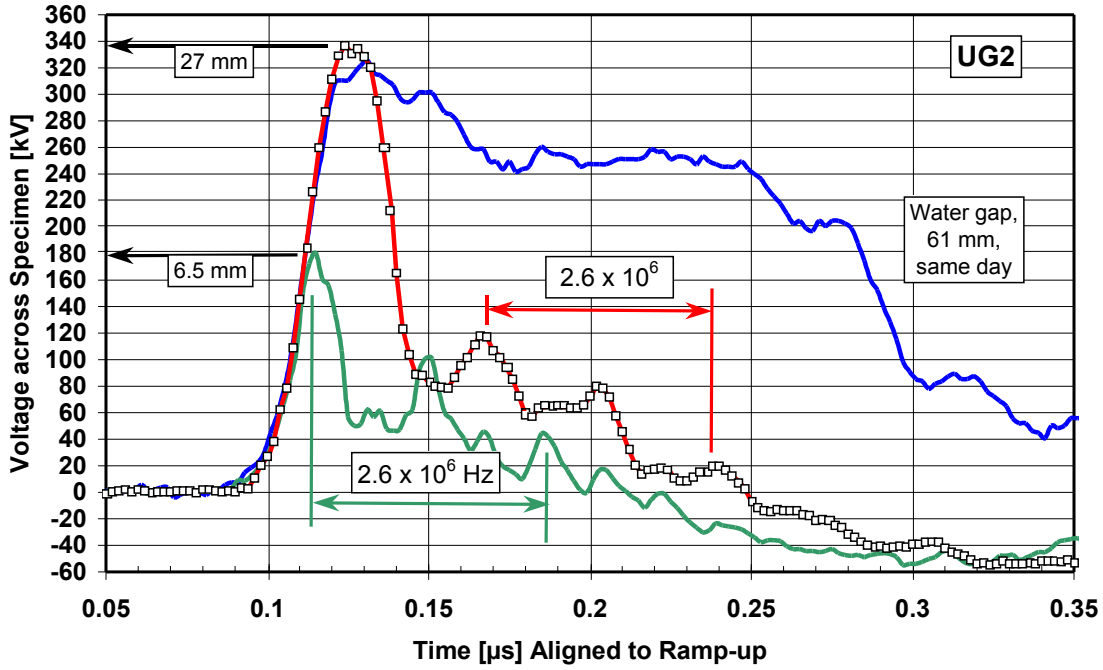


Figure -75: Voltage breakdown patterns for two UG2 specimens and water

Again, a sharp ramp-up is followed by a distinct breakdown associated with a significant voltage drop. After that, the signals seem to oscillate at a frequency of 2,6 x 10^6 Hz while decaying further. White markers were used in the red curve above to demonstrate the individual data points. They revealed that a total of five data points were actually measured at the highest recorded voltage of between 320 and 340 kV.

The electric field strength per millimetre of specimen thickness at dielectric breakdown is significantly lower than the value obtained from the 8-mm-thick specimens. A summary of the evaluated test data is given in Figure -76 below.

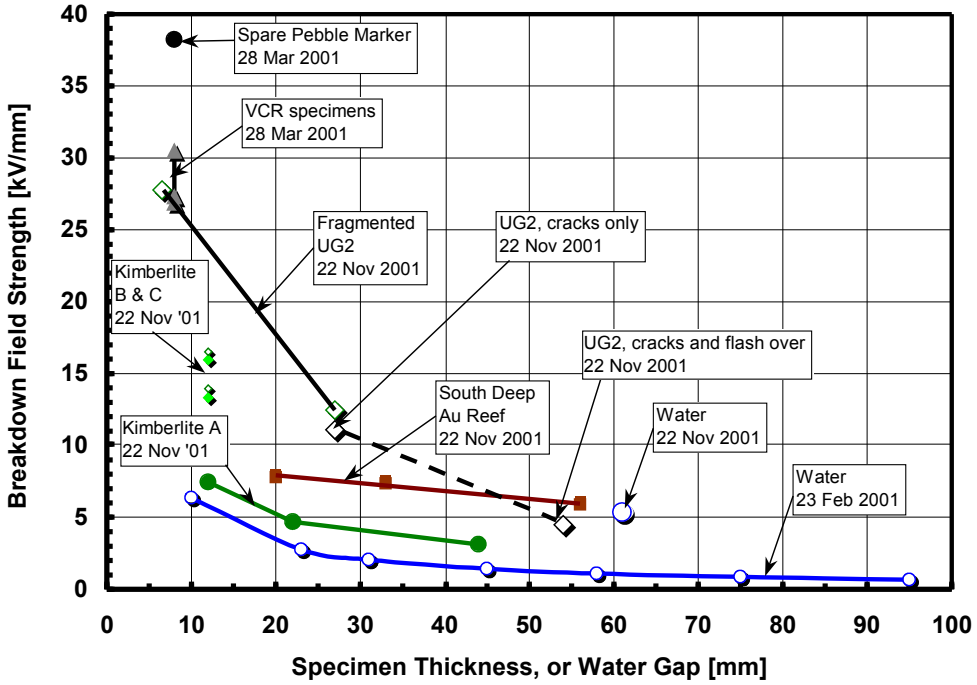


Figure -76: Summary of breakdown field strengths vs. thicknesses

The Kimberlite 'A' specimens had a significantly lower breakdown voltage compared with the other Kimberlite 'B' and 'C' specimens with a thickness of 12 mm, and with the gold and platinum specimens. Water displayed a smooth relationship on the test day of 23 February 2001, and the previously discussed anomaly of the delayed discharge with a 45 mm water gap did not appear again.

8.10 Electron Microscope Images

Electron microscope images were taken from the Lava sample, which was one of the four rock types used at FZK in their continuously operated Frank-0 test rig during the visit by the author. Figure -77 shows the surface of tensile-fractured Lava on the left, whereas traces of the plasma are shown on the right. A further enlargement of the area inside the white rectangle is presented in Figure -78.

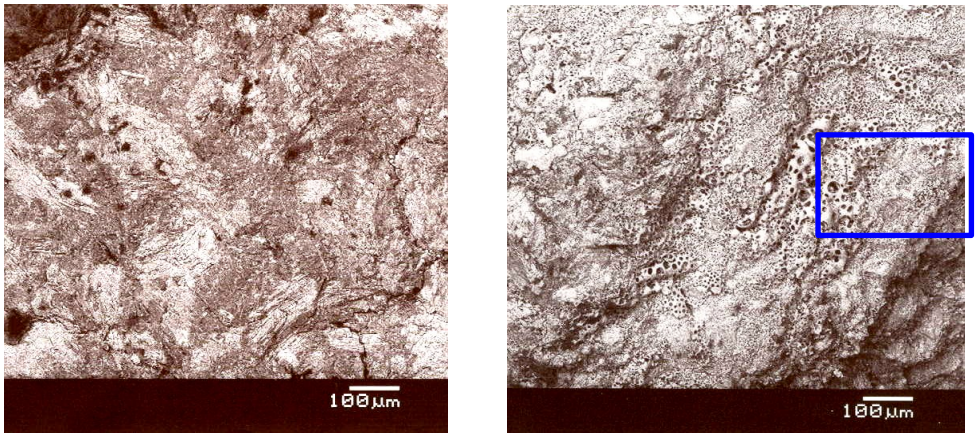


Figure -77: Electron microscope images – Tensile-fractured lava (left) and evidence of small plasma traces (right)

Plasma gas was initially entrapped during solidification, and thereafter escaped, leaving craters behind, as shown in the enlargement below.

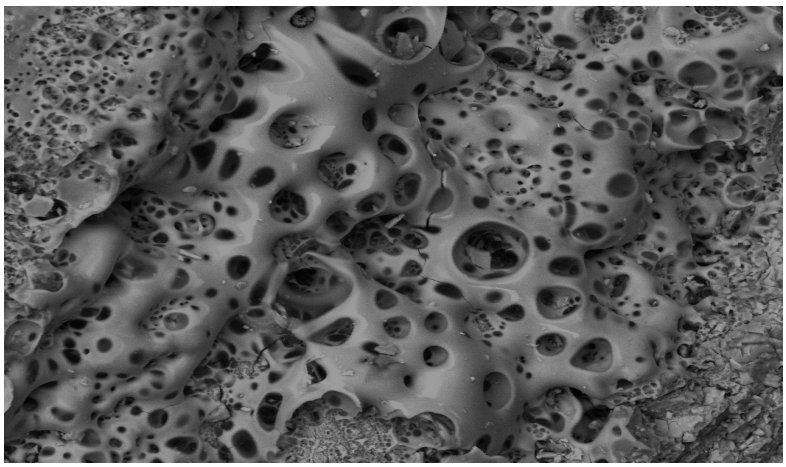


Figure -78: Detailed air-entrapment in solidified plasma (picture width is approximately 300 µm)

From the scale, it is evident that the smallest visible air bubbles were in the order of only 1 µm, with the largest bubble not exceeding 20 µm.

8.11 Summary

Test specimens with various geometries and thicknesses were successfully fragmented. Voltage and current signals were recorded before, during and after electric discharge through rock or water. The comparisons of the signals revealed that non-reef samples and water tests generally display a delay of the discharge after ramp-up of the voltage across the specimens. Contrary to this, the reef samples displayed a sudden voltage drop, when discharge took place as soon as the voltage had ramped through a critical threshold.

Some indicative correlation was established between the geophysical rock properties, measured for a 16 MHz excitation, and the breakdown voltage required for fracturing. Pure quartz materials did not fit that correlation due to the absence of conductive pathways.

Over the specimens tested for each reef type, the breakdown voltages appeared to be linear to the specimen thickness. UG2 materials required the highest breakdown voltage, followed by gold reefs, with Kimberlite specimens requiring the smallest breakdown voltage.

After each discharge, the residual energy seemed to oscillate within the electric circuit at a frequency of $2{,}6 \times 10^6$ Hz. This made accurate energy consumption assessments impossible.

The evidence of consolidated plasma found in some specimens confirms the nature of fragmentation by superheating of material along the electric discharge path. However, no plasma was found in the reef specimens.

9 DISCUSSION OF RESULTS AND OBSERVATIONS

9.1 Potential Effect on Flotation Recovery

The electric discharge created visible burn marks on the UG2 material (Figure -79). This may impact negatively on the platinum group metals (PGM) recovery process and thus may put a stop to any further exploratory work on this technology for platinum mining, aimed at hydrohoisting of electrically comminuted run-of-mine (ROM) materials.

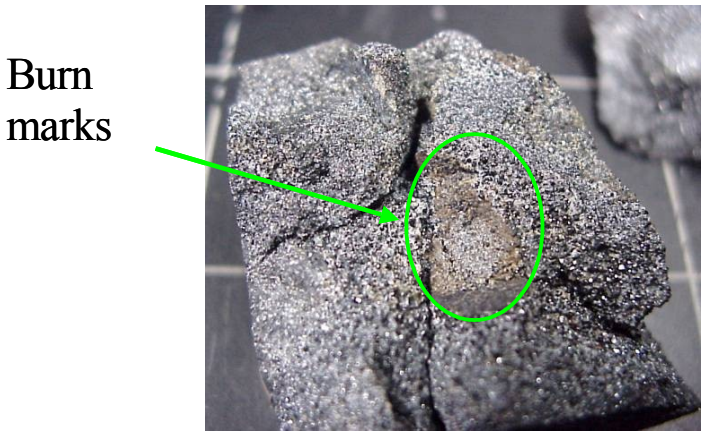


Figure -79: Electric discharge burn marks at UG2 fracture plane

Naturally, the UG2 ROM material provides a high amount of fines, and conventional wet screening appears to be effective enough to readily provide about 60 % of the mined-out reef for potential hydrohoisting purposes.

9.2 Selective Fracturing along Grain Boundaries

At the beginning of the research, it was expected that fracturing would take place along dominant grain boundaries due to the higher mineralisation providing a preferential conduit for the dielectric breakdown.

Inspection of the breakage paths and patterns, however, indicated that the single discharge is so sudden, powerful and violent that the discharge cannot follow the detailed paths of grain boundaries. Fragmentation directly through larger quartz particles within gold reef samples was observed, as well as irregular paths through the very homogeneous UG2 samples.

9.3 Effect of Ore Body Type

9.3.1 Gold reef material

The Elsburg Formation reef and VCR specimens and were the most suitable reef types. Irrespective of the test specimen's shape and thickness, all discharges resulted in successful fragmentation, creating a large new surface area of the broken fragments, including finer particles.

9.3.2 Foot wall and hanging wall rock types

Many of these samples could not be fractured at all, even with up to four successive attempts. It was hoped that each discharge, although failing to go through the specimen, would damage the specimen with the external shock wave created from the discharge through water. However, during ramping up to higher charging voltages of the Marx generator, premature discharges through water occurred before higher field strengths could be applied across the rock specimens.

9.3.3 Platinum reef specimens

Due to their higher conductive content, it was anticipated that the UG2 and Merensky reef specimens would fragment more easily than the Kimberlite specimens. However, the field strength required to create successful fragmentation was much higher than for Kimberlite samples of similar geometry. Both Kimberlite and UG2 are more homogeneous in grain size distribution than, for example, the Elsburg Formation specimens (gold reef), which contained large pebbles of quartz.

The initial discharge through a large UG2 sample, and the created, uneven fragment, are shown in Figure -80 below with an arrow showing the contact point of the electrode.

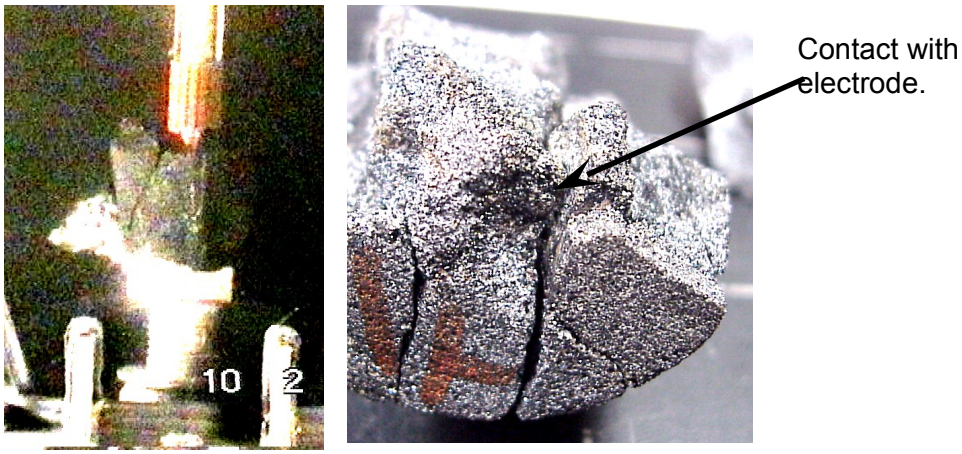


Figure -80: Fragmentation discharge and remaining cracks inside the 40-mm-thick UG2 specimen

A subsequent sampling campaign of ROM material from platinum mining operations revealed a very high amount of fines in the ROM. These could be wet-screened underground to enable hydraulic transportation of the fine fraction only, instead of trying to break up the large rock particles.

A unique feature was observed in a Merensky specimen. A wide plasma trace was evident, similar to the plasma trace in the large Kimberlite sample, and a large crack remained perpendicular to the plasma and fracture plane. This confirms the explosive nature of the electric discharge, but also shows that a single discharge does create only limited fragmentation. As soon as the primary crack results in fragmentation, the pressure breaks down and no force remains to further open up the secondary crack, resulting in the remaining 'tensile cracks' shown in Figure -81.

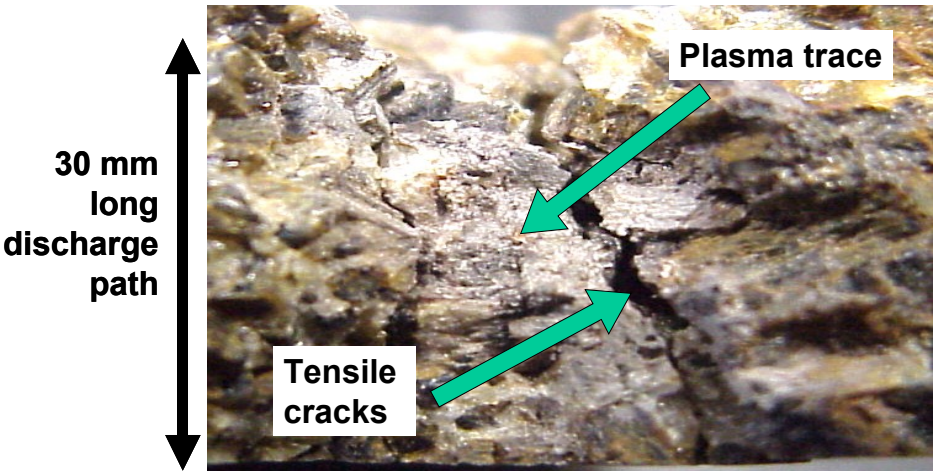


Figure -81: Plasma trace through a 30-mm-thick Merensky reef specimen and remaining tensile cracks

9.3.4 Kimberlite specimens

The Kimberlite samples appeared to be ductile rather than brittle. A soon as they were exposed to water in the comminution chamber, the material absorbed moisture. This, however, did not seem to affect the discharge path. The fragmentation patterns created pie-shaped segments, with few fine particles created. However, during the removal of the fragments from the chamber, some corners of the fragments just fell off after having absorbed some moisture.

The largest specimen fragmented during the entire study is shown in Figure -82 below.



Figure -82: Plasma traces through 56-mm-thick Kimberlite 'A' sample

The single discharge simply split the specimen into two halves. The fact that it was not scattered into many pieces means that any diamonds hidden within a half would remain undetected, unless more discharges were to create smaller fragments.

This also means that a photo showing the liberation of a diamond published by Andres (1989) may have been a coincidence only, unless the diamond had a substantial size to affect the field strength concentration in such a way that it attracted the discharge to pass along the diamond/Kimberlite interface or grain boundary. The core samples available to the CSIR did not contain any diamond material, and therefore no actual assessment of this aspect is possible.

9.3.5 Foscor specimens

This material fractured into a few pie-shaped pieces, when the specimen was 10 mm thick. A typical sequence is shown in Figure -83.

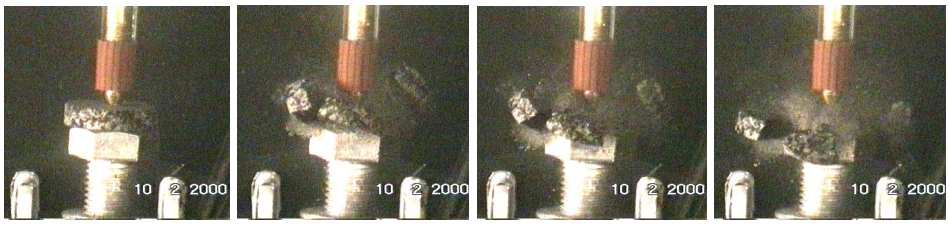


Figure -83: Fracture sequence of 10 mm Foscor specimen

Only a limited application for electric rock breaking would be envisaged for this rock type, thus no systematic tests over a variety of thicknesses were conducted. In contrast to the gold reef specimens, which showed no plasma traces whatsoever, the 30-mm-thick Foscor sample showed plasma traces similar to the ones found in Merensky reef and Kimberlite. The hour-glass-shaped plasma trace is shown in Figure -84 below.

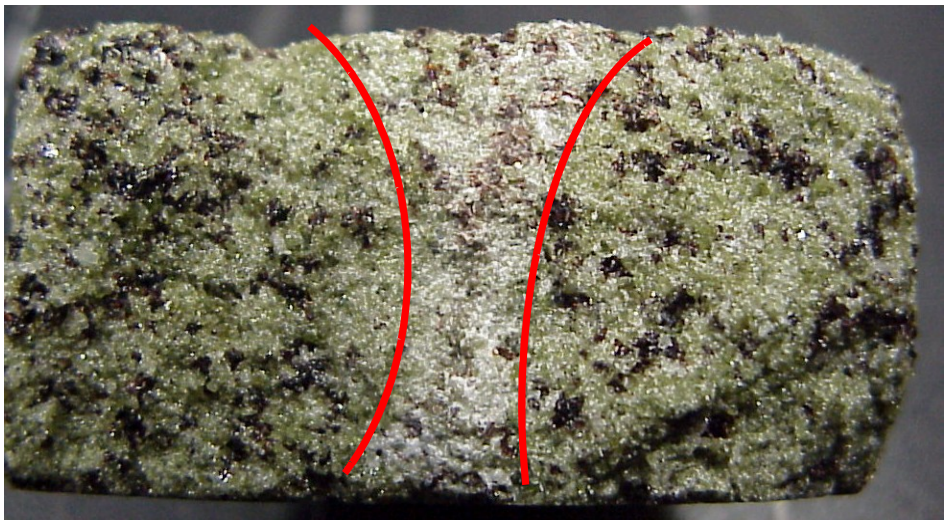


Figure -84: Hour-glass-shaped plasma trace through 30 mm Foscor specimen

9.4 Utilisation of High-Speed Photographic Evidence

9.4.1 Unwanted flashovers

The photo on the left in Figure -85 below shows a flashover on the left side of the specimen. The photo on the right shows part of the unfragmented specimen being pushed away as a result of the flashover.



Figure -85: Undesired flashover next to rock

Detailed attention to the condition of the water and the changes that occur in it during a test programme may be necessary to increase understanding of gas development and flashovers.

9.4.2 Carbon Leader Reef footwall, 'blown off'

Small-diameter Carbon Leader Reef footwall samples were tested and found to be unsuitable for this technology as the discharge preferred to pass through water. The Carbon Leader Reef test specimens were repeatedly 'blown off' the holder without any fragmentation or cracking, as shown Figure -86.



Figure -86: Blown-off, small Carbon Leader Reef footwall sample

This 'refusal' of the discharge to pass through the Carbon Leader Reef specimens clearly identifies the material as being unsuitable for ESWC application. However, at the same time, it highlights that the gold-bearing reef specimens are significantly more suitable, therefore offering a selective mining method, as described in the recommendations in Chapter 12 later.

9.4.3 Cavitation due to moving fragments

The 35-mm-thick, coarsely grained Elsburg Formation reef specimen exploded in an ideal way, creating tensile fractures and leaving no visible evidence of plasma. The specimen was an end-piece of a core so it was not perfectly cylindrical. This can be seen in the top left photo of Figure -87. The second photo shows a whitish cloud in the slipstream of the moving fragments. This could have two origins or a combination of both: gaseous explosion from inside the specimen due to discharge, or cavitation behind the fragments. The following sequence is the most spectacular evidence captured in terms of specimen size and creation of multiple fragments.

The photo on the left in Figure -87 shows the specimen being placed on top of the bolt, representing the bottom electrode. The photo on the right shows the first frame of the explosion during discharge through the specimen.



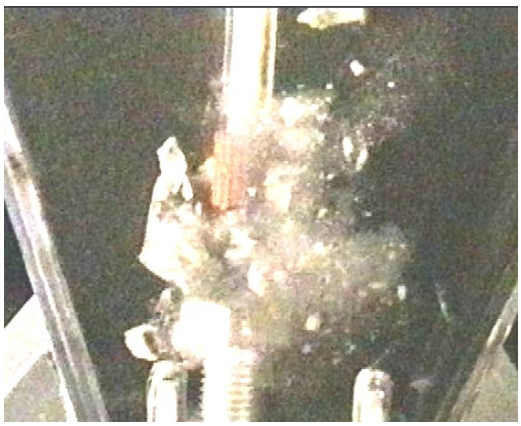
Initial setting of a 35 mm thick gold reef sample.



Gaseous explosion with cavitation and tensile fracturing.

Figure -87: Cavitation evidence for 35-mm-thick coarsely grained gold reef sample, Elsburg Formation (Sony camera)

The next two photos are a continuation of the two photos shown above. The gaseous phase then disappeared gradually in the third frame of the sequence, i.e. the photo on the left in Figure -88. Mainly dust and larger particles are captured on the last frame, i.e. the photo on the right in Figure -88.



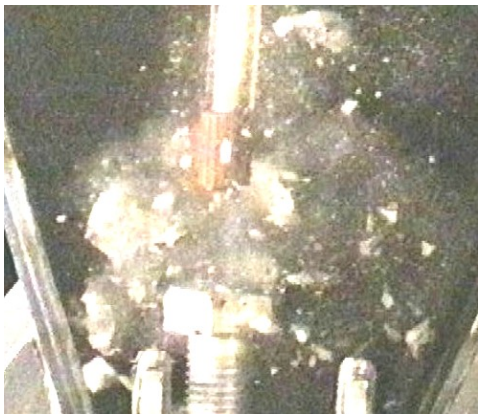


Figure -88: Radial separation of fractured particles (Sony camera)

It is possible that the wider contact area of the metallic bolt distributed the field through the entire cross-sectional area. The majority of the tests were conducted with a pointed electrode, covered with a rubber plug to provide a non-conductive base for the specimens. The plug with the upper electrode in its centre is visible in the right photo in Figure -89.

9.4.4 Raising air bubbles

Significant air bubbles were created with some smaller specimens shown below. The difference from the above gaseous air behaviour is that the bubbles do not collapse, but rather gently move towards the top of the water-filled comminution chamber, as shown in Figure -89.

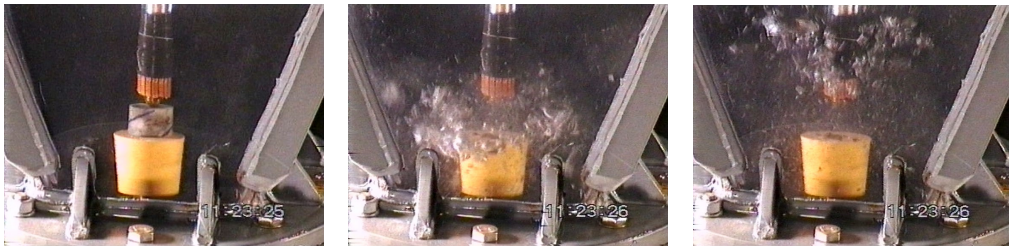


Figure -89: Rising air bubbles (Sony camera)

Detailed attention to the condition of the water and the changes that occur in it during a test programme may be necessary to increase the understanding of gas development and flashovers.

9.4.5 Design of comminution chamber components

The geometry of the inverted pyramid was found not to be ideal. Repeatedly, flashovers were evident at the same location on the bottom left-hand side, as shown in Figure -90. These undesirable paths are much longer than the direct path between the metal electrodes and the rock. This confirms the statement by Whitehead (1951) that the discharge may not always follow the path of the strongest field, assumed to be the shortest path. **N.B.:** Similarly, lightning has been reported to strike objects under a blue sky in the vicinity of a thunderstorm.

The following photos show evidence of the deterioration of the insulation material around the upper electrode.

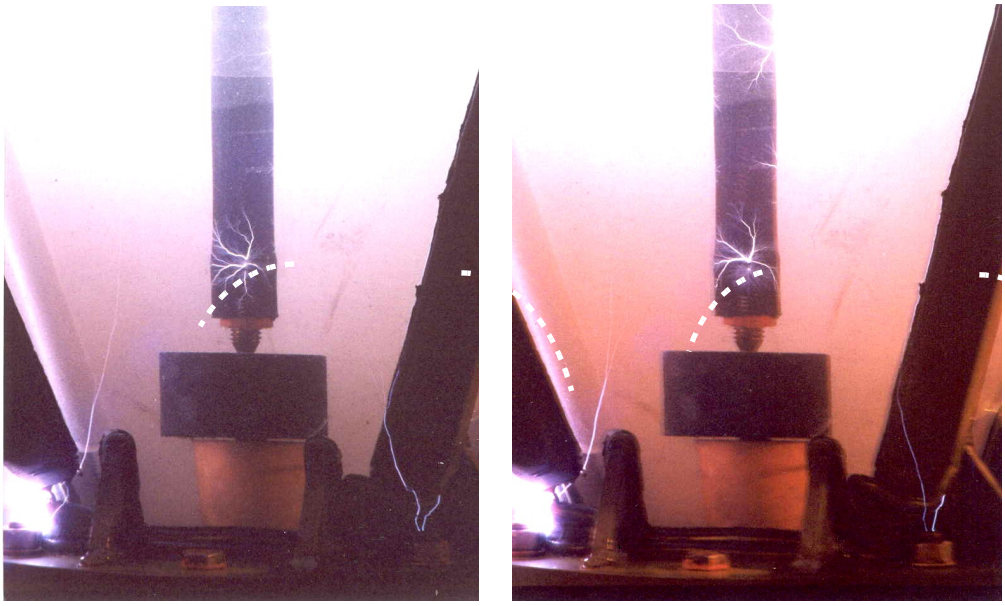


Figure -90: Flashover to an external, metal bolt

The above figure shows that various flashovers originated during two independent discharges at the metallic bolts of the horizontal flange at the bottom right-hand side of each picture. The invisible connection of the white flashovers to the central electrode is assumed to pass through the transparent side-window and the water. The estimated paths are indicated by the dotted white lines inserted into the photos above. After these events, there was no obvious damage to the Perspex window.

9.4.6 Insulation failure for upper electrode

Towards the end of the test programme, the number of unwanted flashovers increased. Figure -90 shows that the flashovers repeatedly terminated at the same location and had passed through the insulation of the upper electrode. It can be concluded that the selected insulation thickness of 5 mm was too thin to remain effective during the test period. Any future test rig should provide at least a 20-mm-thick insulation, which should be based on a well-selected dielectric material, as it will be exposed repeatedly to high field strengths. The electrode and dielectric should be shrink-fitted and water-tight-glued to extend their working lives.

The need for reliable insulation to reduce the occurrence of unwanted flashovers is a major concern if the equipment is to perform with minimal maintenance underground.

9.4.7 Photographic Evidence and Acoustic Emissions

Various camera settings and lighting techniques were tested to capture the high-speed event of electric discharge through water and the rock specimens. The initial rock-breaking process could unfortunately not be captured as the camera equipment and the self-illuminating electric discharge did not complement each other. However, the extent of the explosion was well captured in terms of moving fragments. The biggest discovery made by using the photographic equipment was the exact paths of the unintended discharges and identification of the failure of the insulation material.

Acoustically, a flashover through water, or even through the Perspex window, was duller compared with a successful rock-breaking discharge. Acoustic sound-wave pattern analysis should be used in future tests to gain further insight and to capture signals for the optimisation of analysis and discharges.

9.5 Implications for Underground Equipment

Although the test rig set-up was a first approach without detailed engineering design consideration of the material specifications, already a few fundamental concerns were identified during the practical operation of the rig.

Extremely high voltages, in the order of 30 to 35 kV per mm of rock thickness, are required to facilitate tensile rock breaking by direct discharge through the rock.

The electrical fields are very high and personnel would have to remain at a distance during operation, which is problematic in confined places underground.

Good mechanical coupling between electrodes and rock faces is required to minimise the likelihood of discharge through water paths.

Any metal component, e.g. the bolt in the external plastic flange at the bottom of the chamber, can lead to undesired flashovers. These flashovers consume part of the electrical power, and thus reduce the power available for rock breaking.

There is clear evidence that the coarsely grained, mineralised gold-bearing reef specimens are significantly more amenable to direct discharge than the more finely grained footwall and hanging wall specimens. However, all specimen types showed some variability, even the more homogeneous Kimberlite and UG2 specimens.

9.6 Review of Objectives and Potential Benefits of the Technology

On the basis of having completed some single discharges through various rocks types, which had a well-defined, machined geometry to enable accurate contact with the electrodes, Table -9 summarises the risks or concerns and the anticipated benefits.

Table -9: Potential risks and benefits of ESWC technology

Characteristics	Risks / Concerns	Benefits
Underground use	High voltages Water contamination Underwater operation	High energy into rock samples Potential for mineral liberalisation Integration with Tore® pump
Rock/electrode contact	Unknown for continuous operation, possibly chains over conveyor	
Size control	Limits the tonnage throughput	Screen gap setting is ideal for Tore® pump, requiring coarse, but less than 15 mm, particles.
Requires mineralised grain boundaries	Dependency on rock type	Avoids energy wastage for crushing low-value quartz pebbles.
Low packing density of rocks in continuous mode	Misfires through water	-
Explosion mode	Reduction in packing density per pulse, as particles will move away from electrodes	High energy available within rock only if good mechanical coupling can be ensured.
10 Hz repetition rate for pulsed power	No proper filling of comminution chamber per pulse	Secondary, inefficient comminution by compression of surrounding rocks
Tonnage	Sufficient tonnage needs to be proven (i.e. 10 t/h)	-

Table -9 indicates some potential for an integrated comminution and coarse product pumping system, which would complement future continuous and mechanised mining methods. The table also identifies considerable risks and uncertainties.

9.7 Summary

Electric discharge through rock is violent and takes place along indiscriminate pathways. Footwall and hanging wall specimens appear to be almost immune (inert) to electric discharge. Photographic evidence was essential not only to identify certain weaknesses in the test rig set-up, but also to document the fast processes taking place around the specimens during discharge.

The risks and uncertainties with this unproven technology currently outweigh the perceived advantages of crushing mined reef to sizes suitable for hydrohoisting. Voltage levels have to be high and they increase with rock size. Voltage rise times have to be extremely fast to ensure discharge through rock rather than water. Although systematic tests can be done with single discharges through well-placed specimens, a method needs to be developed to ensure good electrode-to-rock contact for a continuous machine.

10 CONCLUSIONS

Although the dielectric breakdown of insulators is generally undesired, its destructive behaviour has been recognised for many years for electric rock breaking. Scientists and researchers have experimented with pulsed power circuits to purposely create breakdown through materials such as concrete, rock and even electrical appliances for recycling. Tensile stresses can break rock much more efficiently then compressive forces, if only they could be created inside the rock.

Based on single discharges through cylindrical rock specimens, representing typical South African rock types, the voltage requirements and suitable rise times were identified by successful fragmentation. The extent of fragmentation ranged from simply splitting a Kimberlite core sample down the middle, to the creation of a large amount of fine material for the UG2 reef type. Some fragments also displayed fractures as a result of the discharge, but their depth was limited and thus did not result in fragmentation.

The discharge is characterised by extremely fast events in the order of 2 µs. The field strength at which breakdown and discharge took place was between 30 and 35 kV per mm of specimen. After discharge, the current and voltage signals indicated a residual energy oscillation at about 2,6 x 10^6 Hz. It is believed that the electrical impedances and capacities of the circuit components provided some instantaneous surge storage. This resulted at times in ‘ringing’ of the circuit. In the absence of additional instrumentation, the power consumption per fracture could not be determined.

The photographic evidence indicated that flashovers repeatedly took place. This was due not only to decay in the insulation of the electrode, but also to some metal components being present near the comminution chamber. The actual event, showing exactly how the discharge passes through the rock, could not be captured, but insight was gained into the typical streamer and treeing pattern and this was documented with photographs.

Owing to their shapes, the particles from electrically comminuted samples were found to settle marginally faster than impact-crushed particles. This would improve their suitability for feeding the Tore® pump. Unfortunately, a detailed

comparative study on the required geometry and wall thickness of a potential Tore® hydrohoist system had concluded that the three-chamber pipe-feeder would be a more suitable technical option, and any further Tore® work was abandoned. The fines content of Merensky and UG2 ROM material is high and conventional screening would be sufficient to create enough tonnage for hydrohoisting from ROM material.

However, the most likely application for this technology underground could be primary rock breaking in narrow pay chutes, due to the preferential breakage of highly mineralised rock types. If the rock could be mined with this technology on a continuous basis, this would lead to mechanisation for mining of otherwise unmineable reserves. However, the high voltages, surrounding water and confined operating space would necessitate a considerable number of engineering and safety features.

11 RECOMMENDATIONS FOR FUTURE RESEARCH

The indications are that demineralised water would be required as an isolating medium. It would be difficult to maintain high water quality in the underground situation. In experiments conducted at FZK with the Franka-0 equipment, using a polythene vessel, measurements showed the build-up of ozone, hydrogen peroxide and organic acids in the water. Chlorine and salt may react with radicals to form chloroform. The water requirements for the water to be used for an underground plant, as well as the effect of ESWC on the water quality, need to be investigated in detail.

More time must be available to repeat tests with inconclusive results. Many more specimens with similar properties must be acquired and tested to determine statistically sound dependencies.

A larger team of full-time researchers, comprising complementary competencies, such as geophysical, electrical and mineralogical, would be beneficial to follow up interesting leads and to develop a comprehensive understanding of the micro-processes involved with the complex dielectric discharge through various rock types.

However, based on the measured findings of this research that electric discharges prefer reef types with lower resistivity compared with the higher resistivity associated with the footwall and hanging wall, this technology could be considered for primary hard rock mining. If a suitable head could be built as a mining tool, incorporating the two electrodes in a rotating barrel arrangement, this head would create a discharge across its front. The head would be submerged in water and if the rise time would be fast enough, a discharge arc should pass through the mineralised reef, rather than through the water.

With the discharge preferably through the reef horizon, this head would create its own path between the 'inert' hanging wall and footwall. This would be suitable for thin, highly mineralised channels, which are rolling in situ and are therefore not suitable for diamond-saw cutting as a stoping technique. Channel widths between 50 and 300 mm may be suitable for this mining method. Since the head follows the mineralisation automatically, it would simply need to be fed forward to minimise the distance from the electrodes to the reef.

The head could either rotate to drill an auger-like hole, or it could be mounted on an arm that wipes across the face, thereby creating a narrow channel. The self-guided head, which mines reef and finds its own path, was named the 'mining mole' and the concept is shown in Figure -91 below for illustration.

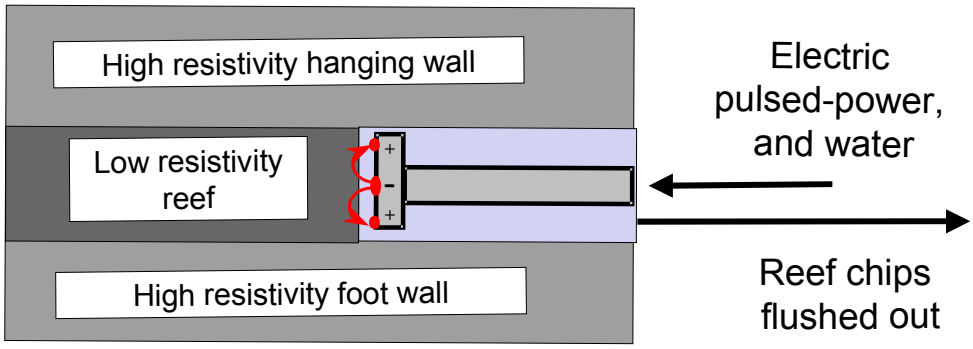


Figure -91: 'Mining mole', based on electric rock breaking

The major challenges for the 'mining mole' would be the provision of a fast voltage ramp-up characteristic right at the head, and the mechanical design of the head to provide shock wave-resistant insulation and reliable electrodes.

12 REFERENCES

Aerie (1996) Electric pulse disaggregation for preferential grain boundary fracture, Aerie Partners, Inc., San Diego, CA, USA.

Andres, U. and Bialecki, R. (1986) Liberation of mineral constituents by high-voltage pulses, *Powder Technology*, *48*, pp 269-277.

Andres, U. (1976) Liberation study of apatite nepheline ore comminuted by penetrating electrical discharges, *International Journal of Mineral Processing, 4*, pp 33-38.

Andres, U. (1989) Parameters of disintegration of rock by electrical pulses, *Powder Technology*, *58*, pp 265-259.

Bergstrom, B.H. (1961) The electrohydraulic crusher, *Engineering and Mining Journal, 2*(2), pp 3-140.

Budenstein, P. (1980) On the mechanism of dielectric breakdown of solids, *IEEE Transactions on Electrical Insulation*, ET-15(3), pp 225-240.

Chard, S.J., Nezhati, K., Delves, J.E., Lockier, A.C., Webber, C.E., Ilgner, H.J. and Parkinson, D.J. (1996) Evaluation of the Tore® for hydrotransport and its application, Proc. 13th International Conference on Slurry Handling and Pipeline Transport, *Hydrotransport 13*, BHR Group, Johannesburg, South Africa, pp 569-590.

CoMRO (Chamber of Mines Research Organization) (1990) Annual Report 1990.

Edinger, W., Neubert, V., Schultheiss, C., Strässner, H. and Wieczorek, H. Process and device for electrodynamic fragmentation of solids – FRANKA.

Haase, H. (1987) Assessment of the Final Report by Battelle on 'Electrical Methods for Fracturing Quartzite, Feasibility Evaluation', pp 1-3.

Hinde, A.L. and Joosub, R.A. (1998) Evaluation of electric pulse disaggregation technology for the liberation of gold from Witwatersrand ores, Mintek Report 14749801, June.

Hoppé, P., Frey, W., Giese, H., Lotz, H., Marek, J., Söhner, H., and Väth, W. (1999) Franka-Stein: A semi-industrial prototype for the fragmentation of concrete, Annual Report 1999, FZK, Karlsruhe, Germany.

Ilgner, H.J. (1997) Innovative slurry pump system for bulk materials. *Mechanical Technology*, Johannesburg, pp 16-20.

Ilgner, H.J. (1999) Innovative concepts for underground comminution and lateral transportation of rock as an alternative to conventional tramming, Paper

presented at the 14th International Conference on Slurry Handling and Pipeline Transport, *Hydrotransport 14*, BHR Group, Maastricht, Netherlands, 8-10 Sept.

Kanellopoulos, A. and Ball, A. (1975) The fracture and thermal weakening of quartzite in relation to comminution, *Journal of the South African Institute of Mining and Metallurgy*, pp 45-52.

Kochanowsky, B.J. and Singhal, R.K. (1966) Recent developments in the techniques of rock fracturing and drilling and their possible application to mining – Part 2, *Australian Mining*, pp 36-39.

Kramers, C.P. (1997) Overseas Visit Report: FZK, Putzmeister, Krebs Engineers, Euro-Pulse, Merpro, and Sonic Process Technologies. CSIR Division of Mining Technology Internal Report.

Kravchenko, V.S. (1961) Dustless breaking of rocks electrically, *Mining Congress Journal*, pp 53-55.

Kroninger, H. (1999) Personnel communications. NETFA Apollo Test Site, SABS, June.

Le Sueur, P.K. (1995) Rock breaking by dielectric breakdown: A review of relevant literature and proposal for practical experimentation, CSIR Division of Mining Technology Report MES 1/95, Aug.

Maroudas, N.G. (1967) Electrohydraulic crushing, *British Chemical Engineering*, pp 558-562.

McGraw-Hill (1984) Dictionary of Technical and Scientific Terms. 3rd Edition, McGraw-Hill Book Company, New York.

McNown, J.S. and Malaika, J. (1950) Effects of particle shape on settling velocity at low Reynolds Numbers, *Transactions, American Geophysical Union*, 31(1), Feb., p 74.

Meyers, M.A. (1994) Dynamic Behaviour of Materials, J. Wiley, New York.

Parekh, B.K., Epstein, H.E. and Goldberger, W.M. (1984) Novel comminution process uses electric and ultrasonic energy, *Mining Engineering*, pp 1305-1309.

Pettijohn, F.J. (1949) Sedimentary Rocks, Harper and Brothers, New York, USA.

Sarapuu, E. (1973) Electro-energetic rock breaking systems, *Mining Congress Journal*, pp 44-54.

Segsworth, R.S. and Kuhn, K. (1975) Electrical Rock Breaking, Department of Electrical Engineering, University of Toronto, pp 39-43.

Swart, P.H. (1999) Pulsed corona pollution control, Paper presented at a One-day Workshop, Potchefstroom University.

Thorarinson, S. (1994) Almenna Bokafelagid, The Viking Press, Inc.

Turner, G. (1999) Personnel Communications, Atomic Energy Corporation, June.

Whitehead, S. (1951) Dielectric Breakdown of Solids, Oxford at the Clarendon Press, London.

Wallmach, T. (2001) Personnel Communication at CSIR Division of Mining Technology.

Young, F.M. (1961). The Secondary Breaking Effect of High-Frequency Electric Energy Applied to Rock Fragments, Montana School of Mines, Butte, Montana, USA, pp. 185-203.

13 BIBLIOGRAPHY

Bialecki, R. (1997) Non-mechanical crushing, Fax correspondence from tests done on 5 May 1997 at Euro-Pulse, London

Bluhm, H. (1997) Industrial applications of high voltage pulsed power techniques: Developments at Forschungszentrum Karlsruhe (FZK), Germany.

Bluhm, H. (1998) Visit Report to the CSIR during Dec. '98 and underground visits.

Budenstein, P., Hayes, P.J., Smith, J.L. and Smith, W.B. (1968) Destructive breakdown in thin films of SiO, MgF_2, CaF_2, CeF_3, CeO_2 and Teflon, *Journal of Vacuum Science and Technology, 6*(2), pp 289-303.

Cooke, N.G.W. and Joughin, N.C. (1970). Rock fragmentation by mechanical chemical and thermal methods. Proc. VIth International Mining Congress, pp 1-5.

Davison, L., Grady, D.E. and Shahinpoor, M. (Editors) (1996) High-Pressure Shock Compression of Solids II, Dynamic Fracture and Fragmentation, Springer.

Farmer, I.W. (1965) New methods of fracturing rocks, *Mining & Minerals Engineering*, pp 177-184.

Goldberger, W.M., Epstein, H.M. and Parekh, B.K. (1982) Two-stage Comminution, US Patent 4.313.573, Feb.

Graham, R.A. (1974) Shock-wave compression of X-cut quartz as determined by electrical response measurements, Paper presented at the Conference on Metallurgical Effects at High Strain Rates, Albuquerque, New Mexico, *J. Phys. Chem. Solids, 35,* pp 355-372.

Haase, H. (1998) Workshop Report: Electric rock breaking, CSIR Division of Mining Technology.

Haase, H. (1999) Visit Report to FZK in January '99, for primary rock breaking and secondary comminution cooperation.

Haase, H., Kramers, P., MacNulty, N. and Willis, R.P.H. (1997) Continuous mechanized mining – Key issue for the future of the industry. Proc. South African Institute of Mining and Metallurgy Symposium, *Maximising Face Utilisation*, pp 1-7.

Haase, H. and Pickering, R.G.B. (1986) The status of non-explosive mechanized mining in narrow reefs. Proc. MINEMECH 86, *Developments in Underground Mining*, pp 1-22.

Ilgner, H.J. and Kramers. C.P. (1996) Pipe wear in vertical backfill distribution columns in South African mines, Proc. 13th International Conference on Slurry Handling and Pipeline Transport, *Hydrotransport 13,* Johannesburg, pp 479-502.

Ilgner, H.J. (1999) Evaluation of electric shock wave comminution, CSIR Miningtek Internal Year-End Report 99-0157.

Ilgner, H.J. (2000) Audit of local equipment for electric shock wave comminution, CSIR Miningtek Internal Year-End Report 2000-0023.

Ilgner, H.J. (2001) Electric shock wave comminution, CSIR Miningtek Internal Year-End Report 2001-0302.

Kanel, G.I., Razorenov, S.V. and Utkin, A.V. (1996) Spallation in solids under shock-wave loading: Analysis of dynamic flow, methodology of measurements, and constitutive factors, Chapter 1 in: High-Pressure Shock Compression of Solids II, Dynamic Fracture and Fragmentation, Springer

Knaur, J.A. and Budenstein, P.P. (1980) Impulse breakdown in PMMA under megavolt, nanosecond excitation, *IEEE Transactions on Electrical Insulation, EI-15*(4), pp 313-321.

Lisitsyn, I.V., Inoue, H., Katsuki, S. and Akiyama, H. (1999) Use of inductive energy storage for electric pulse destruction of solid matter. ieee transactions on dielectrics and electrical insulation, *6*(1), Feb., p 105.

Malan, D.F., Naper, J.A.L. and Watson, B.P. (1994) Propagation of fractures from an interface in a Brazilian test specimen, *Int. J. Rock Mech. Min. Sci. & Geomech. Abstr., 31*(6), pp 581-582.

Mooney, W.M. (1996) Development of Electrohydraulic Slot Miner. Presentation to the CSIR Division of Mining Technology, TETRA Corporation, Albuquerque, NM, Sept.

Nantel, J. (1993) New technologies for the mining industry, *Mining Engineering*, April, p 359.

O'Dwyer, J.J. (1964) The Theory of Dielectric Breakdown of Solids, Monographs on the Physics and Chemistry of Materials, Oxford University Press, Amen House, London.

Ryder, J.A. and Jager, A.J. (2002) A textbock on rock mechanics for tabular hard rock mines, SIMRAC, Johannesburg, ISBN 0-7988-5547-9, p 194.

Sparks, M., Mills, D.L., Warren, R., Holstein, T., Maradudin, A.A., Sham, L.J., Loh, Jr. and King D.F. (1981) Theory of Electron-Avalanche Breakdown in Solids, The American Physical Society.

Telford, W.W., Geldart, L.P. and Sheriff, R.E. Applied Geophysics. Second Edition.

Trump, J.G. and Wright, K.A. (1971) Injection of megavolt electrons into solid dielectrics. *Mat. Res. Bull., 6*, pp 1075-1083.

Zongxian, Z. and Yong, Y. (1993) Effect of temperature on fracture toughness of rock. In: Fracture and Damage of Concrete and Rock, FDCR-2, Edited by H.P. Rossmanith, E & FN Spon., ISBN 0 419 18470 8, p 426.

Zongxian, Z., Yong, Y. and Qing, Z. (1993) Influences of loading rates on the fracture toughness of rock, In: Fracture and Damage of Concrete and Rock, FDCR-2. Edited by H.P. Rossmanith. E & FN Spon., ISBN 0 419 18470 8, p 418.

14 APPENDIX A: FZK draft contract agreement (never been signed)

DRAFT

19. March 1998

AGREEMENT

between

Forschungszentrum Karlsruhe GmbH
Postfach 3640, 76021 Karlsruhe
Federal Republic of Germany

- hereinafter referred to as „ Forschungszentrum“

and

CSIR: Division of Mining Technology
P.O. Box 91230, Auckland Park, 2006
Republic of South Africa

- hereinafter referred to as „CSIR“ -

on cooperation in the field of pulsed power technology

Preamble

WHEREAS:

Forschungszentrum has extensive experience in the field of pulsed power technology, in particular for the fragmentation of solids, such as concrete or natural rock, on the semi-industrial scale. Forschungszentrum has the Fragmentierungs-Anlage-Karlsruhe (FRANKA, Karlsruhe fragmentation plant), which is applied for basic studies on the fragmentation by electric impulses and

CSIR has extensive experience in underground mining technology, in particular for the mining of gold-containing quartzite rock and its transport to the surface and

Forschungszentrum and CSIR**,** hereinafter referred to as the PARTIES, are interested in a Joint Venture on the use of the pulsed power technology for mining and comminution of gold-containing rock, and

The PARTIES envisage that the Joint Venture should entail a DEVELOPMENT PROGRAMME and a COMMERCIAL EXPLOITATION PHASE. The DEVELOPMENT PROGRAMME would entail acquiring data using experimental PLANTS, as described in this agreement, to assess the pulsed power technology, in a rockbreaking and comminution mode for mining of gold-containing rock. The COMMERCIAL EXPLOITATION PHASE would begin towards the end of the DEVELOPMENT PROGRAMME and would continue after conclusion of the DEVELOPMENT PROGRAMME, with the objective of promoting the commercial exploitation of the PLANTS, developed under this Agreement including the generated know-how.

After a successful completion of this Agreement the PARTIES intend to extend the cooperation with regard to other kinds of rock or applications in mining.

THE PARTIES HERETO AGREE AS FOLLOWS:

DEFINITIONS

The following words and phrases shall bear the stated meaning in this agreement, namely:

0.1	CSIR	shall refer to the statutory council established in terms of the Scientific Research Council Act No. 46 of 1988.
0.2	Forschungszentrum	shall refer to Forschungszentrum Karlsruhe GmbH, Germany
0.3	PARTIES	shall refer to the CSIR and Forschungszentrum
0.4	PARTY	shall refer to either Forschungszentrum or the CSIR

0.5 DEVELOPMENT PROGRAMME — shall refer to the first phase of the Joint Venture and would consist of a defined programme of work entailing the assessment of the pulsed power technology, in a rockbreaking and comminution mode for mining of gold-containing rock. The programme of work shall be jointly elaborated and updated in accordance with the intermediate results obtained.

0.6 COMMERCIAL EXPLOITATION PHASE — The COMMERCIAL EXPLOITATION PHASE is a phase of the Joint Venture which would begin towards the end of the DEVELOPMENT PROGRAMME and which would continue after conclusion of the DEVELOPMENT PROGRAMME, with the objective of promoting the commercial exploitation of the plants developed under this Agreement, including the generated know-how.

0.7 CONTRACT RESEARCH — shall refer to elements of the DEVELOPMENT PROGRAMME financed by third parties.

0.8 PLANT #1 — shall refer to an existing plant at Forschungszentrum, based on the use of the pulsed power technology developed by Forschungszentrum, and to be used in the feasibility study to be conducted in ELEMENT #1 of the DEVELOPMENT PROGRAMME.

0.9 PLANT #2 — shall refer to a 5 kW experimental plant, for the fragmentation of broken gold-containing rock in

gold mines, to be constructed by Forschungszentrum and evaluated in South Africa .

0.10 PLANT #3 shall refer to an experimental underground plant which may be constructed following tests to be conducted in PLANT #1 if both PARTIES agree to do so..

0.11 ELEMENT #1 - shall refer to the element of the DEVELOPMENT PROGRAMME entailing the conduct of a feasibility study on PLANT #1 to assess the technical and economic feasibility of the relevant technology in gold-mining applications

0.12 ELEMENT #2 - shall refer to the element of the DEVELOPMENT PROGRAMME entailing developing, building and testing the performance of PLANT #2.

0.13 ELEMENT #3 shall refer to the element of the DEVELOPMENT PROGRAMME entailing the construction of PLANT #3

0.14 ELEMENT #4 shall refer to any further work identified and agreed upon by the PARTIES to be conducted as part of the DEVELOPMENT PROGRAMME.

0.15 TECHNOLOGY shall refer to pulsed power technology for use in mining technology for breaking and comminution of gold-containing rock.

Article 1 - Scope of agreement

The scope of this agreement is as follows:

FIRSTLY, this agreement defines the framework in which the PARTIES shall co-operate in a defined DEVELOPMENT PROGRAMME which will entail:

- conduct ELEMENT #1: as a result of conducting ELEMENT #1, the PARTIES expect to be in a position to define a specification for an experimental underground plant, to be known as PLANT #3

- conduct ELEMENT #2

- conduct ELEMENT #3

- conduct ELEMENT #4

SECONDLY, this agreement defines the framework in which the CSIR and Forschungszentrum intend to collaborate and co-operate in a COMMERCIAL EXPLOITATION PROGRAMME in order to commercialize and exploit plants generated as a result of the DEVELOPMENT PROGRAMME. Thus:

- during the course of that COMMERCIAL EXPLOITATION PROGRAMME the CSIR and Forschungszentrum will conduct negotiations with potential licensees with a view to entering into agreements to manufacture equipment which utilizes the TECHNOLOGY.

- it is envisaged that such licensees shall be manufacturers of equipment and that any licensing agreement would make provision for the payment of a royalty to the PARTIES.

THIRDLY, this agreement defines the arrangements which will apply if either CSIR or Forschungszentrum is unable or unwilling to continue with the joint Venture at any stage, while the other PARTY is able and willing to do so.

Article 2 - Implementation of the Joint Venture

2.1 Basis for decision making

In principle, all decisions relating to the Joint Venture shall be by mutual agreement except under the circumstances contemplated in Article 10.

The PARTIES shall inform each other regularly and exhaustively, in a written report to be submitted to the other PARTY at a minimum frequency of every four months, about planned and completed work and about the results generated under this Agreement. In addition, the PARTIES shall meet at six-month intervals in order to exchange information and discuss their respective activities.

Each PARTY shall appoint a liaison officer in order to make cooperation effective.

2.2 Commitment to conduct ELEMENTS #1 AND #2

The PARTIES make a firm commitment to conduct ELEMENT #1 and ELEMENT #2 of the DEVELOPMENT PROGRAMME, subject to the provisions of 3 and 10 below.

A schedule and detailed planning for ELEMENTS #1 and #2 of the DEVELOPMENT PROGRAMME forms an integral part of this agreement and is appended as Annexure A.

2.3 Basis for conducting ELEMENT #3 of the DEVELOPMENT PROGRAMME

It is expected that, upon completion of ELEMENT #1, the PARTIES will be in a position to decide upon whether to proceed with ELEMENT #3.

The PARTIES will decide whether to proceed with ELEMENT #3 at the appropriate time and such a decision will be taken in the light of experience gained in ELEMENT #1, and the economic circumstances prevailing at the time. Nothing in this agreement shall be construed as placing any obligation upon either PARTY to continue with ELEMENT #3.

2.4 ELEMENT #4 of the DEVELOPMENT PROGRAMME

The scope of ELEMENT #4 will be determined by mutual agreement by the PARTIES, taking into account the results of ELEMENTS #1, #2 AND #3. Neither PARTY has made any firm commitment at this stage to conducting any specific work as part of ELEMENT #4.

2.5 COMMERCIAL EXPLOITATION PHASE

2.5.1 Sharing of the benefits of Commercial Exploitation

In the COMMERCIAL EXPLOITATION PHASE of the Joint Venture, the PARTIES will conduct negotiations with potential partners with a view to entering into agreements to manufacture equipment which utilizes the TECHNOLOGY. Such TECHNOLOGY licensees shall be manufacturers of equipment and it is envisaged that any licensing agreement between the PARTIES and such licensee would make provision of the payment of a royalty to the CSIR and Forschungszentrum. Such royalty or any other benefit, such as licensing fees and the like, shall be apportioned in accordance with the total financial contribution made by each PARTY.

2.5.2. The PARTIES shall provide for two separate internal accounts for the expenditure relating to PLANT #1 and #2, so that the total expenditure on each of the plants can be readily distinguished.

Article 3

Costs of the DEVELOPMENT PROGRAMME

3.1 The expenditure spent by the PARTIES regarding the activities comprising the DEVELOPMENT PROGRAMME shall be on an equal basis.

3.2 Each PARTY shall bear the costs arising to it in the course of implementation of the present Agreement. Such costs would include, inter

alia, the cost of Stamp Duty, registration and the like.

3.3 CSIR shall pay Forschungszentrum the following lump sums in order to cover part of Forschungszentrum's costs of material, equipment and infrastructure incurred by carrying out the DEVELOPMENT PROGRAMME. Such payment is in accordance with the principle that all expenditure by the PARTIES is on an equal basis and in making such payment, the CSIR is merely making a balancing payment to reflect the larger portion of expenditure to be incurred directly by Forschungszentrum in conducting the DEVELOPMENT PROGRAMME:

- Regarding the conduct of test work on PLANT #1 during ELEMENT #1, the sum involved shall be DM 120,000.

- Regarding the development and construction of PLANT #2 during ELEMENT #2, the sum involved shall be DM 150,000.

3.4 Specific arrangements for ELEMENT #3

Forschungszentrum in principle agrees to construct and deliver the pulse generator, including the electrode system, for the experimental PLANT #3 against payment of a lump sum by CSIR to Forschungszentrum. It is noted that such payment represents a balancing payment by the CSIR to re-imburse Forschungszentrum, in order to adhere to the principle of equal payment.

The performance and design specification for PLANT #3 will be defined in the light of operating experience on PLANT #1 and until such experience has been gained, it will not be possible to define the cost of PLANT #3, or the delivery period.

3.5 Payment of duties and taxes

The sums according to Articles 3.3 and 3.4 shall be paid plus legal VAT and

all other duties, taxes or charges which may be levied in Germany or South Africa.

3.6 The sum shall be paid after receipt of invoice of Forschungszentrum.

3.7 Schedule of payment

Progress payments shall be made by the CSIR as follows:

PLANT #1

Description of activity	Amount due on completion (DM)	% of total amount due
Test vessel, Test rock and two-electrode system	***40.000***	***33 %***
Determination of dynamic high voltage breakdown strength of quartzite, granite and lava rock samples	***30.000***	***25 %***
Investigation on high voltage pulse cables, pulse transformers improved electrode configuations	***50.000***	***42 %***
		100%

PLANT #2

Description of activity	Amount due on completion (DM)	% of total amount due
Order of capacitors, charging unit baseframe and Marx housing	***70.000***	***46 %***
Completion of pulse generator discharge vessel, monitors control unit	***50.000***	***33 %***

Shipment to South Africa	***10.000***	***7 %***
Acceptance Tests in South Africa	***20.000***	***14 %***
		100%

Note: All amounts in DM, **not** SA Rand.

3.8 Maintenance of plant

The PARTIES agree that each PARTY shall be responsible for any PLANT maintenance costs incurred while that PLANT is under that PARTY'S control.

3.9 Insurance

The PARTIES shall consult to reach agreement for the arrangements for insuring any PLANT while in transit, as well as allocation of risk to the PARTIES of loss, damage, etc, of the PLANT.

3.10 CONTRACT RESEARCH funding

Both PARTIES acknowledge that CSIR depends on CONTRACT RESEARCH for financing its part of the DEVELOPMENT PROGRAMME. As the intellectual property generated under this Agreement shall not be spread broadly in the course of CONTRACT RESEARCH and the rights of the other PARTY shall be protected, CSIR agrees to obtain the prior written approval of Forschungszentrum regarding all terms and conditions of such a contract and vice versa.

Partners of CONTRACT RESEARCH shall be exclusively potential end users or licencees.

Article 4 - Inventions, Property Rights

4.1. The term „intellectual property" shall include but not be limited to: patentable inventions, inventions which are not patentable, registered

designs, trade marks, data, know how, and reports. It is specifically noted that, in terms of this clause, „joint inventions“ will become owned by both PARTIES jointly and in equal shares. The PARTIES shall consult each other regarding the filing of applications for statutory protection for any item of intellectual property which the PARTIES agree should be given such protection. Moreover, the PARTIES shall provide each other with whatever assistance is required in order to compete the formalities entailed in acquiring joint ownership; such assistance might include, for example, signature of documentation.

4.2. All intellectual property generated shall become the property of the PARTY generating it. Each PARTY shall grant to the other PARTY for the purposes and the term of this Agreement a non-transferable, non-exclusive right of use, which may not be sublicenced, without charge for the intellectual property generated under this Agreement.

4.3. Any further utilization of intellectual property shall be subject to a prior written agreement between the PARTIES, which shall be, in principle, on licence basis.

4.4. Each PARTY shall inform the other PARTY about inventions made within the framework of this cooperation within four months after filing an application.

4.5. If one PARTY elects not to apply for and/or maintaining a share in an intellectual property right to which it is entitled according to paragraph 1 above, it will offer to the PARTY its share in it, at no cost to the other PARTY. The other PARTY shall then be entitled to obtain such statutory protection at its own expense, and shall have full ownership of that particular intellectual property right.,

4.6. Each PARTY shall pay for itself the employee-inventor compensation due to its staff members, except for the case in paragraph 3 above, when the offered right is taken.

4.7. Each PARTY acknowledges that actions of use of information and of objects received from the other PARTY shall not constitute a right of prior use.

4.8. All physical property generated under this Agreement shall become the property of the Party generating it; in case of contributions of both PARTIES the physical property shall belong to both PARTIES according to the ratio of contribution made by each PARTY. The use of PLANT #2 or #3 by CSIR after the term of the Agreement or by third parties during or after the term of the Agreement shall be settled by agreement between the PARTIES in due course.

4.9. Both PARTIES shall be obliged to refrain from the following activities, unless prior written consent has been obtained from the other PARTY:

- Copying or modifying the PLANT #2 or #3 ;
- Selling the PLANT #2 or #3;
- Assigning or transmission of the PLANT #2 or #3 to third parties; or
- Commercially exploiting the PLANTS.

ARTICLE 5

RIGHT OF USE OF INTELLECTUAL PROPERTY DEVELOPED DURING COURSE AND SCOPE OF THE JOINT VENTURE

5.1 All reports and data generated during the course and scope of the Joint Venture and disclosed or transmitted to the other PARTY shall be regarded as confidential and neither PARTY shall disclose such data or reports to a third party without the permission of the other PARTY, unless such disclosure is in accordance with the provisions of 5.2 below. Any permission to disclose data shall be given in writing.

5.2 Each PARTY hereby gives the other PARTY permission to disclose data and reports **-** received by the other Party - in confidence to third parties being potential licencees of the TECHNOLOGY, as contemplated in the

COMMERCIAL EXPLOITATION PHASE of the Joint Venture as described above. Such disclosure shall only take place following the signature of a Confidentiality Agreement by the PARTIES concerned, and the level of disclosure shall only be sufficient to allow the prospective partner to decide whether or not to enter into a commercialization agreement with the CSIR and/or Forschungszentrum.

5.4 The obligation of confidentiality according to paragraph 5.1 above shall not apply to such information and objects for which it can be proved that the information

- has been or is being developed by the receiving PARTY independently of the disclosure;
- belongs to the publicly accessible state of the art at the time of disclosure or falls into public domain later on without the fault of the receiving PARTY;
- had already been the property of the receiving PARTY at the time of disclosure;
- is disclosed to a PARTY by a third party without the obligation of confidentiality.

5.5 The foregoing obligation of confidentiality shall expire five years after termination of this Agreement.

Article 6 - Publications

6.1. All publications and statements shall be in accordance with the general principles described in 5 above. Thus, publications containing information and relating to objects received which, according to Article 5, shall be treated confidentially shall be subject to the prior written consent of the other PARTY.

6.2. In all publications, presentations or other information destined for the public which relate to cooperation under this Agreement appropriate reference shall be made to the cooperation and the partners involved.

Article 7 : Sub-contracting

7.1. In case a PARTY intends to sub-contract any work falling within the ambit of the Joint Venture, the PARTY arranging such sub-contracting shall ensure that the sub-contractor conducts such work in compliance with the terms and conditions of this Joint Venture agreement.

Article 8 - Warranty, Liability

8.1. The PARTIES shall properly perform, to the best of their knowledge and taking into account the current state of the art, all work assumed under this Agreement. Neither PARTY gives any warranties concerning non-existence of pre-existing rights of third parties.

8.20. Liability is limited to intent and gross negligence**,** as far as legally not prohibited.

Article 9 - Personnel Assignment

The following principles shall apply in case of personnel of one PARTY being assigned to the other PARTY:

- The PARTIES shall reach prior agreement in each individual case regarding the staff member to be assigned and the purpose and duration of assignment.

- The employee relationship and conditions of employment of the assignee shall not be affected by the assignment. The remuneration inclusive of all fringe benefits (e.g. social security contributions, accident insurance contributions) shall be paid by the assigning PARTY during the period of assignment.

- The assignee shall conform to the in-house regulations and the safety and security rules inclusive of the respective general and specific instructions of

the PARTY to which he has been assigned.

Article 10 - Duration, Termination

10.1 Tenure of agreement

. Regardless of the date of signature of this Joint Venture, the Joint Venture shall be deemed to come into force **retroactively** on 1 March, 1998. It shall remain in force until 28. February 2002, unless terminated by mutual consent, or by either PARTY.

10.2 Termination by mutual consent

The PARTIES may terminate the agreement by mutual consent at any time, subject to such terms and conditions as the PARTIES may decide upon.

10.3 Termination by one PARTY, without mutual consent

This Agreement may be terminated by either PARTY at the end of each calendar half-year upon three months' notice. The notice of termination shall be in writing to be effective.

10.4 Consequences of termination by one PARTY, without mutual consent

It is contemplated that one PARTY may terminate the agreement because of lack of sufficient funding or changes in funding priorities,. If the other PARTY, upon receiving such notice of termination in accordance with the provisions of 10.3 above, should also elect not to continue, then the following provisions shall apply:

- The provisions in Articles 4 and 5, as well as in Articles 6 shall continue to apply after such termination of this Agreement. However, the provisions in Article 5, paragraph 1 shall continue to apply only for a duration of five years after termination of this Agreement.

If, however, the other PARTY, upon receiving such notice of termination in accordance with the provisions of 10.2 above, should elect to continue, then the following provisions shall apply:

- The PARTIES will reach agreement how a continuing of the Programme of work by the continuing PARTY can be made possible; if necessary including licence agreements for the continuing PARTY or assignment of personnel to the continuing PARTY .

Article 11 - Settlement of Disputes

11.1 The Parties shall make every effort to settle amicably all disputes or difficulties arising from this Agreement without recourse to the courts. In case an amicable agreement cannot be achieved, any dispute between the PARTIES arising from or pursuant to or in connection with this Agreement or the subject matter hereof shall be finally settled under the Rules of Arbitration of the International Chamber of Commerce by one or more arbitrators appointed in accordance with the said Rules.

11.2 The PARTIES agree that arbitration shall take place in Paris with all proceedings in English.

Article 12 - Miscellaneous

12.1. Neither PARTY shall cede or assign any of its rights or obligations in terms of this agreement, without the prior written consent of the other PARTY, which shall not be withheld unreasonably.

12.2. Any modifications and amendments to this Agreement shall be in writing to be effective. This requirement of written form can be waived only in writing.

12.3 Should a provision of this Agreement be or become invalid, this shall not affect the validity of the rest of provisions of this Agreement or the Agreement as a whole. The PARTIES shall attempt in a concerted effort to reach retroactively an agreement on a new valid provision the result of which shall reflect as much as possible the invalid provision which it will

replace.

Article 13: NOTICES

All notices under this agreement shall be in writing and shall be by any means which is confirmed at the time of delivery including telefax, hand delivery or registered mail, but specifically excluding electronic mail, to the PARTIES at their addresses below:

: The CSIR
DIVISION OF MINING TECHNOLOGY
PO Box 91230
Auckland Park,
2006

Forschungszentrum Karlsruhe GmbH
P.O. Box 3640
76021 Karlsruhe
Germany

or at such alternative address or addresses appointed by the PARTIES from time to time which addresses the PARTIES hereto choose as their respective domicilium citandi et executandi.

Thus done and signed on behalf of the CSIR at Johannesburg on this the ..... day of ..... 199..

AS WITNESSES:

_____

AUTHORISED SIGNATORY

1. .....

2. .....

Thus done and signed on behalf of Forschungszentrum Karlsruhe GmbH at ..... on this the ..... day of ..... 199..

AS WITNESSES: ----------

Forschungszentrum
Karlsruhe GmbH

1. .....

2. .....

15 APPENDIX B: Chronological developments and sequence of CoMRo and CSIR involvement with 'electric shock wave comminution' technology

Initiatives	Results	Comments
Search for alternative hard rock mining methods	IEEE and Batelle did some preliminary tests and estimates	No documentation other than the CoMRO Annual Report was found; this is given in the references.
	Aries Partners and Physics International	Some exchange of Memoranda. Lack of funding and high risk appears to have stopped any collaboration.
Search for alternative hard rock mining methods and/or potential use for secondary crushing of mined rock.	FZK in Karlsruhe developed pulsed-power equipment, and visited South Africa as part of their drive to obtain external funding from South Africa.	There appeared to be some mutual benefits, but the CSIR did not secure Innovation Fund money to provide running costs to purchase a unit for South Africa, or to have an engineer working in Germany for 6 months.
	Demonstration tests in Germany "after hours" during exploratory visits to Germany with pulsed power equipment.	Author "tested" four disc-shaped samples at FZK. No clamping arrangement and no provision of instrumentation, just some broken fragments for microscopic analysis in South Africa.
	Euro-Pulse in the UK had a small test set-up with a single discharge and a rock-clamping arrangement.	Some technical aspects from the photos that were obtained by Peter Kramers from his visit to Euro-pulse were used to conceptualise the local South African test rig at the Wits.
	Waste and reef rock lumps, (not machined to any geometry) were tested in an *ad hoc* mode to demonstrate the test rig.	Peter Kramers reported a five-fold increase in 'difficulty' in breaking waste compared with reef.
	Bialecki was very secretive and worked with Andres in the late 1970s on electric discharge for rock breaking.	Andres quoted exorbitant consultant fees to contribute to the South African initiative.

Initiatives	Results	Comments
Assessment of local capabilities to conduct single discharges in a controlled and monitored manner.	Netfa/Apollo and Atomic Energy Corporation (AEC) equipment would require substantial modifications and funds. Apollo had too much energy in their set-up, whereas AEC had too little energy in the small set-up.	Components from Wits' High Voltage Laboratory could be configured for single discharge. A mechanical rock-clamping and sampling mechanism and a water-filled comminution chamber needed to be designed for the single discharge tests. The seasonal work mode at Wits provided time slots for conduct the test.
Systematic, fundamental test work at Wits with different types of South African reef and rock specimens.	Linkage of rock type to breakdown field strength using single discharge in an controlled manner, using water tests as reference.	Good set up for machined specimens, sampling of fragments, gathering of data logged instrumentation and obtaining photographic evidence.

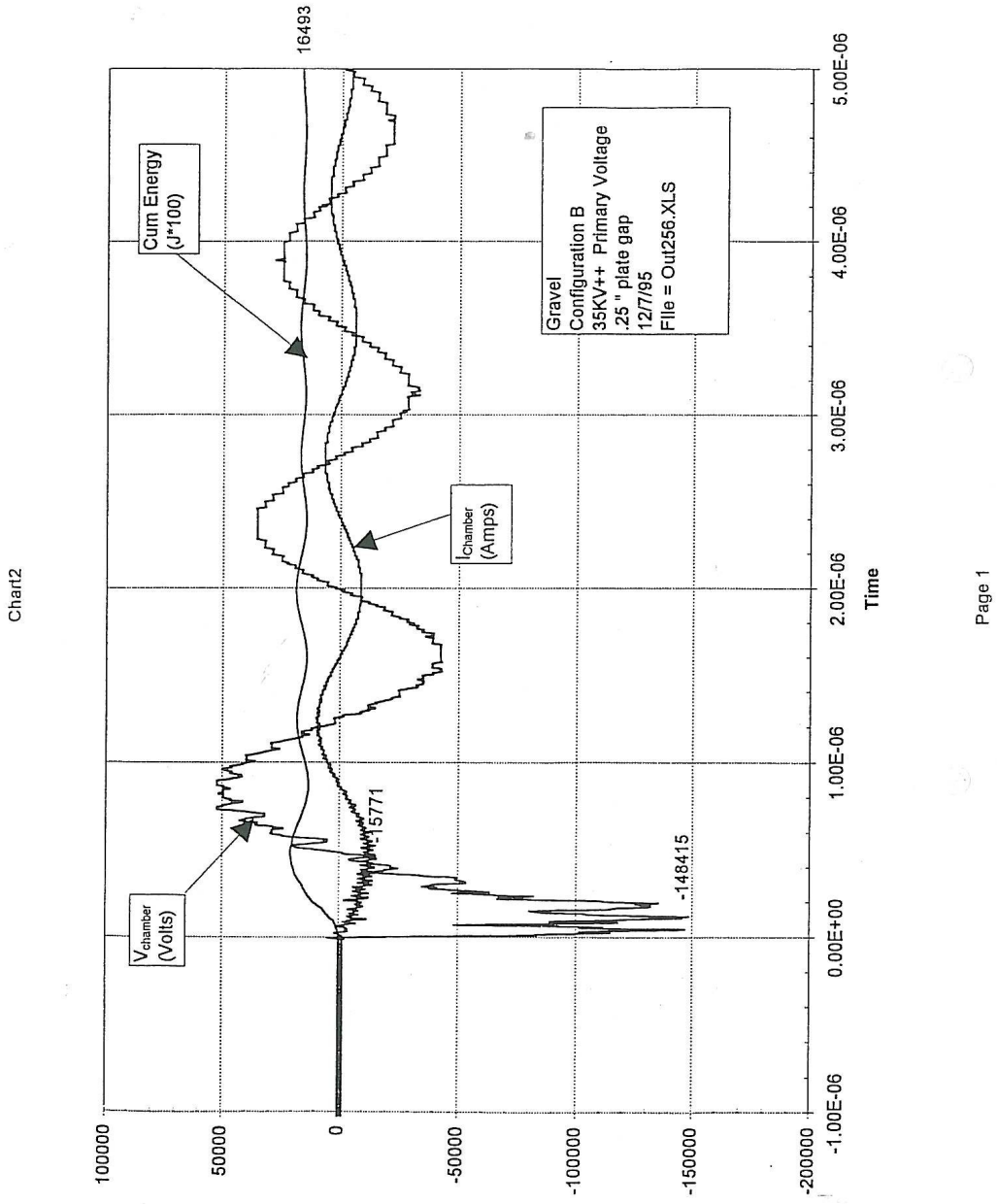
16 APPENDIX C: People significantly involved in South Africa with electric rock breaking for this project

Name and company	Position	Contribution	Comments and related actions by author
Horst Haase, CSIR	Technical Consultant	Initial test work with IEEE and Batelle in Switzerland under CoMRO, late 1980s. Initial liaison with FZK, Germany.	Horst was mentor of the author until his retirement, which was before this study was started, using single discharge in a South African test rig.
Rod Pickering, CSIR	Technical Consultant	Liaison with Aerie Partners, USA, early 1990s.	The available documentation was used in this literature review.
Dr Adrian Hinde, Mintek	Group Leader	Liaison and test work on behalf of Mintek at Aries Partners, using gold reef rock.	Mintek also investigated the technology; the summarised results are provided in this dissertation as part of the technology review for Aries Partners.
Pat Willis, CSIR	Programme Manager	Initiator of electric rock breaking at the face as a mining method. Took UG2 samples to FZK for indicative tests.	Samples were returned to South Africa and analysed by the author as part of establishing a sample results database.
Peter Kramers, CSIR	Research Area Manager	Suggested using electric rock breaking as a secondary comminution method to condition the broken rock for hydraulic transportation by pipeline. Visits to FZK and Euro-pulse (met with Richard Bialecki).	Indicative results from unmachined grab samples of available waste and reef rock. No documentation other than visit report, given in references. Provided pictures from Euro-pulse rig, which is part of the equipment and literature review.

Name and company	Position	Contribution	Comments and related actions by author
Author	Researcher	Conducted only one overseas visit to FZK during the contract negotiation phase between the CSIR and FZK. Entire literature review. Assessment of local equipment and facilities in South Africa. Assessment of success factors; designing of test equipment; specifying the electric circuit functionality; acquisition of suitable photographic facilities and set-up; and planning and conducting of entire test programme. Preparation of all samples and analysis of all results.	Four different rock types were prepared to discs, 4 mm thick and 16 mm in diameter, in South Africa and were then comminuted with the Frank-0 plant for 5 seconds each with a continuously pulsating rig; no rock clamping, no instrumentation. The new Frank-Stein Plant was seen during its construction as it was CSIR's intention at the time to purchase that equipment.
Shawn D. Nielson, Wits Andreas Beutel, Wits	Lecturer at Wits Assistant at Wits' High Voltage Laboratory	Obtaining and calibrating the high-voltage components; taking responsibility for safety in the High Voltage Laboratory; and manually controlling the charging of the Marx generator circuit.	Wits is legally responsible for the safety of the High Voltage Laboratory, and thus an assistant had to be there during all tests.
Philamon Moseme, CSIR Intern	Geologist	Specimen content characterisation by microscope prior to electric discharge.	Employed part time; had left by the time the samples were fragmented.

17 APPENDIX D: Voltage and current traces from other test rigs

The chart below was taken from page 49 of the Hinde and Joosub (1997) reference. It is purely reproduced to demonstrate the smooth wave form of the voltage and the current signal, for comparison with the noisy signals obtained from the unfiltered, not yet optimised electric setup used during this study.



The page below is a direct reproduction of the Andres 1989 reference.

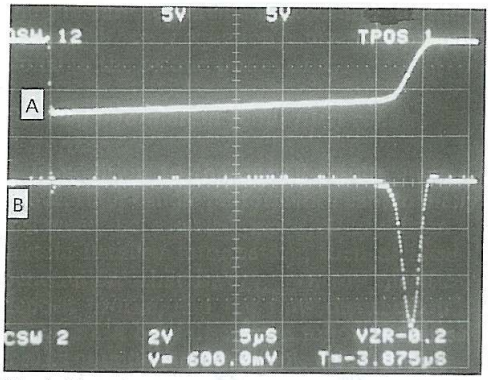


Fig. 4. Wave shapes of a fragmentation pulse in the area of low electrical fields. Scales: 75 kV/square, 5.8 kA/square, 5.0 ms/square.

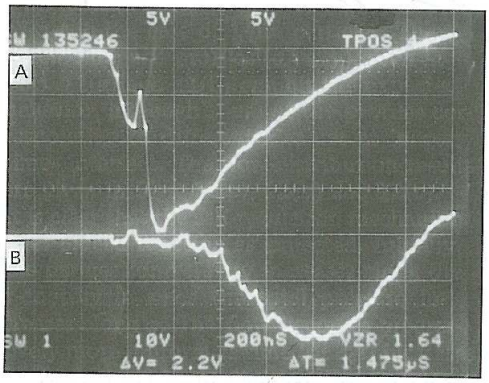


Fig. 5. Wave shapes of the fragmentation pulse in the optimum field area. Scales: 69 kV/square, 0.3 kA/square, 200 ns/square.

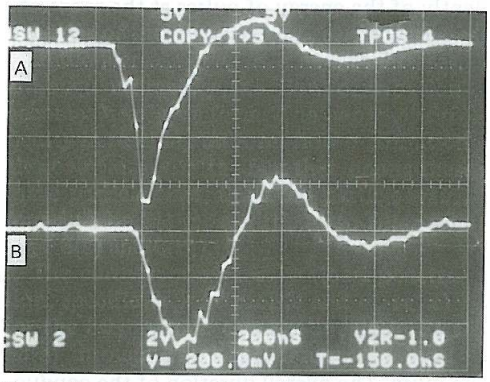


Fig. 6. Wave shapes of a fragmentation pulse in the area of high electrical fields. Scales: 125 kV/square, 0.6 kA/square, 200 ns/square.

shows that with increase in the magnitude of the applied field above 25 kV cm^{-1} and availability of energy beyond 25 J cm^{-1}, the transfer of energy of the pulse through the material takes place under the conditions of electrical breakdown. The area of electrical breakdown, enclosed between graphs 1 and 2, corresponds to pulses which indicate 100% probability of the electrical breakdown, mixed with some percentage of cases where mechanical fragmentation also takes place.

In Figs. 4, 5 and 6 are shown sets of wave shapes of pulses corresponding to the fragmentation events, taking place at different voltages and energies of pulses. The oscillograms are taken in the dual-channel oscilloscope and simultaneously present wave shapes of voltage and of current, passing through the granite sample.

Graphs (Fig. 4) show wave shapes of a fragmentation pulse, impressing a low (27.5 kV cm^{-1}) electrical field across the rock sample and consuming a relatively large amount of energy (120 J cm^{-1}). Graphs (Fig. 5) correspond to the fragmentation pulse which impresses the electrical field of 68 kV cm^{-1}. This field is close to the optimum magnitude for the tested rock (see graph 2, Fig. 2). The energy consumption in this case is lowest (47 J cm^{-1}).

Graphs (Fig. 6) represent the wave shapes of the fragmenting pulse, taking place at the high (100 kV cm^{-1}) electrical field and consuming 62 J cm^{-1}. The parameters of these three pulses are summarised in Table 1.

The fragmentation process, induced by pulses at the low electrical field close to the electrical breakdown limit, is characterised by two distinctive periods of the voltage decay. From the moment of build-up of the potential over the sample until the beginning of the current pulse, a relatively slow linear decay of voltage takes place. An example of such a pulse is the fragmentation pulse (Fig. 4). In this pulse, the slow decay lasts 37 μs. During this time, the current is very small (of the order of several amps) but sufficient for the development of conductive paths, bridging both electrodes. The relatively low electrical field determines the relatively low conductivity of the sample and low rate of development of the conductive paths. When the conductive path is completed, a current surge, accompanied by fast decay of voltage, takes